5-1-1989

Color transformation modeling for printed images using interpolation based on barycentric coordinates

K. Douglas Gennetten

Color Transformation Modeling for Printed Images using Interpolation based on Barycentric Coordinates

by
K. Douglas Gennetten

A thesis submitted in partial fulfillment of the
requirements for the degree of
Master of Science
in the
School of Printing Management and Sciences
College of Graphic Arts and Photography
Rochester Institute of Technology

May, 1989

Thesis Advisor:
Professor Frank Cost

Certificate of Approval — Master's Thesis

Rochester Institute of Technology
School of Printing Management and Sciences
Rochester, New York

CERTIFICATE OF APPROVAL

MASTER'S THESIS

This is to certify that the Master's Thesis of
K. Douglas Gennetten
With a major in Printing Technology
has been approved by the Thesis Committee as satisfactory
for the thesis requirement for the
Master of Science Degree.

Frank Cost
Thesis Advisor

Joseph L. Noga
Graduate Program Coordinator

Miles Southworth
Director or Designate

COLOR TRANSFORMATION MODELING
FOR PRINTED IMAGES
USING INTERPOLATION BASED ON
BARYCENTRIC COORDINATES

All authorized copies *must* be produced with a *color* copier for pages containing *any color content*. Original laser and ink-jet printed copies are available by contacting the author at 4148 Sumter Square, Fort Collins, CO., 80525.

I, K. Douglas Gennetten do hereby *deny* permission to the Wallace Memorial Library of RIT to reproduce my thesis in whole or in part except when in full compliance with the above provisions.

May, 1989
Copy #3

Acknowledgments

It is a pleasure to acknowledge the encouragement and assistance of the many people who have helped in this research project. First of all, Frank Cost who served as the author's Thesis Advisor and provided an invaluable contribution by introducing the author to several persons within R.I.T and R.I.T. Research Corporation who provided insights into the problems studied. The author is indebted to those who read various drafts of all or part of the manuscript, offering many constructive suggestions. These have been Frank Cost, Mark Guldin, Miles Southworth, Burt Saunders, Richard Orr, and Lynn Gennetten. A special thanks to Mark Guldin for meticulously scrutinizing the text flagging the many split infinitives and to Archie Provan for providing valued typographical assistance both during and following last summer's exceptional Typography class.

The author is particularly grateful to Warren "Dusty" Rhodes for his vibrant enthusiasm, expertise, and encouragement, and Richard Orr, a professor in the R.I.T mathematics department for several valuable brainstorming sessions he so willingly hosted. It was upon his original suggestion that the method of barycentric coordinates was studied.

This author is a grateful participant in the Hewlett-Packard Fellowship Program and is thankful for the company's generous additional support in the form of loaned computing and imaging equipment, and for Mary Chappell's many shipments of mail and supplies.

Finally, for steadfast support and encouragement, my heartfelt thanks go to my family – Lynn, Darren, and baby Landon who was born between classes.

K. Douglas Gennetten

Rochester, New York
May, 1989.

TABLE OF CONTENTS

List of Figures

CHAPTER8

ABSTRACT

This document is a report on the research of a potentially superior method of color image transformation for producing rapid and accurate printed color output from a digitized color image. The primary objective is to reduce the complexities, inaccuracies, objectionable artifacts, and processing time common to current methods of color modeling. A new method of vector-corrected mathematical modeling combined with improved color space interpolation is studied. This achievement allows for rapid automatic closed-loop color-match calibration between image capture and output devices.

Currently, digital image creation or manipulation systems rely on image proof printing which is slow and often of poor color fidelity or proprietary. The ideal system would provide optimum color reproduction fidelity and rapid proof printing at a low cost. Existing systems often rely on mathematical models for image conversion for printing. These models are usually a bottleneck in the proofing process and are not accurate enough for many applications. Increasing their accuracy rapidly increases processing time to the point of impracticality well before *graphic arts* quality levels are achieved. A common solution to this problem in larger systems is a massive and tediously generated color look-up table based on actual measured print samples. This method is costly and does not readily accommodate printing process changes such as paper grade or ink color. Attempts to reduce the size of these look-up tables and the large quantity of required sample measurements have been disappointing.

In this thesis, new methods will be reported which should allow practical small-system color proof printing with excellent color fidelity and rapid processing. By eliminating common problems associated with color space interpolation, these new methods make closed-loop control practical with a relatively small quantity of sample measurements which can be automatically printed, scanned, and incorporated into conversion processes.

CHAPTER 1
INTRODUCTION

1.1 PROBLEM AREA

Digital imaging systems, whether for graphic arts applications or for scientific or engineering applications, usually require some form of printed output either as a final product or as a proof. This output optimally preserves the full detail and color content of the digitized image. Several digital electronic color marking engines available today provide the necessary image detail and color gamut potential necessary for realizing these goals. A great deal of processing, however, is required to transform accurately the digitized image to a matching printed image. Transferring digitized image *detail* to printed *detail* is a relatively straight forward process. The problem addressed in this research report is the fairly convoluted processes which are typically required for accurately transferring the digitized image *color* to a matching printed *color*.

Accurate color transformation typically requires either very large and unwieldy look-up tables or very complex and lethargic mathematical models. Large look-up tables are expensive, difficult to modify, and often problem prone due to objectionable interpolation artifacts. Accurate mathematical models are many orders of magnitude too slow for practical rapid output. Compromises often take the form of a less accurate, simplified model.

An optimal system would provide color transformation which is fast enough not to be a significant bottleneck in the users' routine

tasks, accurate enough to justify its use, flexible in its support of various printing inks, substrates, and techologies, and inexpensive to implement. This thesis is a report on an effort to move closer to this ideal.

In order to achieve and maintain the desired accuracy in such a system, *closed-loop feedback* could be employed. This would entail sampling the printer's gamut with some color measurement means. These measurements, if sufficiently accurate, could then be incorporated into an error calculation integrated into the color transformation process. There are several problems with this concept. In a low-cost system, automated color measurement (scanning) usually includes a significant degree of *instrument metamerism*, or color measurement inaccuracy. There are also hurdles to be overcome in the area of gamut sampling and interpolation. The sample quantity must be restricted to far less than the total number of printable, distiguishable colors. Sample dispersion within the printer's color space presents several problems which will be addressed. Once measured, these samples must be placed into the imaging system's color space and interpolated values must be made available between the samples. This task has typically been a weak point in digital systems. Several problems relating to this multidimentional color space interpolation will addressed.

The fundamental investigations of this research are (a) the conception and study of an improved method of interpolation within color space using *barycentric coordinates*, and dissecting the color space into an aggregation of space-filling polyhedra to facilitate interpolation; (b) a method of combining color space interpolation with mathematical modeling to form *vector-corrected modeling;* and (c) a study of means for optimally sampling a printer gamut for maximum sample validity and homogeneity in a uniform color space, consequently providing improved interpolation accuracy and efficiency.

It is anticipated that this research will result in an improved method for producing fast and accurate color transformations for use with digitally-driven, color-marking engines.

1.2 ORGANIZATION

Chapter 1 contains an INTRODUCTION to the research: a description of the problem and an outline of the organization of this document. Chapter 2 will outline the THEORETICAL BASIS for the study. Topics include image reproduction fidelity, subtractive color printing, color transformation and modelling, and multidimensional interpolation and approximation. Chapter 3 is a LITERATURE REVIEW of the field with an emphasis on look-up table and mathematical modeling processes. Chapter 4 contains the HYPOTHESIS and how it relates to the contents of the previous chapters. Chapter 5, the METHODOLOGY, contains a description of the experimental design of the study and the equipment and processes to be used. Chapters 6, 7 and 8 embody the RESULTS OF INTERPOLATION STUDIES, RESULTS OF SAMPLING OPTIMIZATION STUDIES and the RESULTS OF COLOR MODELING STUDIES: an in-depth discussion of the research findings, a discussion of the test data and the results of analysis. Finally, Chapter 9, the SUMMARY, extracts several conclusions from the study making specific comparisons to the literature and prior art. This chapter also suggests several potential avenues of further related study.

An ANNOTATED BIBLOGRAPHY is included for the interested reader along with several APPENDICES containing pertinent data and printed samples.

CHAPTER 2
THEORETICAL BASIS

2.1 IMAGE REPRODUCTION FIDELITY

In graphic arts reproduction, the achievment of image reproduction fidelity can be conveniently segmented into three primary criteria: *detail* fidelity, *color* fidelity and *surface* fidelity. Reproduction of surface properties (when the original is reflection copy) may not be important or even desired. Usually, the surface gloss of the reproduction is specified independently from the original. In the graphic arts, most "originals" are transparencies, leaving surface reproduction indeterminate. All measurements for this study (and most in the graphic arts) incorporate 45/0° geometries which corresponds best to viewing conditions by excluding all specular reflection from gloss.

Detail Fidelity

The detail fidelity of a reproduction is determined by the *spatial resolution* of the printer and the spatial frequency content of the original image. Spatial resolution is specified by a *modulation transfer function (MTF).* It is important to differentiate here between reproduction detail *fidelity* and any objective measure of detail *quality.* Detail quality includes MTF, viewing magnification and the human visual response. The most well known measure of detail quality is *Cascaded Modulation Transfer Acutance (CMT)* [Kriss 77]. This study, however, is only concerned with reproducing the quality as found in the original – with as much fidelity as possible.

Proofing systems, and graphic arts reproductions in general, have minimum MTF requirements which have been discussed in various papers [Johnson 88, Kriss 87, Saarelma 84]. Digitally driven color marking engines of various technologies are available today which generally satisfy the MTF needs for proofing photographic continuous tone images.

Color Fidelity

By far, the more challenging problem in printed image generation is color accuracy. Reproducing images on a substrate by varying the applied quantity of colorant presents a plethora of well known problems—problems not present with reproduction via color displays or photographic prints [Laihanen 88, Yule 67].

Perfect color reproduction is an unrealistic goal. To provide an exact copy of the original which would match *under all illumination conditions* would require a *spectral reproduction.* Spectral reproduction is only practical when the reproduction is made with the same colorants and substrate as used in the original.

For a graphic arts reproduction, *colorimetric reproduction* is the highest practical type of color reproduction. Colorimetric reproduction provides color matching when the original and reproduction are viewed under the *same illuminant and viewing conditions.*

For many reproduction jobs in the graphic arts, accurate color reproduction is eschewed in deference to *preferred reproduction,* where memory colors are intentionally altered from reality. Bluer skies, more tanned skin, and brighter colors are often desired changes from the original record. The most convenient and predictable path to a purposefully altered reproduction is through first providing accurate colorimetric reproduction as a reference point. An in-depth discussion of these and other color reproduction types can be found in [Hunt 87].

Color Error Tolerance

The concept of reproduction accuracy suggests the question: "For graphic arts reproduction, what level of accuracy is desired?" This

question is of course somewhat subjective in nature and effected by many variables. Very little quantitative information has been gathered in this area. One investigation suggests that acceptable tolerance limits for lithographic reproductions is roughly around six CIELAB ΔE color-difference units [Stamm 81]. This form of overall image color tolerancing has one very prominent, though often ignored, flaw: adjacent picture elements of an image cannot have error *differences* any larger than a just-noticeable difference (approximately one CIELAB color-difference unit) when these error differences are *systematically aligned* such as along constant lightness boundaries. This is the type of error produced when a printing or scanning device has less than the optimum gray-level resolution. That is, when the smallest printable or detectable change in color is larger than a just-noticeable difference the objectionable result often presents itself as *false contouring.*

2.2 REPRODUCTION FIDELITY WITH DIGITAL IMAGES

A digital image displayed on a color monitor exists as an array of picture elements, or *pixels,* each assigned a *tristimulus.* This tristimulus is simply three numbers representing the relative amounts of red, green, and blue intensity. These numbers most often refer to a definition of color introduced by the National Television System Committee (NTSC) and standardized for compatible color television image broadcast by the FCC in 1953 [Rzeszewski 83]. Over 35 years later, these standards are still testifying to the validity and applicability of the basic principles underlying the colorimetric standard. Although certainly not the ideal vehicle for color images, the NTSC colorimetric standard has become the vehicle of choice for color images in many disciplines including computer graphics and graphic arts image displays.

The advent of color CRT's used as computer graphics displays and the existence of digital image capture capabilities has greatly increased the demand for rapid digital color printing. This voracious demand has elicited many varied attempts at color printing from digitized images. These endeavors have produced a wide range of

color reproduction fidelity levels. These levels can be classified according to the methods used and the resulting reproduction integrity. On page 2-5 is a chart of just such a classification order.

Level 0 Reproduction

This lowest level of reproduction is, quite unfortunately, still one of the most common incorporated into small systems such as CAD and business graphics printing. With level 0 reproduction, the original image tristimulus *[R,G,B]* is converted pixel by pixel to relative amounts of printed *[C,M,Y]* by simply complementing the tristimulus. For example, if *RED* is an 8-bit integer ranging from 0 to 255 and has a value of 245 then *CYAN* would simply be the 8-bit complement, 10. Increasing *RED* directly causes proportionally decreasing *CYAN*. For the purposes of this discussion, the printer's black ink will be temporarily ignored. All of these levels are valid constructs for either three-color or four-color printing systems. Calculating the amount of the fourth color, black, is a largely separate problem which will be discussed later. For clarity and generalization the chart on page 2-5 treats *[C,M,Y]* and *[R,G,B]* as having a range of zero to one.

Several problems exist here. The values *[R,G,B]* and *[C,M,Y]* are *relative amounts* of some quantity. In the *[R,G,B]* case, it is usually relative intensity: maximum *RED* implies "full-on" *RED* but says nothing about the resulting absolute brightness. Similarly, *CYAN* typically will represent some relative amount of dot area or concentration but indicates nothing about the resulting absolute color lightness or density. With these conditions, tone reproduction is not controlled at all. Highlight and shadow detail is often lost entirely. Gray balance, a very important consideration in graphic reproduction, is not preserved. A gradation of grays may end up being reproduced as a pastel rainbow.

A second problem is caused by the inaccurate assumption that the printing primaries are color complements of the display primaries. To illustrate how fallacious this assumption is, find a printed example of solid ink process primaries and two-color overprints (in any book on basic color theory) and hold it next to a color monitor

COLOR REPRODUCTION FIDELITY LEVELS

General Color Fidelity Levels of Printed Digital Images

Level 0: Complemented RGB Tristimulus Values. Minimum for simple business and CAD graphics. No tone reproduction, gray balance or color correction. Inadequate for natural images.	$C=1-R$ $M=1-G$ $Y=1-B$
Level 1: Single Tone Reproduction Curve. Improved color rendition for business and CAD. No gray balance or color correction.	$C=f_1(1-R)$ $M=f_1(1-G)$ $Y=f_1(1-B)$
Level 2: Multiple Tone Reproduction Curves. Balanced grays. No color correction. Minimum level for many natural images, though inadequate for most.	$C=f_1(1-R)$ $M=f_2(1-G)$ $Y=f_3(1-B)$
Level 3: First Order Matrixing (Masking Eqns). First order color correction, large errors remain. Large color accuracy improvement over Level 2. Minimum level used in graphic arts scanners.	$C=f_1(a_1R+a_2G+a_3B)$ $M=f_2(b_1R+b_2G+b_3B)$ $Y=f_3(c_1R+c_2G+c_3B)$
Level 4: Higher Order Mathematical Models. Polynomial fits and physical models. Heavy computation requirements for high fidelity.	$C=f_c(R,G,B)$ $M=f_m(R,G,B)$ $Y=f_y(R,G,B)$
Level 5: Sampled, Interpolated Look-up Table. Look-up table generated from interpolation of non-orthogonal samples. Accuracy depends on table size and uniformity.	$C=lut_c(R,G,B)$ $M=lut_m(R,G,B)$ $Y=lut_y(R,G,B)$
Level 6: Vector Corrected Math Models. Correction of model through closed-loop feedback. Significant performance gains over 4. Significant efficiency gains over 5.	$C=lut_c(f_c(R,G,B))$ $M=lut_m(f_m(R,G,B))$ $Y=lut_y(f_y(R,G,B))$
Level 7: Massive Look-Up Table. Ultimate accuracy. Perfect color match when in gamut. Inflexible and extremely impractical.	$C=lut_c(R,G,B)$ $M=lut_m(R,G,B)$ $Y=lut_y(R,G,B)$

displaying full-on primaries and secondaries (a PC with a draw or paint program will do nicely). In comparing the two, one can quickly spot significant differences. For example: Printed magenta is much redder than the displayed magenta and, in fact, it is often called "process red." Similarly, printed cyan is considerably bluer than the displayed rendition and is frequently labeled "process blue." Monitor blue is a nearly-unique blue, whereas the two-color overprint blue—cyan plus magenta—is a very purple blue. These fairly dramatic differences invoke large and unavoidable hue errors in Level 0 reproductions.

Note that ideal "block dye" inks requiring no traditional color correction would still not match the monitor colors and thus, at this level, would still result in hue error.

Level 1 Reproduction

Advancing one level on the scale introduces the use of a tone reproduction curve; also called a shaper or gamma curve. This curve is simply a look-up table which is used to convert any value on the relative scale to any other value on the same scale. Any desired curve shape can be used. With this curve, one has the flexibility to correct for basic tone or lightness reproduction. This presents two noteworthy options. Providing *absolute* tone reproduction—assuming the absolute values represented by the relative tristimulus of the original image data are known, or providing *preferred* tone reproduction. With preferred reproduction the image shadows, mid-tones and highlights are mapped (with the curve) into the printer's range from the darkest to lightest printable dot. This process, which is very common in the graphic arts, can insure the reproduction of shadow and highlight detail, preserving the maximum amount of original detail.

Preferred reproduction is used under two conditions: when the original is to be intentionally modified, and when the printer can't reproduce the full lightness range found in the original. Absolute reproduction may be fine only if the lightness range of the image falls within the printable lightness range.

Level 1 reproduction still has a serious problems: Gray balance is missing. Since a single curve is applied to all primaries, equal amounts of *[R,G,B]*, which is gray by NTSC definition, yield equal amounts of *[C,M,Y]*. Equal amounts of real printing inks usually result in a noticeable hue. Also, complementary primaries are still assumed, resulting in large hue errors. Hue error is also introduced by the tone reproduction curves themselves (See [Yule 67] p.121 for details).

Level 2 Reproduction

Giving each of the printing primaries a separate tone curve provides a means for insuring balanced gray reproduction. Gray balance is one of the most important considerations in both synthetic and natural image reproduction. This level, though admittedly faulted, is an acceptable level for many images. Due to the lack of color correction, hue error from primary mismatch and from ink characteristics will still cause objectionable degradation of most originals. The tone-curve induced hue error of Level 1 still remains.

Level 3 Reproduction

This is the first point on the scale at which the mismatch of primaries becomes less of a problem. The improvements up to Level 2 are retained and an additional degree of freedom is added by allowing the relative ink primaries to each individually be a function of *all* of the original primaries. The amount of *CYAN* now is a linear combination of different amounts of each of the complemented additive primaries. This allows one to perform the equivalent of photographic masking [Yule 67]. At this level, first order color correction is possible which enables major color accuracy improvements over level 2; however, large hue errors may remain. This is the highest level obtainable with traditional photographic means in a graphic arts camera. This is also the level at which most commercially successful graphic arts scanners operate [Molla 88]. In these scanners, analog signal processing eliminates any computation bottleneck.

To most, this would be considered the minimum practical level for the graphic arts. It is also the first level at which mathematical

(though not necessarily digital) computation becomes necessary (previous levels only required addressing locations in a look-up table). An important consideration for this level is the choice of primaries. A simple 3x3 transform works much better with uncorrelated primaries. Working in hue saturation and lightness, rather than red green and blue, will give better results; however, this is not often practical due to processing speed considerations.

Level 4 Reproduction

This level has opened up an unlimited foray into higher order mathematical models of the image capture and reproduction processes. The well known Neugebauer equations [Neugebauer 37] fall into this category and are used, in various forms, on many of the newer digital graphic arts scanners.

Computational complexity rapidly becomes an encumbrance at this level, leading to the use of look-up tables for acceleration. Newer scanners using modified Neugebauer equations are sold with initial coarse look-up tables for various printing conditions, then a form of interpolation is performed during scanning [Pugsley 75, Molla 88]. This insures scanning speed at the sacrifice of flexibility to changing printing conditions. Higher accuracy requires increased model complexity—with rapidly diminishing returns. Mathematical models which approximate observed physical phenomena (including modifications of Neugebauer) have a strong advantage over blindly generated polynomial curve fits achieved through regression. They can provide a great deal of flexibility to changing conditions.

Rapid printing of a displayed image is rendered impractical by any use of an accurate color transform based solely on mathematical modeling. In such systems, where timeliness is critical, a compromise in the form of reduced accuracy is usually administered.

Level 5 Reproduction

All previous reproduction levels assumed a fixed set of scanning and printing conditions and materials. Graphic reproduction jobs en-

compass the use of various reproduction technologies and mediums. Each variation can effect the image reproduction and may require a unique solution to guarantee fidelity. Simply changing from one paper grade to a different grade of the same paper color can cause startling shifts in printed hues. Because of the large number of possible printing conditions, only a few of the most general are modeled in the newer graphic arts scanners. Happily, with printing standards such as the Specifications for Web Offset Publications (SWOP), these generalizations combined with skillful press operation can meet adequately the behests of most publications. The ideal reproduction system would automatically compensate for changes in the imaging processes from capture or generation to final printing.

Automated control systems operate on the principle of *closed-loop feedback*. The process control parameters are measured and compared against a standard. Any detected error is then fed back into the controls of the system and used for correction. In a graphic reproduction system, the size and location of the press or printer gamut could be automatically measured for any given set of printing conditions. This data then could be fed back to the image transformation process to make any detail (edge enhancement) or color corrections necessary to enable the desired response. An ideal system might have an on-line feedback system which would continuously make corrections. This could guarantee the best possible reproduction if the image carrier could also be modified continuously (which is possible with most electronic printing technologies but *not* with traditional plate presses). It is important to note that this feedback automatically provides the best possible gray balance and facsimile tone reproduction (assuming no measurement error); without any explicit control over these traditional metrics.

Level 5 reproduction is based on a sampled look-up table. This level does incorporate feedback error control although not necessarily continuous closed-loop feedback. The available accuracy is determined by the size of the gamut sample, the accuracy of sample measurements, and the method of interpolation used for the look-up table. The sample size necessarily is much smaller than the total

number distinct printable colors. Colors not found in the sample are generated through approximation or interpolation techniques. These techniques, discussed in section 2.3 and Chapter 6, often induce *false contours* and other objectionable artifacts. The avoidance of these problems dictates a minimum look-up table size which is typically very large. This presents two hurdles. First, the immense tables required are far too large to be practical for small systems available now (1989). Admittedly, this limitation will diminish with time. The second problem, however, is more serious: the logistics associated with the large sample size become impractical, especially from a printing and measurement perspective.

This reproduction level is used for building large look-up tables to be sold with high-end digital scanners.

This thesis involves a new color-space interpolation methodology which promises to eliminate these major weakness of current interpolation schemes.

Level 6 Reproduction

Level 6, perhaps the pinnacle of practical digital image reproduction levels, is formed by combining the previous two levels to form *vector-corrected* look-up tables. This level promises to provide a significant improvement over all of the lower levels discussed up to this point. By combining a mathematical model with closed-loop interpolated correction techniques, both discussed in Chapter 6, this method would perform an effective three dimensional curve fit between the samples for each printed primary. This could substantially reduce the computation complexity and table size requirements of Levels 4 and 5 respectively.

Level 7 Reproduction

Included primarily for academic rigor, this unequivocally impractical level is nonetheless the most color-perfect. Each distinguishable printable color—counting into the millions—is printed, accurately

measured, and stuffed into a look-up table of colossal proportions. The result, even if plausible, would be dreadfully inflexible.

2.3 COLOR SPACE INTERPOLATION FOR IMAGING SYSTEMS

Reproduction levels 5 and 6 both require some form of approximation to calculate the required printer stimulus for generating colors which fall between the known points of the look-up table. These known points are refered to as *knots.* Interpolation between these knots within a color space requires three or four (depending on the number of inks and the method of black stimulus calculation) interpolations of a one-dimensional stimulus (amount of ink) calculated within three dimensions of color space.

Three facets of image color fidelity determine the approximation requirements. Individual pixel color error between any two reproductions must be less than about 6 CIELAB ΔE units. The allowable color error between the *original* and the reproduction is usually quite a bit larger and much more difficult to predict. Finally, adjacent pixels must not have spatially-systematic errors of more than about one ΔE unit. These tolerances will be studied in Chapter 6

Approximation and Interpolation

Free-form curves and surfaces play an essential role in the construction of 3D objects for synthetic (computer-generated) images. Such a curve or surface is generated from a set of points in two or three dimensions. Methods for generating a curve or surface from these points are well known [Böhm 81, Thalman 88], and can be classified into two categories: *interpolations* and *approximations.* An approximation generates a curve or surface which passes near but not necessarily through the specified anchor points. Conversely an interpolation is guaranteed to pass through them. Approximations generally have the advantage of preservation of *second-order continuity* while interpolations may have undesirable kinks. Interpolation methods include: linear interpolation, parabolic bending, m-splines, and for surfaces, Coons interpolation. Approximation methods include Bézier, B-spline, and ß-spline approximations and weighted averaging. A

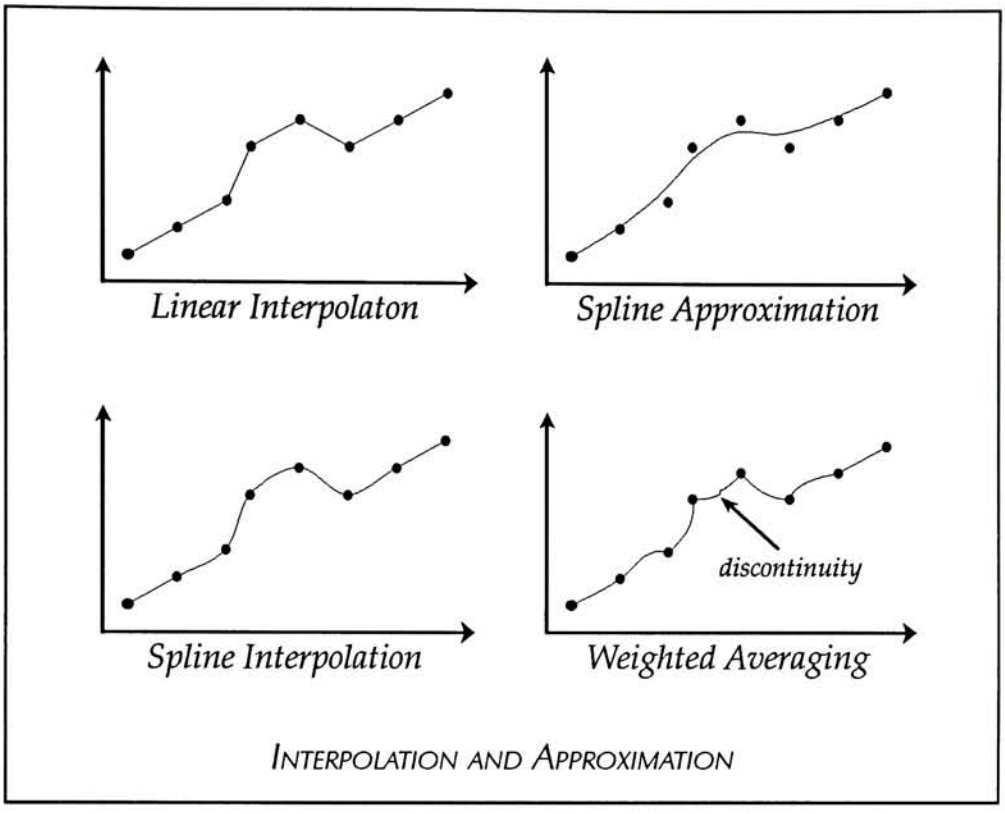

INTERPOLATION AND APPROXIMATION

comparison of these two categories as applied to two-dimensional curves is shown in the diagram on this page.

Interpolation may be generally more appropriate for color space calculation because of the measured status of the knots. The values at the knots are known matches and ought to be used as is. The advantage of differentiability found in approximation techniques probably has little impact in color fidelity and is most likely far less important than adhering to the knots. The absolute color error caused from imperfect interpolation between the knots is likely to be far more deleterious than the kinks at the knots (These topics will be an area of preliminary study for this research.)

INTERPOLATION IN FOUR DIMENSIONS

The color space problem is in four dimensions: a stimulus dimension being approximated in three color dimensions. None of the given

interpolation and approximation references address this higher dimension which is of no value for computer image synthesis. Preliminary investigation seems to indicate that anything higher order than linear interpolation is nearly formidable in four dimensions. And linear interpolation in four dimensions—*true* linear interpolation—is in itself a hurdle which has yet to be applied (and reported) to color space interpolation. Existing methods of color space interpolation, discussed in the next chapter, fall short of true linear interpolation and have several problems. One of the more serious flaws can best be illustrated with the two dimensional equivalent: weighted or *boxcar* moving averages. The fourth graph in the diagram on page 2-11 illustrates the problem. When calculating an average based on some fixed quantity of unevenly spaced nearest neighbors, the calculated average will more likely than not exhibit a discontinuity when one neighbor is exchanged for another. As one progresses through the space, adding and dropping neighbors to the averaging calculations, these discontinuities become commonplace. This can result in small but very noticable *spatially-systematic error* in the observable form of false contouring. Note also that this form of approximation accentuates the non-differentiable kinks at the knots.

The principal difficulty in generating an interpolated look-up table is the uneven (non-orthogonal) spacing of the knots when mapped into the desired color space; leading one to the use of weighted averaging (and its associated problems mentioned above). In an ordered orthogonal sample set, the in-between colors are calculated from the eight surrounding neighbor colors at the corners of the "box" containing the desired color. This is done with *trilinear interpolation* [Pugsley 75]. This method doesn't inherently exhibit the discontinuity problem of weighted averaging; however, weighted averaging is most often the method used for arriving at the orthogonally ordered sample set!

An improved method of color space interpolation in four dimensions, which may eliminate all of the problems common to the current methods, is one of the major studies in the thesis. The results of this study begin in Chapter 6.

CHAPTER 3
LITERATURE REVIEW

Several published papers address color transformation accomplished with look-up table acceleration and closed-loop feedback. These papers are individually reviewed below.

3.1 FRANK R. CLAPPER: CLOSED LOOP COLOR PREDICTION

Perhaps the earliest discussion of *closed-loop* color prediction is that of Frank R. Clapper [Clapper 1969]. Clapper's primary thrust, however, was the possibility of introducing digital computers and linear regression as a replacement for the established role of analog computers. This would allow, he asserted, the electronic graphic arts scanner to be calibrated for nearly optimum performance with any given set of reproduction conditions. With such a digital system, one could take three values corresponding to the red, green, and blue densities of the original as input, and determine the three output signals given an array of traditional potentiometer settings. The object was to collect a large number of input data sets for which the corresponding outputs are known and perform a linear regression between them—establishing a least squares fit of the scanner potentiometer settings.

Clapper's experimental verification was in the form of a painting reproduced with two differently colored sets of inks. The color gamut of the painting was judged to be reproducible with both sets of inks. The two reproductions, included in [Clapper 1969], do come quite close, though clearly not perfectly, to a visual match. A direct

observation of the achievement can be observed through close examination of the same color areas between the two reproductions. A sizable difference in dot structure can be found. Clapper's results were fairly successful. This technique, however, is of limited accuracy, especially around the periphery of the gamut.

Clapper makes no mention of the immense speed mismatch between the analog and digital implementations. This method uses a single set of complicated equations for the complete range of colors. These equations are very time consuming, especially when their complexity is increased to reduce inaccuracies. This consideration alone makes this method impractical, especially for continuous or near continuous feedback. He also makes no mention of measurement error caused by instrument metamerism and the possibility of dissimilar original versus reproduction print viewing conditions. Though Clapper suggests the use of direct closed loop feedback, he did not actually achieve such, due to his scanners inability to read reflection copy. A separate program was devised to calculate the hypothetical scanner-reflection values.

3.2 NATHANIAL KORMAN: CLOSED LOOP LOOK-UP TABLES

In 1971, Nathanial I. Korman was awarded a United States patent for a method and apparatus for closed-loop color matching using look-up tables [Korman 1971]. This patented method, more clearly described in [Korman 1972-1] can be summarized as follows:

Test prints are made on the target output process. These prints contain the 512 possible combinations of a set of eight different dot sizes for each of the cyan, magenta, and yellow inks. The dot sizes of the black separation are given by an arbitrarily chosen function of the cyan, magenta, and yellow dot sizes. This function was chosen so the black is printed only when all of the other three are present. The dot size of the other three is reduced when black is added (partial GCR). The patches are scanned with the target input device thereby generating a table of input tristimulus and correlating output excitation. This data is then inverted and interpolated to allow prediction of the needed excitation of the output process from any input tristimulus.

The approximation method used is described in [Korman 1972-2]. First, the tabular values of c,m,y dot percentages and their resulting L*a*b* values are inverted and placed in a look-up table. (Korman and Yule's paper actually predates the CIELAB color spaced definition, but they use a lightness-redness-blueness space which is similar. For discussion purposes, L*a*b* will be used). The result is a three dimensional look up table with L*, a* and b* as its address. The known c,m,y are then dispersed in an unpredictable fashion within. At this point, without explanation, Korman and Yule talk of approximately 40 orthogonally arranged c,m,y,k values at exact 10 unit spacing within the L*a*b* space. How they got to this point is a critical element in any evaluation of the integrity of their method, yet this is left unanswered. They either simply chose the best fitting points out of the 512 test patches or, at best, they might have done a weighted average of nearest neighbors. Since this step was not discussed, they probably took the simpler route. This problem is one which has plagued most published attempts at sampled look-up table reproduction.

Once they have a well-ordered table of dot percentages, they then create a sister table of "interpolation coefficients." These coefficients are simply the first order terms of the Taylor series expansion of a three-space function. For each entry in the data table, several entries are generated for the interpolation table. These are calculated directly from the surrounding entries in the data table and are simply the changes in dot percentages of each ink in each direction. A new color's cyan could then be approximated as:

$$C_{new} = C_{near} + \partial C/\partial L^*(L^*_{new} - L^*_{near}) + \partial C/\partial a^* (a^*_{new} - a^*_{near}) + \partial C/\partial b^* (b^*_{new} - b^*_{near}).$$

This approximation is done for all inks and is done for four near neighbors of the color being approximated. These four neighbors are chosen arbitrarily except that they attempt to have them enclose the color in question. These four approximations are then reduced to one; again, without explanation. They are probably simply averaged; perhaps in a weighted fashion.

This procedure has several shortcomings. Korman admits his algorithms fail near the periphery of the gamut due to the inability to find data points surrounding the unknown point. "Smoothness" of the reproduction is also a problem. Sudden jumps in color are observed. Korman states "we believe the jumps will be eliminated by an averaging method of calculating the interpolation coefficients, by reducing the interval between tabular values [i.e. larger look-up tables], and by using 128 steps instead of 64 in the tone scale" [Korman 1972-2]. No later papers exist on this subject by this author. The actual causes of these jumps are likely due, at least in part, to the arbitrary selection of surrounding points. This will be discussed in detail in Chapter 6.

3.3 PETER C. PUGSLEY: LOOK UP TABLE COLOR PREDICTION

In 1975, Peter C. Pugsley of Pinner, England was granted a US patent for a Colour Correction Image Reproducing Methods and Apparatus [Pugsley 1975]. This patent, which references Korman's 1971 patent, makes no use of closed loop feedback. Pugsley first fills a small look up table with algorithmically generated values. Then, during scanning, actual printed values are determined by an on-the-fly approximation from surrounding table values. The approximation method used is different than Korman's in two significant respects. First, the known values start out orthogonal and predictably spaced; probably through a great deal of time consuming iterations on proofed test patches and some form of weighted-average interpolation. Secondly, Pugsley uses the eight nearest neighbors forming the enclosing cube. He incorporates trilinear interpolation at this point which is less than ideal; however, most of any existing aberations would have probably occured in the prior interpolations required to achieve orthogonally placed known values. Trilinear interpolation will be discussed in greater detail in Chapter 6.

CHAPTER 4
HYPOTHESIS

4.1 INTRODUCTION

Interpolation within color space is an important component of rapid color transformation of digitized color images. A rapid transformation based on mathematical models, vector-corrected mathematical models, or interpolated gamut samples requires the speed advantages realized with look-up tables which have been pre-determined from a model and/or measurements based on the expected printing conditions. The color reproduction fidelity requirements and the interpolation methods, place a lower limit on the size of this look-up table (including any real-time sub-interpolation extension of the look-up table). Historically, these constraints have either forced sample and table sizes far too large to be practical for small and medium sized imaging systems or they have resulted in fidelity or speed compromises.

4.2 THE HYPOTHESIS STATEMENT

Traditional color space interpolation methods can be replaced with interpolation methods derived using *barycentric coordinates* in four dimensions, combined with an ordered partitioning of the color space into a *space-filling aggregation of polyhedra.* The result will be interpolations which will generate *zero color step error* for a color gradation between any two points within the printable gamut.

4.3 SUPPLEMENTAL DETAILS

This hypothesis, if verified, will provide the basis for a significant improvement over current modeling methods, moving a step closer to the previously described ideal system.

The stated hypothesis explicitly calls for *analytical* verification. No images are involved other than synthetically generated test images. Any natural images processed using these results will be strictly supplemental in nature, and are non-essential for testing the hypothesis. This hypothesis does not involve testing system-level reproduction fidelity. Color reproduction fidelity through an entire system is a function of many things—such as colorimetric integrity of scanned input—which are beyond the scope of this research.

"Zero error" as stated in the hypothesis does not include the inevitable computational artifacts such as finite numerical computation range and round-off errors. These, and other sources of error, will be studied and discussed in Chapter 6.

CHAPTER 5
METHODOLOGY

5.1 BARYCENTRIC INTERPOLATION

Verification of the hypothesis demands the derivation and procedural description of interpolation in four dimensions using *barycentric coordinates*. The derivations and associated computation implications will be formulated sequentially from the simplest two-dimensional case to the three-dimensional case, then finally to the four-dimensional conclusion. Due to the spatial nature of this problem, extensive illustrations will be generated to aid in the research process and to document the results. These will be incorporated into Chapter 6.

5.2 PARTITIONING AND SAMPLING OF THE COLOR SPACE

Optimal color space interpolation necessitates rigorous attention to two particulars. Firstly, the samples or knots should approximate a homogeneous distribution within the visual color space (which, in turn should be closely approximated by the imaging systems color space). Secondly, interpolations should be performed within *tetrahedrons.*

Sample Distribution

Initial characterization of a printer's gamut will provide the necessary information required for developing an efficient sampling scheme. This procedure will include characterization of color rate-of-change as a function of gamut location and independent variation of each of the printer's primary stimuli. Potential problems include serious perceptual non-homogeneity and gamut inflections which might, for example, generate matching colors for two dissimilar inputs. This characterization, it is hoped, will show strong useful similarities between all reflection copy ink printing technologies.

At least two processes will be fully characterized: ink-jet printing and offset lithographic printing. Additional studies of pertinent parameters will be performed on other variations.

Interpolation Hulls

The smallest number of points which can describe the vertices of a three-dimensional solid is four: an *irregular tetrahedron.* Linear interpolation will provide unique solutions at each point within this four-vertex convex hull. Using more than four points to describe an interpolation hull introduces an *overdetermined* condition. No unique solution exists for any interpolation within. In chapter 6, it is hoped, it will be shown that this is the root of a large portion of color space interpolation complications.

A substantial challenge which has hampered previous efforts in this area [Saunders 88] is the task of space-filling with polyhedra such that no interstitial spaces remain while keeping the polyhedra sizes approximately uniform and avoiding overdetermined conditions. It is hoped that this research effort will bring to fruition a new method which achieves these goals.

5.3 COMBINING MODELING AND SAMPLE INTERPOLATION

An interesting extension of the potential improvements over current methods of sampled color space interpolation is the process of combining mathematical modeling with closed-loop sample interpolation. This could provide a form of *vector-corrected* modeling which might vastly improve the practicality of mathematical models in environments where speed is critical.

This possiblity will be studied with the results being described in Chapter 8.

CHAPTER 6
RESULTS OF INTERPOLATION STUDIES

6.1 INTRODUCTION

Regardless of the means of color modeling or transformation used, fast conversion of digitized images to amounts of printed ink—where the time required for conversion is on the same order of magnitude as the time for printing—requires the use of look-up tables resident in memory. Filling these look-up tables through the use of a mathematical model is fairly straightforward once the model is determined. Filling the tables through the use of measured gamut samples, as with Level 5 fidelity (page 2-5) and higher, is a much more illusive problem which requires *interpolation* or *approximation*. In any practical implementation the size of these look-up tables is limited to well under the total number of printable colors. Furthermore, this total number of colors (See Chapter 7) is far more than is practical for a calibration test target. This fact necessitates sub-sampling of the printable gamut. A gamut sample might, for example, include only 512 colors which are printed under the target conditions and then colorimetrically measured. These color samples are spread throughout the gamut of printable colors. Though these samples may be spaced in an orderly fashion in the printers' color space (equal dot-percentage spacing, for example), when mapped into the system's color space (the space used for image color representation), they become rather unpredictably spaced (see diagram on next page) on a mesh that is not Cartesian, i.e. it has tabulated function values at

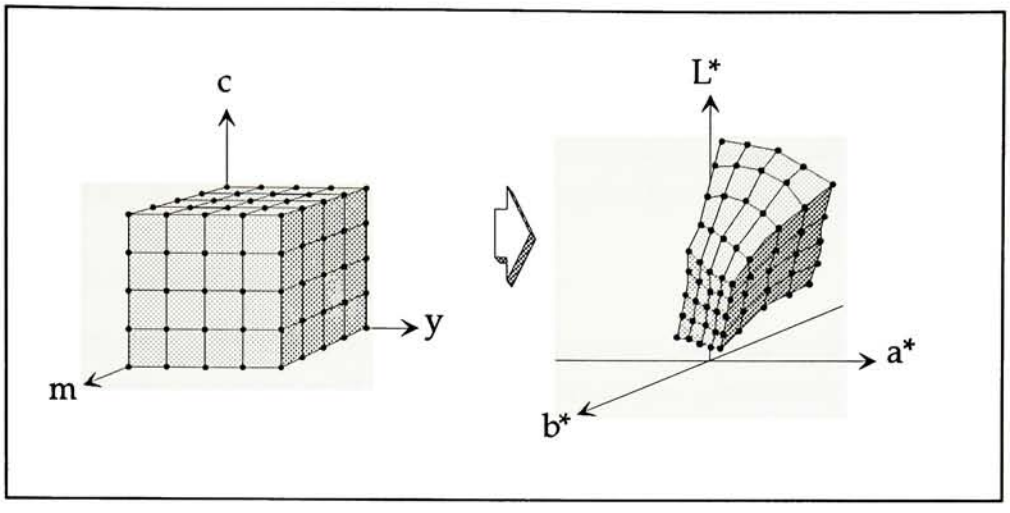

"random" points in 3-dimensional space rather than at the vertices of a rectangular array. In order to be useful, a system's color space must provide access to equally spaced orthogonal values. Each value consists of an input color (the address of the location within the table) and a matched set of printer-specific ink parameters (such as C,M,Y, and K dot percentage) required to reproduce the input color. One starts out with an orderly array in C,M,Y space which allows convertion of C,M,Y ink values to color space coordinates. This array is then inverted to allow conversion from color to C,M,Y—but this inverted array is now a disheved arrangement of values unpredictably scattered through the color space (a discussion of K, the black printer, is postponed until Chapter 8).

This chapter is a report of studies dealing with the topic of color space interpolation given these undesirably scattered samples: generating a full, well-behaved look-up table from an unpredictable mélange of known values.

6.2 INTERPOLATION AND APPROXIMATION REQUIREMENTS

Determining a value associated with a point in space based on known values at other near-by points requires some form of interpolation or approximation—and inevitably results in some amount of error when compared with the *correct* value for that point. The

sensitivity of the system to that error of course is dependent upon what the system is used for. In the case of interpolating color space for printed images this tolerance for error must be carefully understood prior to any investigation of interpolation or approximation alternatives since they can directly impact image fidelity.

Color Error Tolerance and Error Types

From this study, three important aspects of color tolerance in image reproduction have surfaced: (1) constant (or gradually changing) color error. (2) systematically arranged step color error, and (3) non-differentiable boundaries in color error (where the rate of change of color error suddenly increases or decreases). The first two considerations were allude to briefly in §2.1.

Type 1: Constant or gradually changing error is the most common and typically the largest constituent of color error in a reproduction. This is where, for example, skin is too blue or a tomato is orange. Detail is not altered by this type of color error. The error is either constant (a color cast) or changes in concert with the image color detail. The color error has no spatial frequency content higher than that of the image area where it exists and the error gradation, if any, is *in phase* with the image color detail. Tolerance for this type of error is a complex function of image content and viewing conditions but in general it is quite large, especially when the original is not available for comparison. Color television, color photography, and color printing all typically have relatively large (much greater than just-noticeable) Type 1 error when compared to their respective original scenes. The cognitive aspects of human vision make putting limits on acceptable levels of Type 1 error a formidable task. Fortunately there are useful simplifications.

Type 1 error can conveniently be classified in two sub-types: (a) error between any two reproductions (color difference) and, (b) error between the original scene and the reproduction. The tolerance for the first sub-type is usually much tighter than the second. A recent study suggests that not greater than six CIELAB color difference units as an acceptable range for variation among offset

lithographic reproductions [Stamm 81]. Other conditions, such as corporate logotype color tolerances, can be even more demanding. When considering tolerances for the second sub-type (b) one can refer to the many studies on this and related subjects (See the section *Colorimetry and Color Science in the Graphic Arts* in APPENDIX A, the ANNOTATED BIBLIOGRAPHY). Useful information can also be obtained from evaluations of successful reproduction systems such as color TV [Rzeszewski 83] and color copiers. A recently introduced color copier from Canon has become quite successful and well regarded. A colorimetric evaluation of this copier operated by an experienced technician (at the Rochester Institute of Technology Media Services department in the Wallace Memorial Library) has shown color errors with process ink originals to be an average of over 15 and as high as 30 CIELAB color difference units on an "excellent" copy. The complete set of data for this Canon copier evaluation and further discussion is included in APPENDIX E.

Type 2: Systematically arranged step error is a condition unique to digital imaging systems and is distinguishable by its characteristic *false contouring*—an effect similar to *posterization* in the graphic arts. A common cause of Type 2 error in inexpensive PC-based equipment is an inadequate number of gray levels somewhere within the image reproduction process. More expensive digital imaging and proofing systems usually incorporate at least the minimum number of levels required for good image fidelity [Johnson 88]. Another frequent cause of Type 2 error is interpolation artifacts resulting from inferior multidimensional interpolation schemes. This problem occurs in a broad range of digital imaging systems including some graphic arts scanners and is expensive to minimize [Korman 72-1, 73]. This thesis, and specifically this chapter, introduces an inexpensive method for eliminating this and other significant problems relating to color modeling.

Tolerance for Type 2 error is very low. Just-noticeable false contouring is objectionable, suggesting that the tolerance is less than one just-noticeable difference. A CIELAB color difference unit can be used as an estimate of just-noticeable differences. However, it has been shown that just-noticeable differences can range from 0.5 to 5 difference units for a population of normal observers [Berns 88].

Type 3: Non-differentiable boundaries of color error result from some interpolation and approximation techniques as mentioned in §2.3. This error is caused by the lack of smoothness and optimum curvature in the interpolated values. Multidimensional interpolation which is free from first derivative discontinuities (not to mention higher derivatives) is difficult to implement when dealing in two input dimensions [Thalman 87] and nearly formidable with three. Before expending a large amount of effort on minimizing this error type, it would be desireable to evaluate its impact on image fidelity. A test image was devised which exhibits ranges of Type 1 and Type 3 color error from zero to very large. These images and discussion of their design and use is included as APPENDIX D. The results of this test show one important fact: Type 3 error can be very large before it is noticeable—so large, that the Type 1 tolerance limits will almost certainly prevent its noticeable appearance. This has tremendous implications for color space interpolation as will be discussed later in this chapter.

6.3 MULTIDIMENSIONAL INTERPOLATION AND APPROXIMATION

Most books on numerical methods examine the topic of interpolation and approximation. Few, however, give much space to the multidimensional case. Often, a statement is included such as "for multiple dimensions, each dimension can be interpolated separately as above." Although this can be done, it will most often result in discontinuities in the interpolated function. This author found no references (out of at least two dozen books on numerical methods) that addressed the situation of non-Cartesian knots: known points with irregular distribution within the n-dimensional space.

In multidimensional interpolation, we seek an estimate of some function or process through the use of an n-dimensional grid of tabulated locations within the function or process where each tabulation has an associated one-dimensional scaler representing the function or process value. When these values are on a Cartesian mesh the methods of bilinear or trilinear interpolation are often used.

Bi- and Trilinear Interpolation

Bi- and trilinear interpolation rely on the concept of a *grid square* and *grid cube*, respectively, where all the tabulated points lie on the vertices of the grid. The formula for bilinear interpolation is

$$f(x, y) = (1 - t)(1 - u)f_1 + t(1 - u)f_2 + u(1 - t)f_3 + tuf_4$$

where $f(x, y)$ is the interpolated point surrounded by the rectangle of four points: f_1 and f_3 on the low-x edge and f_1 and f_2 on the low-y. and the factors t and u are the fractional distances (ranging from 0 to 1) which the point falls into the interior of the square along the x and y axes. For example, if the rectangle ranges in the x-dimension from $x=1$ to $x=2$ and the interpolated point is ¾ of the way in on the x-dimension then $t=0.75$. The three dimensional equivalent – trilinear interpolation – is a natural extension to the common bilinear case

$$\begin{aligned} f(x, y, z) = {} & (1 - t)(1 - u)(1 - v)f_1 \\ & + t(1 - u)(1 - v)f_2 \\ & + u(1 - t)(1 - v)f_3 \\ & + v(1 - t)(1 - u)f_4 \\ & + tu(1 - v)f_5 \\ & + tv(1 - u)f_6 \\ & + uv(1 - t)f_7 \\ & + tuvf_8 \end{aligned}$$

where $f(x, y, z)$ is the interpolated point in space surrounded by a hexahedron delineated by eight vertices: f_i for $i=1$ to 8. One might notice the distinct similarity to the Neugebauer equations which are, in fact, trilinear interpolations.

The n-linear method has several important characteristics. First, as mentioned before, it requires well ordered knots – and is thus not usable for the first interpolation of the gamut samples mapped into a colorimetric space. Second, n-linear methods are frequently only "close enough for government work" as one text put it. As the inter-

polating point wanders from grid to grid the interpolated function changes continuously, adapting to the over-determined situation in an orderly, but not truly linear, fashion. However – this is the third characteristic – the *gradient* of the interpolated function changes discontinuously at the boundaries of each grid – that is, the boundaries are non-differentiable. These characteristics make trilinear interpolation, which is just varient of averaging, useful for *sub-interpolation* at the final stages of the color prediction process, but less useful as a total solution without resorting to a large gamut sample size.

Moving Average Interpolation and Approximation

Most existing color space interpolation schemes (and as far as this author is aware, *all* published schemes) use some form of moving average as a technique for handling the randomly spaced knots problem. For every interpolation, an algorithm is used to locate several surrounding knots and perform a weighted average to determine an approximate value. This method can take the form of either interpolation or approximation (§2.3).

The single most substantial problem with using this method in color space is the unavoidable Type 2 errors from function discontinuities. Consider, for example, an algorithm that locates the six nearest neighbors for interpolation. A color gradation from color ***A*** to color ***B*** (where color ***B*** is not near-by) would start out using an initial set of six knots. At some point, as the interpolated color progresses from ***A*** to ***B***, one of the initial six knots will no longer be one of the *closest six*. It will consequently be dropped and supplanted with a new near-by knot. There is no reason why the contribution of the dropped knot will be exactly equal to that of the new knot – a step change in the function is therefore inevitable. The only means of reducing the problem is through increasing the number of knots.

True Linear Interpolation: Barycentric

For color space interpolation, n-linear methods have one prominent failing: they cannot operate with disordered knots. A secondary weakness is their inexactness: they provide true linear interpolation

only for a select set of functions. Bilinear interpolation, for example, is exact only for functions of the form $u(x, y) = a + bx + cy + dxy$. To overcome these shortcomings, a method of interpolation used in *finite-element analysis* will be considered.

Recently the method of finite-element analysis has become widespread for solving problems in continuum mechanics. This method entails segmenting a plane into an aggregation of irregular triangles. Associated with each triangle vertex is a one-dimensional function value (e.g. mechanical stress). A formula can be applied to a point within any triangle using the three surrounding function values to effect a *linear interpolation* of the function. Unlike the overdetermined methods described above, this method uses only three points: the minimum to describe a plane. These points are used to calculate a weighting factor for each corner. These factors are the *barycentric coordinates* of the point being interpolated. The physical significance is illustrated in the diagram below showing a triangular see-saw. The fulcrum corresponds to the point being interpolated and the weights – adjusted to provide perfect balance – are proportional to the contribution of the function value at the associated corner. The larger the weight, the greater is that corner's contribution the the interpolation. When balanced, the fulcrum lies at the *center-of-mass* of the combined weights – hence, the term *bary-* (mass) *-centric* (center). This method, used for linear interpolation in triangular grids, will be extended to *space-filling tetrahedral aggregations* in the following sections of this chapter.

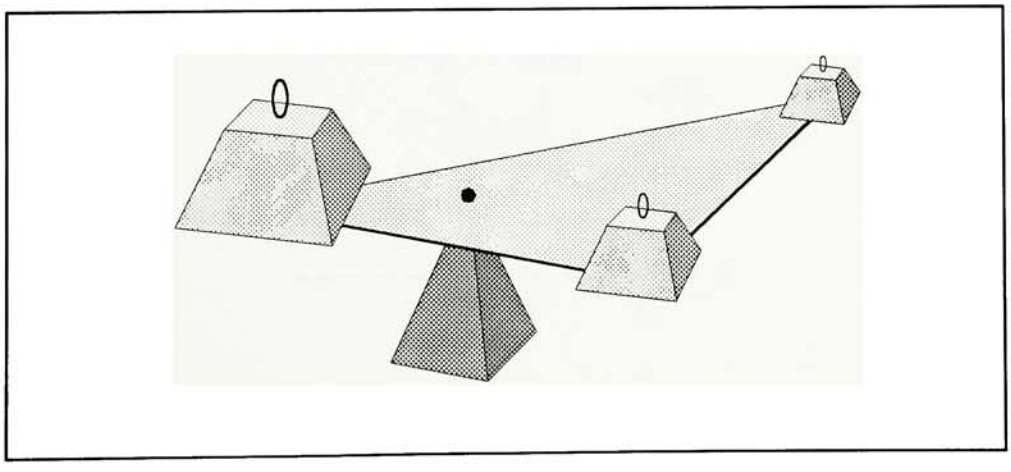

6.4 DERIVATION OF BARYCENTRIC INTERPOLATION

ONE DIMENSION: (1D INTERPOLATION IN 2-SPACE)

Let $P_i = (x_i)$, $i = 1, 2$, be the vertices of a line segment L. Then any point $P=(x)$ in the line can be uniquely expressed by the equation

$$P = \theta_1 P_1 + \theta_2 P_2 \qquad \text{where } \theta_1 + \theta_2 = 1.$$

In fact, the θ_i, which are called *barycentric coordinates* of P, are determined from the following set of equations:

$$\begin{aligned} \theta_1 x_1 + \theta_2 x_2 &= x, \\ \theta_1 + \theta_2 &= 1. \end{aligned}$$

The interior of the line is characterized by the inequalities

$$\theta_i > 0, \qquad i = 1, 2.$$

When defined as above, P is the center of mass (centroid) of the two masses θ_1 and θ_2 located at the vertices of the line (at P_1 and P_2). If u is a *linear function* of P then it follows that

$$u(P) = \theta_1 u(P_1) + \theta_2 u(P_2)$$

This and the above set of two equations are solved for *linear interpolation* in the straight line.

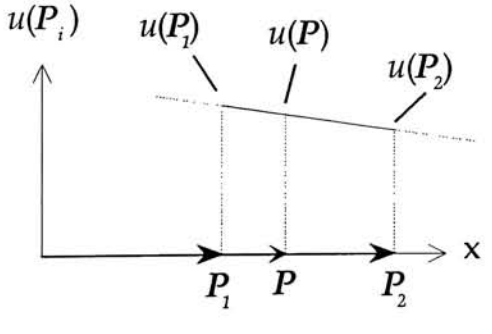

1D BARYCENTRIC INTERPOLATION

Two Dimensions: 2D interpolation in 3-space

Let $P_i=(x_i, y_i)$, $i=1,2,3$, be the vertices of a triangle T. Then any point $P=(x, y)$ in the plane can be uniquely expressed by the vector equation

$$P = \theta_1 P_1 + \theta_2 P_2 + \theta_3 P_3 \qquad \text{where } \theta_1 + \theta_2 + \theta_3 = 1.$$

Again, the θ_i are the *barycentric coordinates* of P, and are determined from the following set of equations:

$$\begin{aligned} \theta_1 x_1 + \theta_2 x_2 + \theta_3 x_3 &= x, \\ \theta_1 y_1 + \theta_2 y_2 + \theta_3 y_3 &= y, \\ \theta_1 + \theta_2 + \theta_3 &= 1. \end{aligned}$$

The interior of the triangle is characterized by the inequalities

$$\theta_i > 0, \qquad i = 1, 2, 3.$$

P is the center of mass (centroid) of the three masses θ_1, θ_2 and θ_3 located at the vertices of the triangle (at P_1, P_2 and P_3). If u is a *linear function* of P then it follows that

$$u(P) = \theta_1 u(P_1) + \theta_2 u(P_2) + \theta_3 u(P_3)$$

This and the above set of three equations are solved for for *linear interpolation* within *triangular planes*. $\theta_1 = 0$ is the equation for side P_2P_3 and similarly for the other sides.

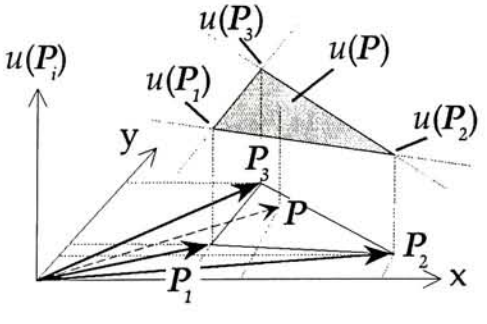

2D Barycentric Interpolation

THREE DIMENSIONS: 3D INTERPOLATION IN 4-SPACE

Let $P_i=(x_i, y_i, z_i)$, $i=1,2,3,4$, be the vertices of a tetrahedron T. Then any point $P=(x, y, z)$ in space can be uniquely expressed by the vector equation

$$P = \theta_1 P_1 + \theta_2 P_2 + \theta_3 P_3 + \theta_4 P_4 \quad \text{where } \theta_1 + \theta_2 + \theta_3 + \theta_4 = 1.$$

Once again, the θ_i are the *barycentric coordinates* of P, and are determined from the following set of equations:

$$\begin{aligned}
\theta_1 x_1 + \theta_2 x_2 + \theta_3 x_3 + \theta_4 x_4 &= x, \\
\theta_1 y_1 + \theta_2 y_2 + \theta_3 y_3 + \theta_4 y_4 &= y, \\
\theta_1 z_1 + \theta_2 z_2 + \theta_3 z_3 + \theta_4 z_4 &= z, \\
\theta_1 + \theta_2 + \theta_3 + \theta_4 &= 1.
\end{aligned}$$

The interior of the tetrahedron is characterized by the inequalities

$$\theta_i > 0, \quad i = 1, 2, 3, 4.$$

P is the center of mass (centroid) of the four masses θ_1, θ_2, θ_3 and θ_4 located at the vertices of the tetrahedron (at P_1, P_2, P_3 and P_4). If u is a *linear function* of P then it follows that

$$u(P) = \theta_1 u(P_1) + \theta_2 u(P_2) + \theta_3 u(P_3) + \theta_4 u(P_4).$$

This and the above set of four equations are solved for *linear interpolation* within *tetrahedral solids*. $\theta_1 = 0$ is the equation for plane $P_2P_3P_4$ and similarly for the other planes.

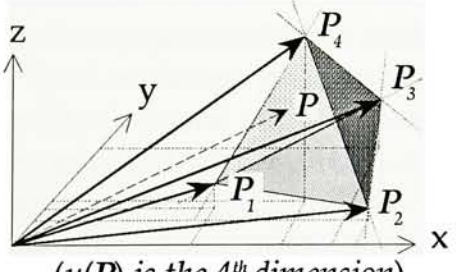

($u(P_i)$ *is the* 4^{th} *dimension*)

3D BARYCENTRIC INTERPOLATION

6.5 SPACE-FILLING WITH IRREGULAR TETRAHEDRA

In §6.3 it was shown that true linear interpolation of a scaler quantity within color space (or any 3D space) requires that the knots, the known (measured) scaler values, be grouped into quadruples to form tetrahedrons. In §6.4 a method for linear interpolation with these tetrahedrons – the method of barycentric coordinates – was derived. This section will now address the task of *space-filling* with these interpolated tetrahedrons.

Geometric Considerations & Requirements

In order to implement barycentric interpolation within a color space containing a cluster of knots, three conditions must be met during the process of segmenting the knots into tetrahedra.

(1) The aggregation of tetrahedra must be space-filling. In order to provide interpolation at any point within the space representing the printable gamut, each point must be contained within one, and only one, tetrahedron or on the boundary between two tetrahedra. There must be no interstitial spaces between tetrahedra.

(2) All interfaces between tetrahedra must be oppositely congruent. This provision, which can be violated without violating provision (1), insures polyhedra packing such that their faces, edges, and vertices make contact with oppositely congruent counterparts of adjacent polyhedra. The interface between two tetrahedra making contact over some positive area (as opposed to tetrahedra making contact through common vertices or edges) is a pair of oppositely congruent, triangular faces.

(3) Deviations from the regular tetrahedron must be limited. A regular tetrahedron, one of the five *platonic polyhedra*, contains edges, faces and dihedral angles (the internal angle formed by two faces that meet along a common edge) which are all equal. Extensive deviation from this nominal shape will inflict degradation in the interpolation accuracy. Given these restrictions, methods of polyhedra aggregation will now be investigated.

Crystal-Growing Aggregation

Keep in mind that the interpolation knots (three dimensions of color and one dimension of printed primary – usually dot percentage) are dispersed in an unpredictable (but hopefully not a wildly non-homogeneous – see Chapter 7) fashion within the color space. The smallest convex polyhedron containing *all* of the knots is a close approximation of the size and shape of the printable gamut. This large polyhedron must be partitioned into space-filling tetrahedra while accommodating the Three Conditions outlined above. This provides an aggregation of tetrahedra for interpolation, with linear functions throughout the interior of each tetrahedron and with continuity being preserved at the boundaries.

To begin the process, four neighboring knots in the center of the gamut are chosen as the vertices of a tetrahedron which serves as the nucleus of the aggregation. Succeeding tetrahedra are formed by combining a nearby knot with three knots of an existing tetrahedron thereby affixing it to the "growing crystal." The two-dimensional equivalent of this process – a plane-filling aggregation of triangles – is shown in the diagram below. Two problems which arise in space-filling can be illustrated in the 2D example. First, there are multiple ways to partition the plane – picking a nucleus triangle (tetrahedron) does not cause an immediate crystallization of re-

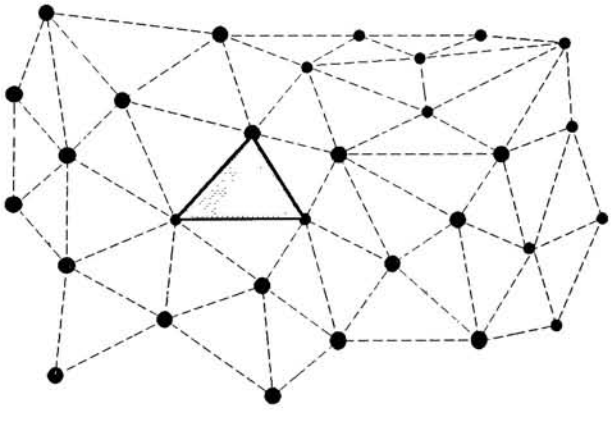

2D Crystal-Growing Aggregation

maining triangles (tetrahedra) to occur. For example, pick any four neighboring knots in the plane which define an irregular four-sided polygon. This polygon can then be partitioned into two triangles in two separate ways. This is shown—along with the third dimension being interpolated—in the diagram below. It is obvious that these interpolation triangles must be used in matched pairs. Performing an interpolation between two points within the four-sided polygon using a triangle from one pair for the first part of the interpolated function and a triangle from the other pair for the last part of the function will clearly cause a step discontinuity in the result. As an aside, this diagram also clearly illustrates the fact that four points form an over-determined system for linear interpolation in two dimensions, just as eight points give an overdetermined system in 3D. So now there must be some intelligence interjected into the process: picking the best of the available options for partitioning.

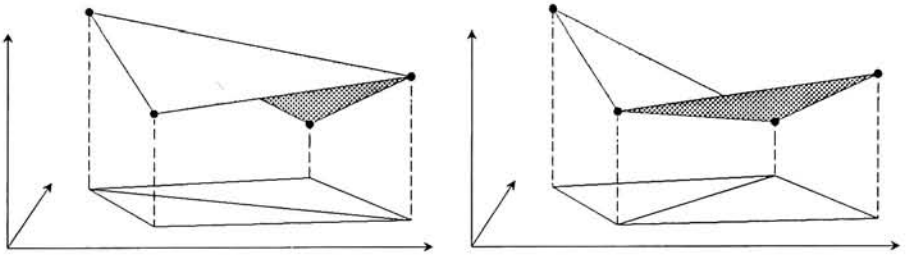

2D Linear Interpolation in a 4-Sided Polygon

A second somewhat related problem is that of *creeping distortion.* As triangles (tetrahedra) are added to the growing crystal, they may be forced into unacceptably oblong shapes. This process is beginning in the upper right corner of the triangle aggregation illustrated on page 613. Clearly, this must be monitored and circumvented when excessive. This task is quite onerous especially in the case of tetrahedral space-filling. Algorithms for the three dimensional search-

ing needed for evaluating the alternative growth paths are quite complex and akin to solving a 3D maze. These algorithms must be capable of multiple levels of backtracking. For example, an aggregation might be half done only to find out that one of the first few tetrahedra to be added (and all succeeding tetrahedra) would have to be changed to ameliorate a growing distortion problem which became unacceptable many tetrahedra later.

A figure of merit relating to shape distortion (or more correctly: interpolation accuracy degradation *caused by* shape distortion) must be formulated. Of course, optimal interpolation hulls would be regular polygons or polyhedra. The degradation of interpolation accuracy occurs in an exponential manner exhibiting significant amounts only after fairly large deviation from the nominal hull shape. Error analysis, discussed in §6.8, can be used to arrive at an equitable threshold criteria for distortion. The figure of merit might be, in the case of triangles, a check of angle sizes: whenever any two angles both become close to 0° or both close to 90° an elongated triangle exists. For tetrahedra, the same condition would apply to any *three* dihedral angles (the nominal dihedral angle is $2\sin\sqrt{3}/3 = 70°31'44"$). This suggests a conceptually fairly simple test. Another possibility, again for the case of triangles, could be the calculation of area normalized by the dimension of the longest edge of the bounding Cartesian rectangle. For tetrahedra, the *volume* would be normalized by the largest edge of the bounding *box*. Tetrahedral volume is easily calculated using matrix algebra. In some cases of poor sample homogeneity it may be advantageous to drop or add some samples to improve distortion growth problems.

After extended consideration this author has come to the conclusion that the algorithms needing for this method of aggregation are beyond the scope of this research effort. This apparent impasse was overcome with the innovation of a radically different method of aggregation.

PARTITIONED-CUBE AGGREGATION

The printable gamut of a printing process, often represented as a cube in dot-percentage space, is distorted when mapped into another color space. Although the degree of distortion is a function of the new color space, generally it is not more severe than a two- or three-to-one ratio of the resulting longest and shortest edges of the cube (See Chapter 7 for extensive data and discussion on gamut shape in CIELAB space). This information can be used to justify an alternate gamut partitioning technique. The original gamut cube can be thought of as an aggregation of sub-cubes delineated by the sampled slices through the gamut cube (neither the aggregate cube nor the sub-cubes need have all three dimensions equal. That is, the cubes can be right-angled hexahedra with three pairs of unequal faces). When the gamut is mapped into another color space, these sub-cubes all become distorted along with the cube—but they remain as a contiguous space-filling aggregation of (now irregular) hexahedra. If these sub-cubes, then, can be further partitioned into tetrahedra without violating—anywhere within the gamut—the Three Conditions of space-filling, the task will be consummated.

A systematic investigation of cube partitioning into tetrahedra has shown four general modes (a complete analysis and proof is included in APPENDIX B). Three of these modes are shown in the diagram on the next page.

All three modes shown are space-filling as required by the first of the Three Conditions and only eight knots, the eight corners of the cube, are used as tetrahedral vertices.

The first mode yields five tetrahedra: one regular tetrahedron and four right-angled tetrahedra. Within the cube these tetrahedra meet Condition 2 with shared interfaces. When several copies of the cube are stacked, this condition is violated unless the cubes are appropriately rotated. The first diagram on page 6-18 illustrates the minimum cluster of mode A cubes with the required symmetry for stacking side-by-side and directly above and below each other. This cluster can be reduced by half if assembled with each layer being offset by one cube.

PARTITIONING THE HEXAHEDRON

MODE A: FIVE TETRAHEDRA

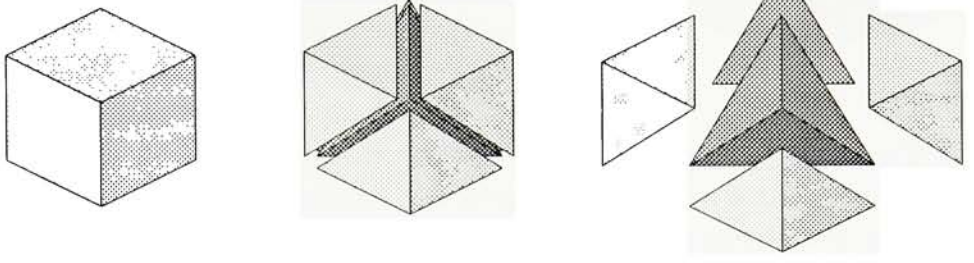

MODE B: SIX TETRAHEDRA

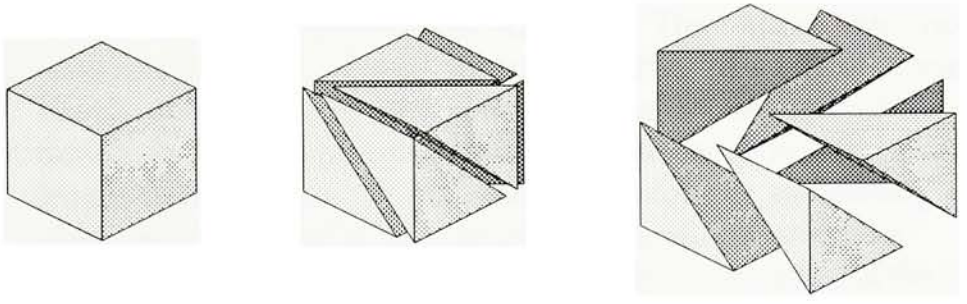

MODE C: SIX TETRAHEDRA

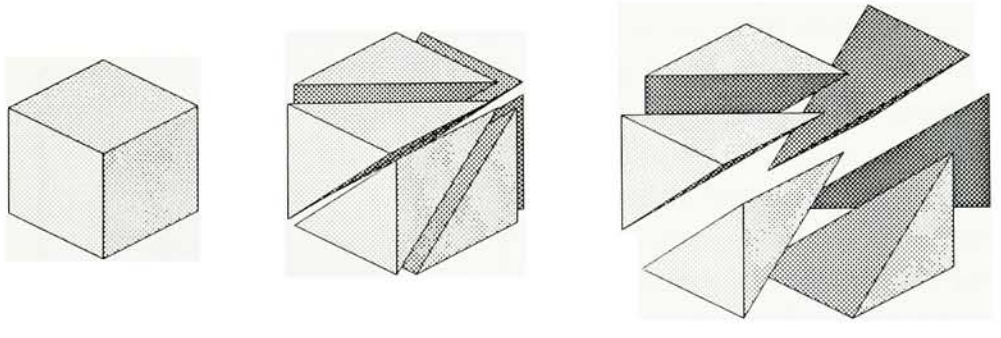

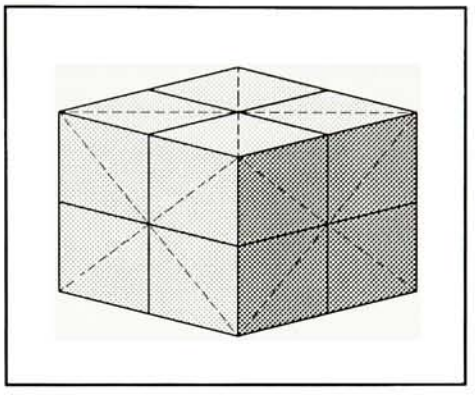

The central tetrahedron in the mode A cube is twice the volume of the remaining four. This two-to-one size difference is exacerbated by the distortion of the gamut which contributes another factor of about two- or three-to-one to size distortion. A size range of six-to-one, though not egregious from the interpolation perspective, is certainly worse than hoped for and is improved in modes B and C.

Both modes B and C are constructed with a single tetrahedron and its mirror image leading to the improvement over mode A: no size difference. Mode B includes a family of variations of which, strictly speaking, Mode C is one. Careful inspection of Mode B will reveal an infraction of Condition Two: Observe the two tetrahedra which share the top face of the cube. They share two, not the required three, vertices. The lower vertex of each of these two tetrahedra fall in opposite corners of the bottom face of the cube. Such an arrangement would lead to step errors at this interface in the interpolated function. This mode also requires assembling a specially oriented cluster prior to three dimensional stacking.

Mode C as mentioned above is actually one member of the family of cubes formed with this prototype tetrahedron. This mode is clearly the best of all possible cube dissections. *All of the Three Conditions are securely achieved.* The inherent symmetry also allows direct stacking: opposing faces of the cube contain matching diagonals, leading to simpler procedures for sequencing through the interpolation of the gamut. This symmetry is achieved by slicing the cube in half on three planes placed at 60° intervals pivoting along an internal diagonal of the cube (See diagram this page). The diagram shows the top view of a cube sitting on end

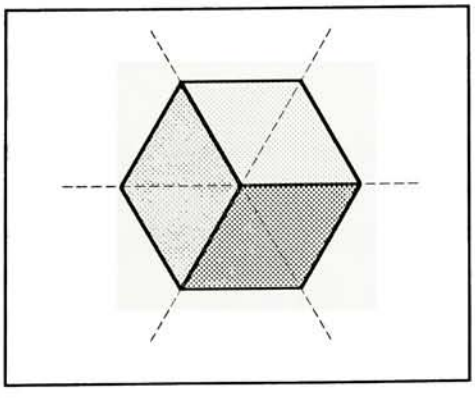

such that the diagonal is projected as a point and the dashed lines delineate triangular projections of the six tetrahedra. A fourth mode (found in APPENDIX B) also satisfies the Three Conditions but contains three different tetrahdron shapes in each cube. This is not really a problem, but Mode C is preferable.

6.6 NUMERICAL METHODS FOR BARYCENTRIC INTERPOLATION

Using the results described in the previous sections of this chapter, especially §6.4 and §6.5, color space interpolation has been reduced to an ordered interpolation of a space-filling aggregation of irregular tetrahedra. All addressable points within each tetrahedron are calculated using the methods of barycentric interpolation derived in Section 6.5. These tetrahedron interpolations dictate three primary tasks: Finding which points from the color space (a lattice of Cartesian points equally spaced according to a pre-determined color resolution) are contained within the tetrahedron being interpolated; and, for each point, solving a set of equations to determine its unique set of four barycentric coordinates; then finally applying these coordinates toward the calculation of the interpolated primaries. One method of addressing the first task borrows from the results of the second task which will consequently be discussed first.

Solving a Linear System

For each point in the three dimensions of color space for which a fourth dimension (printed ink) must be interpolated, a linear system of equations must be solved. This system, derived in §6.5, is expressed by the vector equation

$$P = \theta_1 P_1 + \theta_2 P_2 + \theta_3 P_3 + \theta_4 P_4$$

with only three of the four barycentric coordinates being independent. Then any point $P_i=(x, y, z)$ in space can be uniquely expressed by the equation

$$P = \theta_1 P_1 + \theta_2 P_2 + \theta_3 P_3 + (1 - \theta_1 - \theta_2 - \theta_3) P_4.$$

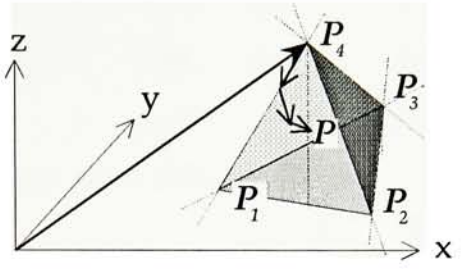

Rearranging the terms this becomes

$$P = P_4 + \theta_1(P_1 - P_4) + \theta_2(P_2 - P_4) + \theta_3(P_3 - P_4).$$

In this form the equation has an interesting physical significance. The point being interpolated, represented by the three-dimensional vector P, can be envisioned as the head-to-tail concatenation of four vectors (see above diagram): The first one, P_4, traverses from the origin to the surface of the tetrahedron; the second, a fraction of $(P_1 - P_4)$, to move part way along the P_1P_4 edge; the third, a fraction of $(P_2 - P_4)$, to traverse part way into the center of the $P_1P_2P_4$ triangular face; and finally the fourth vector, $(P_3 - P_4)$, for the trip into the volume of the tetrahedron to point P.

Replacing the fourth barycentric coordinate with a function of the first three, the linear system becomes

$$\begin{aligned}
\theta_1x_1 + \theta_2x_2 + \theta_3x_3 + (1-\theta_1-\theta_2-\theta_3)x_4 &= x,\\
\theta_1y_1 + \theta_2y_2 + \theta_3y_3 + (1-\theta_1-\theta_2-\theta_3)y_4 &= y,\\
\theta_1z_1 + \theta_2z_2 + \theta_3z_3 + (1-\theta_1-\theta_2-\theta_3)z_4 &= z.
\end{aligned}$$

The color space coordinate for which an interpolation is being calculated is (x, y, z). The vertices of the tetrahedron undergoing interpolation are (x_i, y_i, z_i), for $i = 1, 2, 3, 4$. The unknown barycentric coordinates are θ_i for $i = 1, 2, 3$, and $(1 - \theta_1 - \theta_2 - \theta_3)$.

Rearranging and collecting like terms this system becomes

$$\begin{aligned}
\theta_1(x_1 - x_4) &+ \theta_2(x_2 - x_4) + \theta_3(x_3 - x_4) + x_4 = x,\\
\theta_1(y_1 - y_4) &+ \theta_2(y_2 - y_4) + \theta_3(y_3 - y_4) + y_4 = y,\\
\theta_1(z_1 - z_4) &+ \theta_2(z_2 - z_4) + \theta_3(z_3 - z_4) + z_4 = z.
\end{aligned}$$

Represented in matrix form this becomes

$$\begin{bmatrix} (x_1 - x_4) & (x_2 - x_4) & (x_3 - x_4) \\ (y_1 - y_4) & (y_2 - y_4) & (y_3 - y_4) \\ (z_1 - z_4) & (z_2 - z_4) & (z_3 - z_4) \end{bmatrix} \begin{bmatrix} \theta_1 \\ \theta_2 \\ \theta_3 \end{bmatrix} = \begin{bmatrix} (x - x_4) \\ (y - y_4) \\ (z - z_4) \end{bmatrix}$$

The *explicit determinant formulas* for the inverse matrix and for the solution of a linear system of equations is known as *Cramer's Rule.* This method is very uneconomical in numerical calculations with the exception of 2×2 and 3×3 matrices and some matrices with very special structure. Larger matrices are much more efficiently handled with techniques such as *Gaussian Elimination* and *LU-Decomposition.* The task of interpolation with four barycentric coordinates entails solution of a 3×3 system, hense Cramer's rule will be used.

Cramer's rule can be stated as follows [Schneider 82]: Let A be a nonsingular $n \times n$ matrix and let b be a vector in R^n. Then the components of the unique solution $x = (x_1, x_2, \ldots, x_n)$ of $Ax = b$ are

$$x_i = \frac{\det A_i}{\det A}, \quad i = 1, 2, \ldots, n,$$

where A_i is the matrix obtained by replacing the ith column of A by b. The determinant of a 3×3 matrix can be computed as follows

$$\det \begin{bmatrix} a & b & c \\ d & e & f \\ g & h & i \end{bmatrix} = aei + bfg + cdh - gec - hfa - idb.$$

Using these formulae, an equation for each barycentric coordinate can be implemented.

Finding Points Within the Tetrahedron

Each tetrahedron within the aggregation possesses a unique quadruplet of color space coordinates which delineate a convex hull. Interpolation within the convex hull of the tetrahedron requires the identification of interior color space coordinates for which the interpolated fourth dimension (in this case usually an amount of ink) is desired. That is, to interpolate within the hull, one must first identify which points of the orthogonal lattice lie on or within the hull.

Given a coordinate C in color space, and a tetrahedron T in the same color space defined by four vertices t_i for $i=1,2,3,4$, a test can be designed to determine if C either (a) falls outside of or (b) falls on or within the convex hull bounded by T.

One such test results as a direct outgrowth of the calculation of the barycentric coordinates associated with C. This is simply the test for non-negative barycentric coordinates:

$$\theta_i > 0 \qquad i = 1, 2, 3, 4.$$

Any negative coordinate indicates a point outside of the hull. This test requires heavy computation, however, and is a sort of "wasted calculation" whenever the test fails.

Several optimizations are possible. First, a rectangular box can be placed in alignment with the color space axes and around the hull such that it is as small as possible while still completely enclosing the hull. The tested points can then be immediately limited to the volume of the box. (See the diagram on next page). Yet this box still contains, on average, six times the volume of the tetrahedral hull. Testing each point would then still require quite a large overhead of calculation. This overhead may not be of much concern since this interpolation process need occur only once for each change in printing conditions (paper, process or ink change).

The quantity of tested points can be further reduced through procedural optimization. A simple improvement will be realized by this simple procedure: Proceed through the box always in one direction along one axis (e.g. from min to max L* or RED) with the other two axes remaining constant. Test until within the hull; interpolate

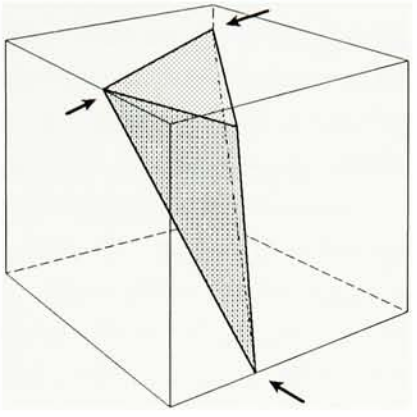

Arrows indicate points of contact.

SMALLEST BOX ENCLOSING A TETRAHEDRON

until the edge of the hull; then stop. The remaining points along that particular path are known, without testing, to be outside the hull since the hull is convex. This simple improvement will yield, when applied to all axes, a reduction of the worst case overhead of out-of-hull tests from 500% to 250% above optimum and the average to less than half that – much less than half if R,G,B space is used rather than L*a*b* since the printed gamut "cube" is more closely aligned with the axes. This alignment leads to tetrahedrons which come closer to fitting into the corners of the interpolation box. As the tetrahedron approaches a perfect fit within the box (similar to those shown on page 6-10) the wasted testing approaches zero.

This procedure for finding the points within a tetrahedron can be described as a state diagram and is included, with illustrations and additional text, as APPENDIX C.

An alternative method for finding the points falling within the tetrahedron follows. An extensive equation could be used to describe the volume given the four vertices. This equation could then be applied, using the limits of the bounding box described above, to determine the range of in-volume values. For example, if an x and y

value (which fall within the bounding box) are inserted into this equation, it would produce the range of z values, if any, which fall within the tetrahedron. This method would still involve trial-and-error searching; but only in two dimensions. The equation required is quite complex and additional study would be necessary to determine if this method would allow any practical improvement. Since this task is a once-per-calibration procedure, the time difference between these two methods may well be insignificant.

When performing these point-locating procedures, it is important that for each tetrahedron all points in the volume *and on the surface* be included. This will introduce the possibility, exaccerbated by inevitable computation error (see next section) of interpolating some boundary points twice. Once for each of the two bounding tetrahedra. This will produce insignificant increases in calculation time; but no objectionable interpolation artifacts.

Interpolation of the Printable Gamut

For each interpolated point in color space, four barycentric coordinates are calculated. The coordinates are used for interpolation of the printers primaries as outlined in §6.4. Each tetrahedron has associated with each of its four vertices the color space coordinates of the vertex—used for barycentric calculations—as well as a value for each printed primary. These values represent a relative amount of ink coverage or density. For each interpolated point, all of the primaries—usually cyan, magenta, yellow, and possibly black—are interpolated from their respective vertex values. Each color is interpolated using *the same quadruplet of barycentric coordinates.*

Once the entire color space is interpolated, the gamut is in the form of evenly spaced orthogonal values throughout the volume of printable colors. The color difference between any two adjacent colors must less than a just-noticeable difference to provide adequate gray level resolution thereby preventing false contouring.

From the data introduced in Chapter 7 it will be shown that this can require as much as 1.6 million color space locations (with the low end being far less. See discussion in §7.4). Each location will typically require 4 bytes of storage, one for each primary. This brings the memory requirements to 6.4 megabytes. This is still quite a large and expensive requirement for the technologies of the latter part of the 1980's. The next section describes a method – combining barycentric interpolation with trilinear interpolation – for greatly reducing the memory requirements without sacrificing significant image quality. Also, as discussed in Chapter 7, working in an RGB color space rather than an opponent color space such as CIELAB can significantly reduce storage requirements due to the fact that the ink gamut fits much more efficiently leaving less surrounding out-of-gamut space.

6.7 COMBINING METHODS: SUB-INTERPOLATION

By this point it should begin to be obvious why the next chapter, on gamut sampling, is so important for this research. In order to reproduce an image with good fidelity using digital methods, an adequate quantity of well spaced printable colors must be accessible within the printing gamut. Any increase over the minimum acceptable spacing between these colors will introduce objectionable banding. If color transformation is performed through the use of a look-up table, this table must either be large enough to hold *all* the different printable colors – resulting in a multi-megabyte memory requirement – or there must be some post-look-up-table interpolation. Two methods investigated are worth noting: Real-time trilinear sub-interpolation and real-time interpolation using pre-calculated partial differentials. Both of these methods will be described in this section. The desired reproduction speed and the available system hardware will determine to what extent this sub-interpolation has practical justification.

Trilinear Sub-Interpolation

In the results of §6.2 it was found that constant or gradually changing color error is far less noticable or objectionable than systemati-

cally arranged step error, for a given error size. This finding can be used to advantage when sub-interpolating to finer color spacing than that provided by the initial barycentric-interpolated look-up table. Any sub-interpolation beyond the well behaved barycentric interpolation, must not introduce any step error and must keep any error to an appropriate minimum. The initial interpolation provided an equally spaced cubic lattice of colors – precisely what is needed to allow trilinear interpolation. The nature of trilinear interpolation, as mentioned in §6.3, is such that it preserves continuity (introduces no step error) at the boundaries of the interpolation hull – in this case a sub-cube. Also, because of the relatively small size of the interpolation sub-cubes, any introduced gradually changing color error will fall well below the threshold of noticability found in the research reported in §6.2.

An example of practical application of trilinear sub-interpolation in a small limited-memory system could break up 8 bits (256 levels) per printed primary into 5 bits of barycentric interpolation and 3 bits of trilinear interpolation. This gives a look-up table of $(2^5)^3 \times 3 =$ 98,304 bytes. The average size of the tri-linear interpolated sub-cube (From results described in Chapter 7) would be less than four CIELAB color difference units with the resulting introduced color error (the far less noticable gradually changing Type 1 variety) being less that one difference unit.

The three bits of real-time trilinear interpolation will slow down the transformation process to some extent. This extent is a function of numerical computation power determined by such things as clock speed, processor word size, and presence of any math co-processor. Each printed pixel will require one trilinear interpolation regardless of the breakdown of the barycentric vs. trilinear interpolation. The point of this breakdown (the split of the 8 bits between barycentric and trilinear), then, is likely to be driven mainly by memory availability. The only speed factor would be precipitated upon elimination of the sub-interpolation altogether: color transformation at look-up table speeds.

PARTIAL-DIFFERENTIAL SUB-INTERPOLATION

The principal dissadvantage of trilinear sub-interpolation over comprehensive barycentric interpolation is speed – not color fidelity. The villain in this case are the multiplications required (page 6-6). These multiplications can be reduced by using the method of precalculating a second look-up table containing the rate-of-change of ink amount as a function of each of the three input color coordinates then using these *partial-differentials* to speed up the calculations. This method, used by Yule and Korman ([Korman 73], see §3.2) has the same susceptibility to step error, however, as other inferior interpolation methods and must be used only for small-distance interpolation.

6.8 SOURCES OF ERROR

Numerical systems are influenced by many types of errors. Some are relatively difficult to regulate; others can be reduced or even eliminated by redesigning procedures or calculations. Several types of errors as related to color modeling and interpolation will be considered.

(1) *Errors in Input Data.* Samples of the printable gamut for an output device will have some error. This error may be dominated by systematic deviation or temporary disturbances. The most likely source is systematic error from imperfect color measurement or poor control of the printing process. The first can be reduced by approaching the CIE standard observer spectral measurement sensitivities. Alternatively, the imperfect color measurement can itself be modeled to provide a mathematical transformation to a best approximation of CIE colorimetry. Temporary disturbances will be present in both the printing and measurement of gamut test patches. These may or may not be controllable and should be evaluated within the perspective of color tolerances discussed in §6.2. Note, also, that any measurement of color necessarily has some small amount of round-off error.

(2) *Round-off Errors During Computation.* If the computation device being used cannot handle the required number of digits for a multiplication (e.g. the exact product of two 8-bit numbers requires 15 or 16 bits) the product must be rounded off. With the use of modern low-cost 16- and 32-bit computers, along with high precision computation languages, this need not be a problem for color imaging where calculations on an individual pixel are not that extensive and are not numerically unstable. When working with color calculations for imaging, errors of much less than one-half percent of full scale are not noticeable – this is well within the capabilities of today's systems

(3) *Quantization Error.* When limiting each primary to a fixed number of gray levels, there will be an associated error when in-between levels are desired. This type of error is minimized to insignificance by providing enough gray levels such that the steps are unnoticeable. The image capture and gamut sample measurements also have a small quantization error.

(4) *Simplifications of a Mathematical Model.* The idealizations made during the process of designing a model will cause error. This is particularly important for the first five levels of reproduction color fidelity outlined in §2.2. For levels 5 and 6, errors will result from the idealization associated with the interpolation or approximation method. This source of error is of major importance and is discussed throughout this thesis with special emphasis in Chapter 7.

(5) *"Human" Errors.* These errors should be virtually eliminated through automatic calibration in a color imaging system. No numeric data entry or manual color measurement would be required.

CHAPTER 7
RESULTS OF PRINTING GAMUT STUDIES

7.1 INTRODUCTION

In previous chapters, arguments have been made supporting the need for characterizing the size, shape and internal structure of the printable gamut of a digital image proofing process. This chapter addresses the subject of gamut characterization. The gamut is defined as all possible printable colors given a particular fixed paper-ink-process printing environment. Colorimetric analysis of the gamut surface provides the important measurement of the limits of printable colors. Any transformed image element which falls outside of the gamut of printable colors must, if printing is desired, be preprocessed and brought back into the interior of the gamut. This requires a detailed knowledge of the gamut surface.

The internal structure of the gamut, combined with the surface measurements, is also quite important for gamut sampling considerations. A gamut's internal *color rate-of-change* varies throughout the gamut in a process-dependent, difficult-to-predict manner. This problem is particularly troublesome to model with mathematical methods—especially in the extremities of the gamut. A knowledge of the structure of this internal rate-of-change can provide important information in the modeling and sampling optimization process.

7.2 GAMUT MEASUREMENT

Two different printing process categories are considered in this study: offset lithography and Hertz continuous ink-jet. Test images are first synthesized by printing color step gradations distributed through the entire expanse of the gamut. This is most easily done by *slicing* the gamut, a number of times, perpendicular to each of the three subtractive primaries. For example, while holding *CYAN* constant, patches are printed with several variations of the amounts of *YELLOW* and *MAGENTA*. Then the amount of *CYAN* is changed and the process repeated. The steps might be in dot percentage from 0% to 100%in 5% steps—giving a total of 20^3 samples. These 8,000 patches are clearly too many for any manual method of color measurement. Fortunately, adequate information can be obtained by only measuring a small subset of these patches.

Gamut Boundary

The method of space-filling using partitioned hexahedrons (Section 6.5) requires that gamut samples be placed in parallel—though not necessarily equally spaced—planes slicing through the color cube of the printer's color space. This forces equal sample count along any quadruplet of four parallel edges. For example, the four edges of the color cube connecting the zero-yellow face to the solid-yellow face (that is, the edges with gradations: white-to-yellow, magenta-to-red, blue-to-black, and cyan-to-green) all have the same quantity and spacing arrangement of samples. When mapped into an approximately uniform color space such as CIELAB, the distortion alters the size of each edge differently. This introduces an unavoidable degradation of sample dispersion homogeneity throughout the gamut. This non-homogeneity impacts the usefulness of the samples for interpolation or for regression analysis for modeling. Any deviation in sample spacing impacts interpolation efficiency: effecting the number of samples required to cover the gamut. Large deviations can effect the interpolation accuracy. Data gathered for this study provides three-dimensional gamut boundary information which can be used for this distortion analysis.

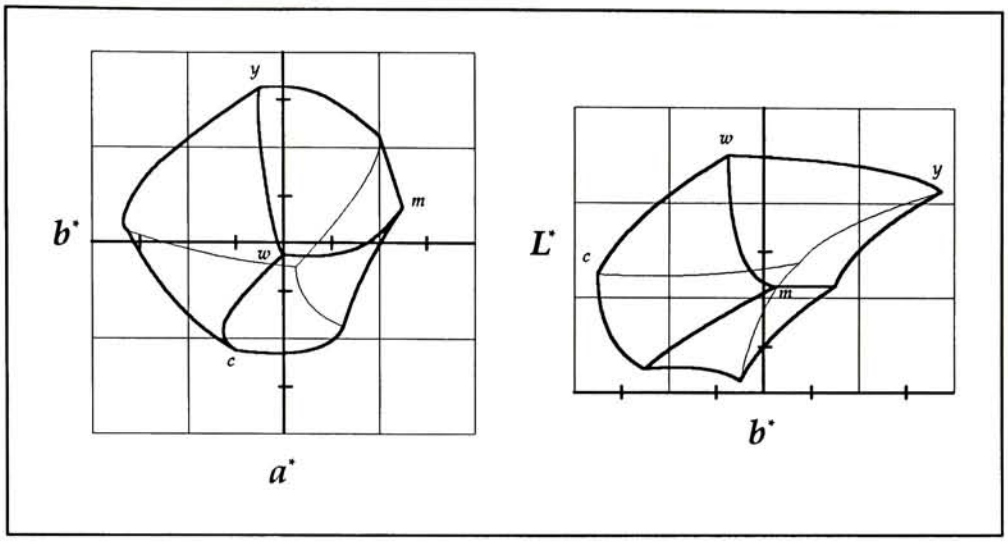

Measurements along all 12 edges will locate the outline of the gamut in color space and measurements along lines bisecting all faces (e.g. all surface measurements where one primary is at 50%) will provide valuable information relating to the concave or convex nature of the gamut. The edge and face data combined with data gathered along internal bisecting planes can provide sufficient information for sampling optimization studies. This gamut surface measurement data can be plotted as 2D or 3D projections in a color space. This provides a useful visual tool for gamut comparisons. The diagram at the top of this page shows two 2D projections of a gamut in CIELAB color coordinates.

Gamut Homogeneity

Interpolation and approximation methods require a collection of known points, called *knots*, of the function or process in question. These knots are then used to generate estimated values for in-between areas. The distance between these knots directly impacts the error associated with the estimates. The estimation process may ignore curvature and simply re-create the function as a straight line between knots (*n*-linear interpolation, §6.3) or it may attempt to imitate the expected curvature of the process (higher order interpo-

lation or modeling). The method chosen can dramatically impact the resulting error. In the color space context, this error is the Type 1 constant or gradually changing error. This, and two other types of error and their associated tolerance characteristics in the graphic arts were described in §6.2. Once the interpolation or approximation process is determined, a minimum sample spacing can be determined for each point within the gamut to achieve a desired minimum color error. To facilitate this gamut characterization, the measured data may be plotted as a partial derivative of the color along any path within or on the gamut. This is only a first step used to flag areas of high rate-of-change. Once these areas are found, they must be analyzed in three dimensions. The important parameter for sample spacing, whether for regression analysis and model building or for direct interpolation, is the maximum distance between the actual gamut path and the straight-line path connecting any two adjacent samples. The farther apart the samples, the larger this difference *if the actual path is not straight.* Even though the actual path in color space may not be straight, this maximum distance may still be small due to the direction changes possible in the path. This concept is illustrated in the diagram below. The diagram shows an example of a gamut path (say, for example, samples along the magenta-to-red edge of the gamut) of nine possible printable colors represented by the dots. The arrows, from color ***P*** to the dashed lines, illustrate the increasing

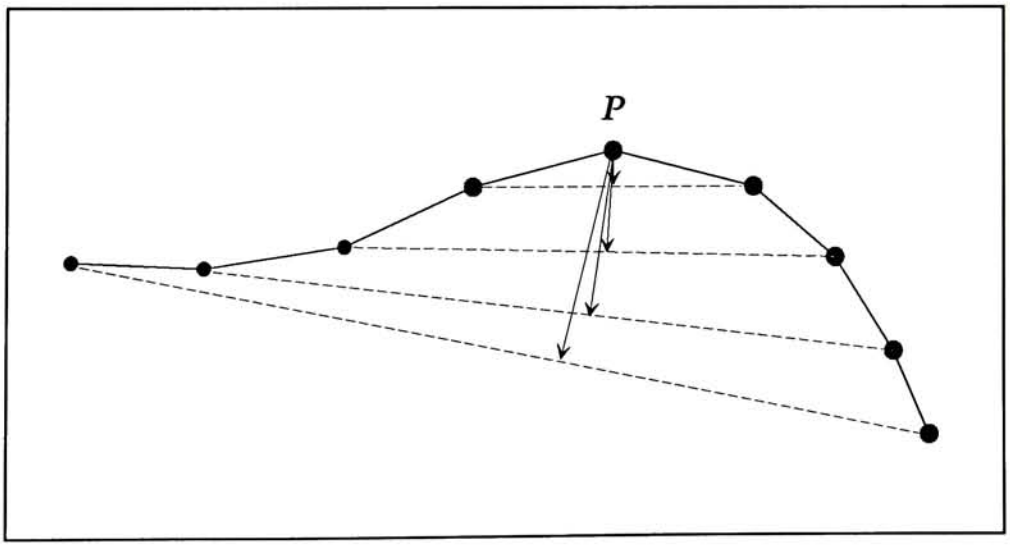

Euclidean color error possible from straight-line interpolation between samples spaced at increasingly larger distances apart. As can be seen from the diagram, the actual distance is very much a function of the path taken by the gamut. Increasing the sample spacing in some areas of the gamut may not significantly increase the associated interpolation or model error. In fact, the sample spacing can be varied throughout the gamut to optimize the process. This is most conveniently done by varying the spacing of the sample *slices* which lie perpendicular to the axies of the primaries in printer C,M,Y space. The three dimensional color data gathered for this study, included as APPENDIX F , provide the necessary information for performing this analysis.

7.3 RESULTS OF INK-JET GAMUT MEASUREMENTS

The first section of APPENDIX F contains plotted color measurement data for a printed test image from an Iris series 3000 ink-jet printer. This printer is capable of printing 300 spots per inch and 32 spot sizes. Through bayer dithering, 256 gray levels per primary are supported. This is a Hertz type continuous flow ink-jet printer.

The test image (a sample and detailed description is in the appendix) contains color patches distributed along all 12 edges of the color cube. The number of drops-per-pixel (spot size) is known for each color patch and is used as the ordinate for all the graphs. Color measurements were made using a Minolta Chromameter. This colorimeter was calibrated to measure CIELAB color coordinates for the 2° Standard Observer using illuminant D65.

Gamut Boundary

There are two general ways to look at gamut distortion: vertex-to-vertex distance, and edge length. These two parameters are not equivalent due to the curvature of the edges. The ink-jet data exhibits approximately a 2.8:1 ratio of maximum to minimum vertex-to-vertex difference and a 3.1:1 ratio of maximum to minimum edge

length. This will lead to a minimum of a 3.1:1 sample-to-sample spacing range despite the choice of slice spacing. The following table shows, for each of the 12 edges, the edge length and vertex-to-vertex edge distance including normalized values for each.

COLOR CUBE DISTORTION STATISTICS

Color	— Edge —		— V-to-V —	
W-Y	128.17	2.0	89.97	2.6
W-M	129.74	2.0	82.11	2.4
W-C	125.41	2.0	66.13	1.9
Y-G	198.35	3.1	94.51	2.8
Y-R	171.79	2.7	95.07	2.8
M-R	64.31	1.0	34.2	1.0
M-B	138.83	2.2	72.72	2.1
C-B	106.17	1.7	62.96	1.8
C-G	162.14	2.5	92.69	2.7
G-K	133.81	2.1	90.44	2.6
B-K	68.72	1.1	35.94	1.1
R-K	147.97	2.3	86.5	2.5

This is certainly not a problem for interpolation accuracy and, thought not optimum, is not too bad for sample efficiency. This ratio can be observed in the CIELAB color space projections found on pages F-4 through F-6. Notice, especially from the L*b* projection, the distinct wedge shape of the gamut. It is particularly interesting to note that the addition of magenta causes a strong reduction of the gamut extent in the direction of yellow variation. The solid magenta face is the smallest of the six—giving rise to the wedge shape.

GAMUT HOMGENEITY

A wealth of information about a printable gamut can be obtained through data such as those found in APPENDIX F. Perhaps the most important function of this data is in the optimization of gamut sample dispersion. From this data one can determine the optimum points for slicing the gamut into hexahedrons. Consider the cyan vectors (the four edges of the color cube where cyan varies from zero to maximum density) plotted on page F-9 and repeated below in simplified form. This data is the *cumulative* color change along the

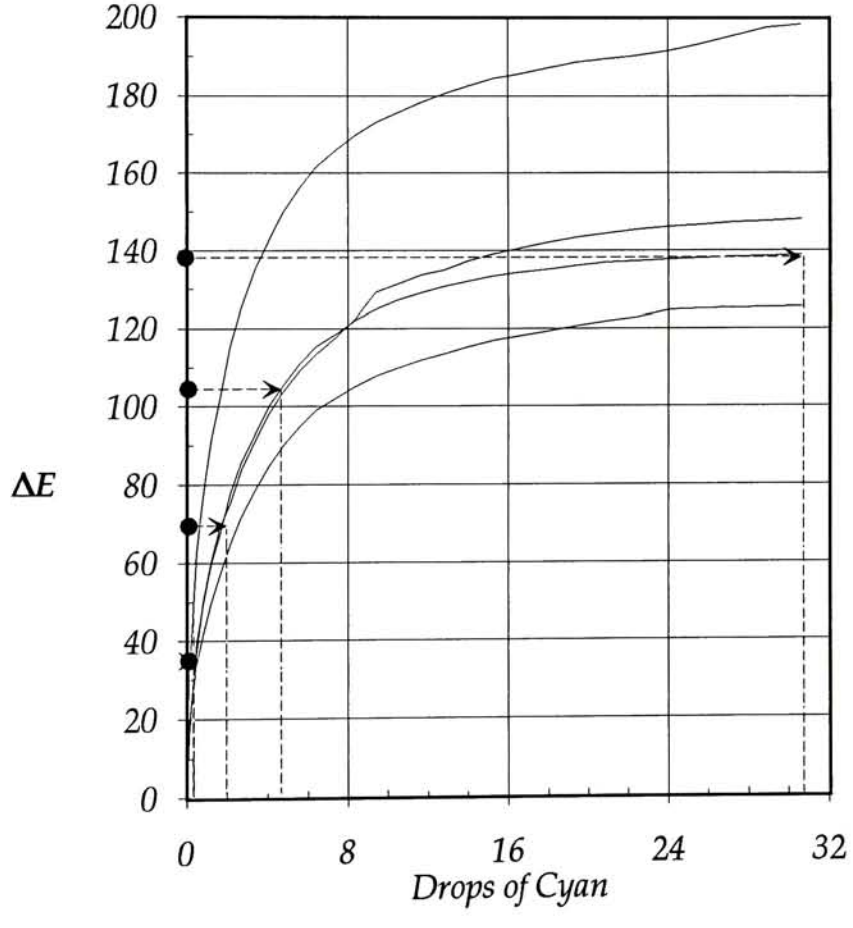

GAMUT SLICING — CYAN VECTORS

distorted edges of the gamut. For maximum sample efficiency, the color change between sample slices, on average, should be the same for all the slices of a primary. In the diagram, the magenta-to-blue curve has been divided into four equal-color-change segments. This produces four unequally space points on the ink-amount axis. This is repeated for the other three curves, generating additional sets of four points which will most often closely coincide with one another. The average position of the four groupings would be a good estimate of the most suitable slice boundaries. There is one important consideration which was left out. Notice the large difference in the slice widths on the drops-of-ink axis. More importantly, observe the severe flattening of all the curves—for the yellow and magenta vectors as well. For this printer, it may very well be advisable to exclude a portion of the printable gamut from being used at all. The gamut extension from the last few drops of ink is so small it may not be worth considering (this seems to support the manufacturer's recommended default settings which limit the drops to well under 31). There are other reasons for truncating the gamut. On page F-10 and F-12 there are quite severe inflections in the latter part of the CIELAB curves. Three of the four yellow vectors (W-Y, M-R, C-G) all exhibit a breakdown in the expected monotonic behavior of b^*. If drastic enough, this kind of performance can introduce situations of multiple ink combinations producing the same color. Clearly, this is unacceptable. Fortunately, for this device the problem only occurs very close to the high drop-count end of the edges where ink efficiency is already quite poor. Gamut slicing then must be preceded by careful examination of the behavior of the color rate-of-change at and near the boundaries of the gamut.

As mentioned earlier, another crucial contribution from gamut homogeneity studies is aiding in the determination of sample count—the number of slices in each of the three primaries (See Chapter 8 for a discussion of how the 4th-color black enters in). The primary concern is containment of type 1 color error introduced from interpolation between samples. The table on page 7-6 quickly identifies the yellow-green edge as the one with the largest overall color change. This edge (plotted on page F-13) exhibits the largest

rate-of-change of a^* for the entire set of edges. Actually, it is the second derivative which is most important: the rate-of-change of the rate-of-change revealed in the sharpness of curvature of the color coordinate plots. Again, the Y-G edge is the most extreme; with several close contenders. Although and automated analysis of the data for type 1 error versus sample spacing could be developed, the plots can quickly be visually inspected to locate the worst offenders for further analysis.

Combining the slice-spacing methods, the type 1 color error requirements, and the desired modeling method (straight linear interpolation versus vector-corrected models), one can systematically determine the sample quantity required. Assuming linear interpolation and type 1 color error limit of six CIELAB units (quite conservative), the data indicate that eight slices will provide more than enough accuracy. This results in 512 samples; a very reasonable number which could be included in a single test print and a single scan. Using vector-correction methods discussed in Chapter 8, this could likely be reduced to four slices, or 64 samples.

Much more can be gleaned from these data than is possible within the scope of this chapter. One item worth mentioning is the effects of digital halftoning and dithering. By placing all of the ΔE-per-drop curves together, one can observe correlation at points of significant pattern change in the halftoning pattern. This barely noticeable with the Iris printer due to its exceptionally high resolution. This "jitter" in the ΔE curves is particularly troublesome for any efforts to mathematically model a printer with good accuracy.

7.4 RESULTS OF OFFSET LITHOGRAPHY GAMUT MEASUREMENTS

Gamut Boundary

A comparison of the CIELAB projections of the S. D. Scott offset lithography (pages F-23 to F-25) with that of the ink-jet projections reveals striking similarities in gamut shapes. The similarly wedge-shaped solid shows sharp contraction of the yellow vectors contain-

ing maximum-density magenta. This is also evident from the color-change data of the yellow vectors plotted on page F-26. The distortion statistics tabulated below show a 4.5:1 range of edge lengths and a 4.5:1 range in vertex-to-vertex distance. This is larger distortion than that that of ink-jet, but combined with inherent tetrahedral distortion for Mode C partitioning, still provides a total distortion range which is well within the desired maximum of one order of magnitude.

COLOR CUBE DISTORTION STATISTICS

Color	*— Edge —*		*— V-to-V —*	
W-Y	94.37	3.84	82.28	3.82
W-M	79.29	3.23	72.29	3.36
W-C	63.68	2.59	55.19	2.57
Y-G	74.58	3.04	64.96	3.02
Y-R	110.78	4.51	96.45	4.48
M-R	24.57	1.00	21.51	1.00
M-B	71.20	2.90	61.49	2.86
C-B	40.48	1.65	38.95	1.81
C-G	65.83	2.68	57.89	2.69
G-K	56.26	2.29	46.78	2.17
B-K	30.68	1.25	26.96	1.25
R-K	76.14	3.10	60.11	2.79

Notice how the edges do not exactly connect in the CIELAB projections. This discontinuity is too large and systematic to be measurement error. It is likely due to the fact that these patches were not all printed with exactly the same conditions. There likely were several plates and press runs involved. This is an interesting reflection of offset press color printing accuracy.

Comparison of the overall gamut size and location of the offset data with that of the ink-jet data reveals an interesting and very pertinent fact. The offset gamut falls almost entirely within the ink-jet gamut. This speaks well for ink-jet proofing—*if* the color transforms provide the requisite fidelity.

Gamut Homogeneity

The internal behavior of the offset gamut exhibits one strong difference from the ink-jet data: The color changes much more linearly with dot percentage. The most prominent deviations from the straight line tend to be in the highlight dots from 0% to 10% (observe this on the yellow-to-red data, for example). This is as expected and in fact is probably why 5% patches are included in the S. D. Scott Color Guide with the otherwise 10% spacings.

A troublesome characteristic of the offset data is the high "jitter" content of the CIELAB color curves. This hampers efficient modeling efforts and reduces the attainable sampling efficiency given a set of color error limits—more samples are required to capture the essential nature of the gamut. This jitter is not likely related to any measurement error. Exactly the same measurement conditions were used for the offset and the ink-jet samples.

CHAPTER 8
CLOSED-LOOP COLOR REPRODUCTION

8.1 ADVANTAGES OF CLOSING THE LOOP

Feedback control systems have long been used for their ability to monitor and control system related error. "Closing the loop" in a color image printing system has typically been an impractical task. With new digital image scanning and printing devices, closing the loop becomes a practical potentiality. Feedback from measured color patches printed under actual conditions can be used to control the error in a color transformation process. This ultimately could provide continually optimum color fidelity. The diagram on the next page illustrates the flow of information in a digital color image reproduction system.

The target printing device is used to generate a synthetic image containing samples of the printable gamut. These samples are then scanned using the system's image input device. The data is automatically extracted from the scanned image and provided in appropriate form to the color transform process. In operation, an original is scanned and the data is processed with the color transform (look-up tables generated from the scanned samples) and printed. The result is the best possible color match producible with a color transform. Producing a transform in this manner creates a *composite* transform which accommodates both the scanning and printing processes together in one step. The degree to which it is imperfect will be affected by several considerations discussed in a later section in this chapter.

CLOSED-LOOP COLOR REPRODUCTION

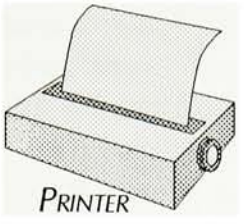

PRINTER

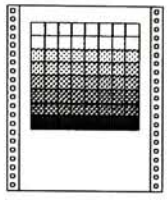

GAMUT TEST

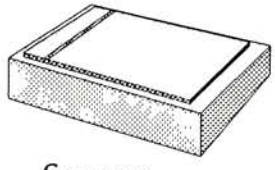

SCANNER

ORIGINAL

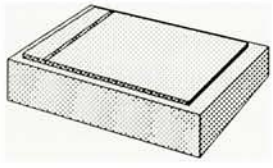

COLOR TRANSFORM

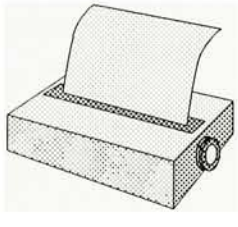

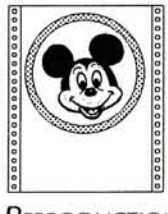

REPRODUCTION

8.2 VECTOR-CORRECTED MODELING

For speed considerations, the color transform is processed by way of a look-up table. This table can be filled with direct interpolation of the samples, by a mathematical model, or by a *vector-corrected mathematical model.* The process of vector correction can best be illustrated with a simplified example.

The diagram below illustrates a one-dimensional function (math model) which is to be vector corrected. The dots represent the known values (knots) of the actual parameter being modeled. Each knot has an error vector associated with it. These vectors are used to create a curve of interpolated error. This error curve is then added to the original model to generate the vector-corrected model. This new model retains the desirable curvature of the original model.

This method can be applied to color space interpolation and modeling. There are non-differentiable points introduced into the

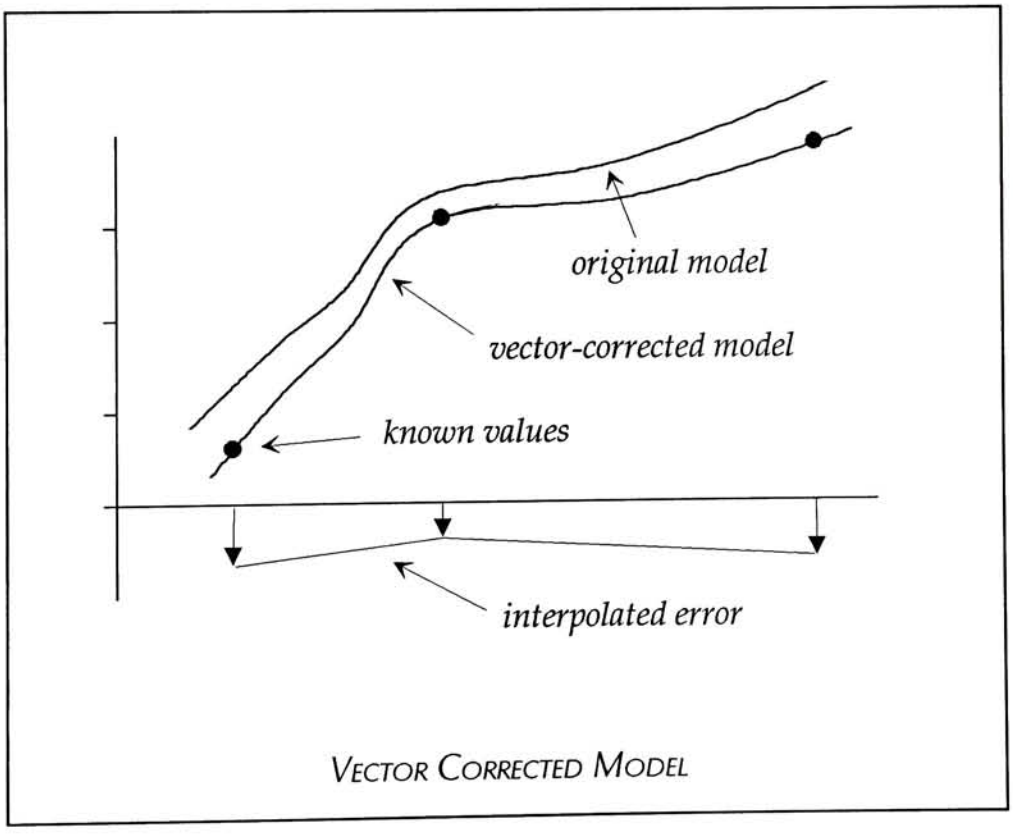

VECTOR CORRECTED MODEL

model at the knots; however, as revealed in the color error study of §6.2, this Type 3 error is of little consequence and can be ignored. The curvature provided by the original model—which hopefully has some physical significance—allows spacing of the knots to be wider leading to a simpler and more efficient calibration process. Vector-corrected mathematical modeling, first introduced in Chapter 2 as Level 6 color reproduction fidelity, promises to provide vast improvement over traditional mathematical modeling methods.

8.3 CLOSED-LOOP CALIBRATION ACCURACY

The color transformation process can be used to accommodate either only the printing process—converting color from, for example, CIELAB values to CMYK values—or it can accommodate both the printing and scanning processes by converting scanned data (usually RGB) directly to printed CMYK. The first, where the "original" is stored digital data, relies on image data which is colorimetric; the second does not. A color transformation which includes both the scanning and the printing processes may be more efficient by avoiding two separate transformations; however, this eliminates a possible path through any color space used by an image editing/display system. Such a single-transformation system would be ideal for a color copier application.

Perfect colorimetric reproduction fidelity for all types of originals is only possible with a trichromatic image capture device which mimics human vision (standardized as the CIE Standard Observer). Any deviation (an *anomalous trichromat*) will cause instrument metamerism. Illumination of the original with a source other than that used for viewing will also exacerbate the metamerism problem. Instrument metamerism exhibited by the input scanner will cause greater loss of color reproduction fidelity when several colorant types are used for originals. This loss can be minimized, but not eliminated (nothing can totally eliminate this), by closed-loop calibration (*including* the scanner) for each original type. If the spectrophotometric characteristics of the original pigments are the same or very close to those used for the printing process, a closed loop

calibration can greatly minimize the loss of fidelity caused by instrument metamerism. Newer generations of scanners are coming closer to being true colorimeters but one can not yet achieve graphic arts levels of fidelity with low-end CCD scanners without some minimal transformation of the data. As an example, hue error data for a Sharp JX-450 CCD scanner is plotted on pages 8-6 and 8-7. This scanner is designed to generate 24-bit color in accordance to the NTSC standardized primaries. Page 8-6 illustrates the hue error resulting from scanning an RIT Process Separation Guide on a matte substrate; using the standard NTSC matrix for converting RGB to XYZ tristimulus. The marker colors indicate the scanned patch colors: cyan, magenta, yellow, red, green, blue and their respective 50% tints. Several unexceptably large hue shifts are present. On the following page, and optimized 3x3 transform is applied. This transform was generated through a regression analysis of all the patch color readings. The result of this simple transform is quite a remarkable improvement. This indicates a generally good colorimetric performance and leaves quite a bit of latitude for achieving, for example, total system hue error performance as good as the Canon copier (APPENDIX E).

Closed-loop calibration, as illustrated on page 8-2, for exact reproduction requires that the original and reproduction are both reflection copy or transmission copy. Reproducing a reflection copy from a transmission original usually involves gamut compression; a topic which is beyond the scope of this thesis. Closed-loop calibration of non-compressed color reproduction will yield the quickest path to such *preferred reproduction* processing. Using a look-up table based system certainly does *not* preclude the inclusion of "knobs" in the system for image modification to meet the demands of preferred reproduction.

An obvious, and often ignored, precondition for useful closed-loop calibration of any feedback system is the need for control dynamics which are fully capable of tracking process variations. System stability may need to be analyzed to determine the necessary sampling frequency for the feedback. Of course, the ideal system would be fully automated with effectively continuous sampling and would provide much more latitude for process variation.

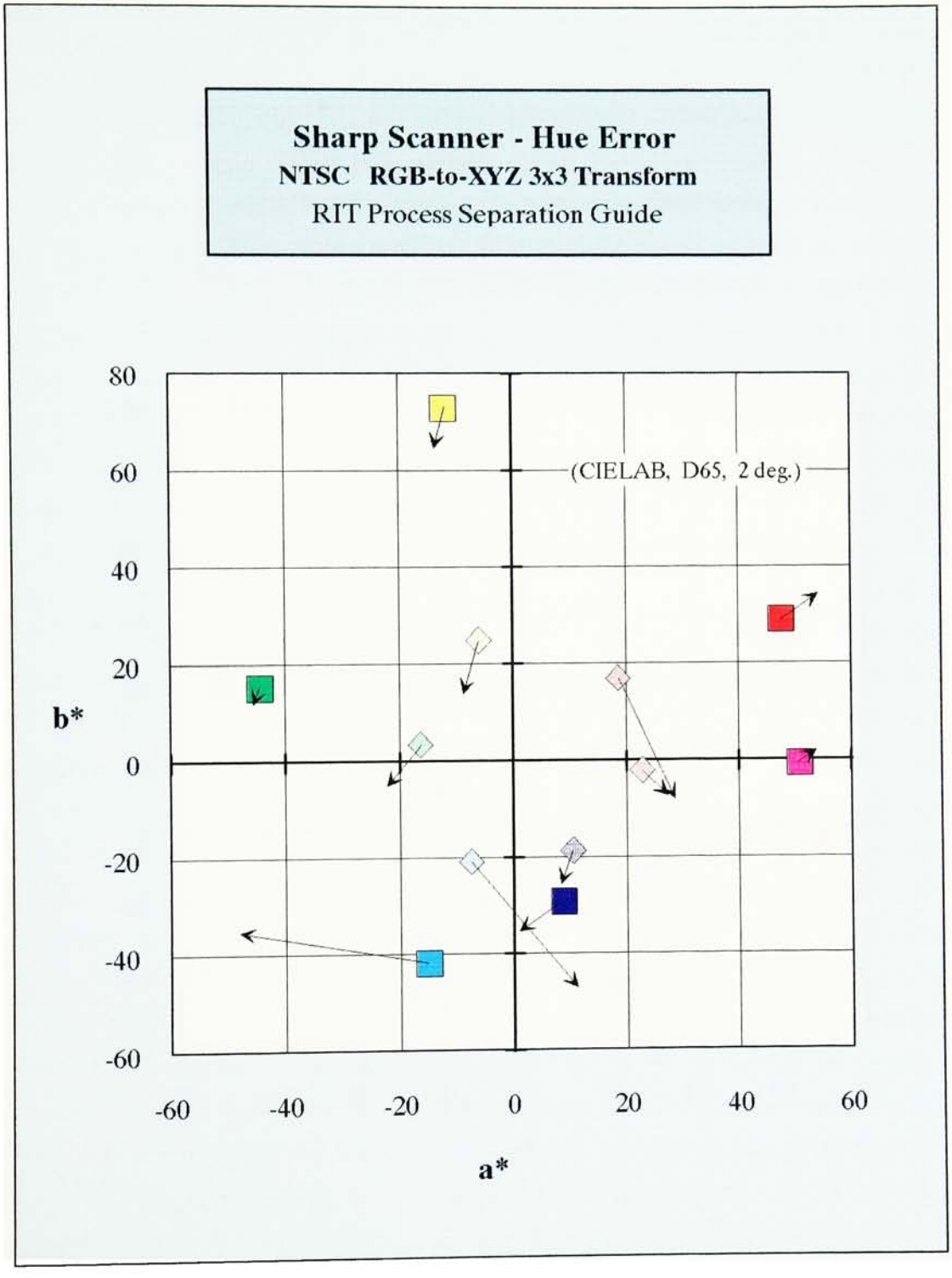
Sharp Scanner - Hue Error
NTSC RGB-to-XYZ 3x3 Transform
RIT Process Separation Guide
(CIELAB, D65, 2 deg.)
80
60
40
20
0
-20
-40
-60
b*
-60
-40
-20
0
20
40
60
a*

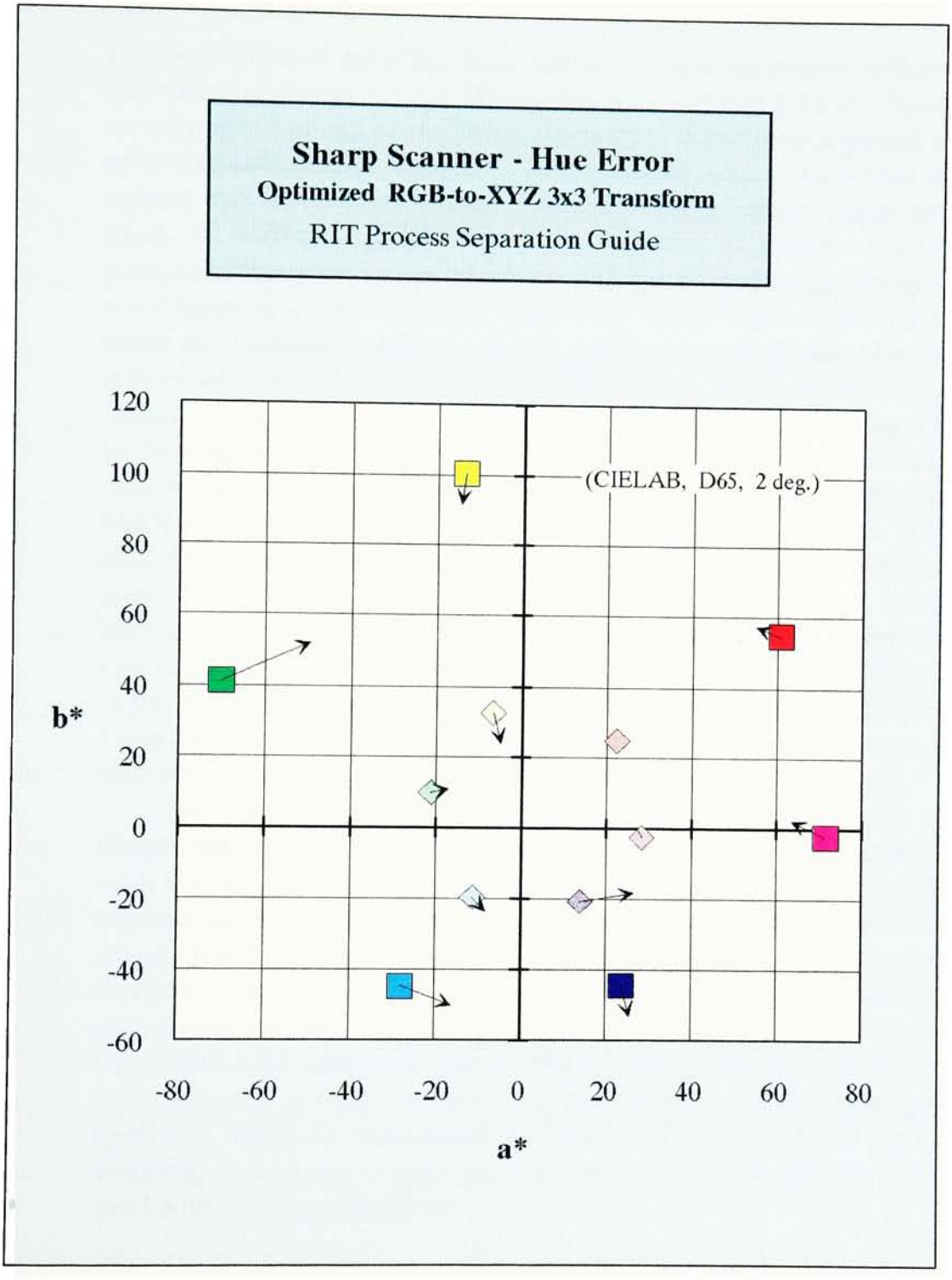
Sharp Scanner - Hue Error
Optimized RGB-to-XYZ 3x3 Transform
RIT Process Separation Guide
(CIELAB, D65, 2 deg.)
b*
a*
120
100
80
60
40
20
0
-20
-40
-60
-80
-60
-40
-20
0
20
40
60
80

8.4 FOUR-COLOR PRINTING

The perception of color has been known for centuries to be a three dimensional phenomenon. Theoretically, any three inks not lying on a straight line can be used to create a three dimensional gamut of printable colors. Any number of additional colors can be added to extend this three-color gamut. When more than three colors are used—as with the common four-color printing processes—a large portion of the printable color gamut can be created using multiple combinations of the available primaries. This creates a dilemma: there are multiple solutions to the problem of predicting the required ink amounts to produce a specified color. This is another case of an over-determined system. The four-color problem is analogous to having four equations in three unknowns. One must decide which right answer is desired. This is usually done by having the black ink amount be a function of the other three ink amounts. This can, and often does, lead to color reproduction problems if not performed carefully. For example, when adding black to a color previously created with cyan, magenta, and yellow, in order for exactly the same color to be reproduced, unequal (and very difficult to predict) amounts of the three primaries must be removed. Objectionable Type 1 color error is the common result. This has been a notorious problem area for graphic arts scanners.

Color transformation modeling based on measured samples of the printable gamut (closed-loop transformation) is not beleaguered with this problem. A simple solution presents itself. The black ink amount can be a simple function of the other three with no concern for any resulting hue shift since that shift becomes a predictable and integral part of the system being modelled. If the same simple conversion of three ink amounts to four ink amounts is used for both the closed-loop sampling and for the normal printing, it becomes automatically compensated during the process control through feedback. Based on considerations other than color (such as paper wetness, and gamut extension), the amount of black printer used can be an arbitrary decision.

CHAPTER 9
SUMMARY

9.1 SUMMARY AND CONCLUSIONS

Digital color printing and imaging technologies are currently in a state of rapid evolution. Image processing and image printing technology, in particular, have taken great strides in this decade of the eighties. In most respects, these advancements will continue with a veritable endless avalanche of new and better applications; however, in one respect the grandest attainable heights are fixed and certainly achievable in the near future. That is the aspiration of rapid and accurate "push-of-the-button" reproduction of a digitized color image. Both the speed and accuracy of current digital color printing sub-systems present deficiencies which bar them from greater acceptance. In this report, these problems have been addressed and potential solutions have been studied which show verifiable potential for significant progression toward the ideal.

Color transformation is at the heart of the reproduction process and is where the problems, and opportunities, reside. The first problem plaguing previous attempts of rapid and accurate color transformation is the disordered spacing of gamut sample measurements when inverted to form color-tristimulus-to-ink-amount conversion tables.

Chapter 6 reports of an extension of the technique of barycentric coordinates which can be used to perform an interpolation between any four points defining a tetrahedron. By partitioning the gamut

samples into a space-filling aggregation of tetrahedra, one could then interpolate within each and be insured of continuity at the interfaces between. The challenge of partitioning was resolved through a devised method of systematic partitioning of the printable gamut in to hexahedrons which were subsequently partitioned into hexahedra ready for barycentric coordinate interpolation. In order for this method to be practical, tetrahedra distortion must be kept in check. This was shown to be achievable, largely due to the results of Chapter 7.

The gamut studies of Chapter 7 illustrated the gamut boundary and homogeneity characteristics of two general printing processes: ink-jet for proofing, and offset lithography for on-press printing. The distortion statistics gathered for these gamuts reveal conspicuous similarities and pertinent differences. These data were used to evaluate sample-spacing requirements for provision of color fidelity levels common to the graphic arts. A synthetic image of 512 test patches was shown to be more than sufficient for barycentric-based color transformation under the most demanded color accuracy requirements.

In Chapter 8, closed-loop color transformation was addressed with special emphasis on practical considerations such as scanning accuracy. Vector-corrected modeling was discussed as a possible refinement enabling a reduction in the 512 color measurements.

Verification of the initial hypothesis—whether or not one could perform a continuous and uniform interpolation given a disordered assortment of knots—was accomplished well with the combination of hexahedron partitioning and barycentric coordinate-based interpolation. Further, and perhaps equally important, these methods were shown to provide a means of color reproduction accuracy throughout the entire gamut which are superior to the much more time-consuming mathematical modeling techniques in common use.

9.2 RECOMMENDATIONS FOR FURTHER STUDY

This research has opened up several avenues of further study. Perhaps the most obvious is incorporating the reported results into a working system and performing image reproduction color fidelity analyses under varying conditions. Sample spacing could be varied to observe the effects these results have indicated will occur. Variation in the amounts of on-the-fly sub-interpolation could be investigated for speed trade-offs. Other means of sub-interpolation, such as the partial derivatives method, could be analyzed for speed enhancement possibilities.

The possibility of combining barycentric interpolation with vector-corrected math modeling promises to reduce significantly number of gamut samples required for a given fidelity. This could be verified with a system implementation. This is perhaps the most exciting possibility since it might provide rapid closed-loop system calibration with a small test image.

APPENDIX A
ANNOTATED BIBLIOGRAPHY AND REFERENCES

COLORIMETRY AND COLOR SCIENCE IN THE GRAPHIC ARTS

[Berns 88] Berns, Dr. Roy, Private communication, Studies at the Munsell Color Science Laboratory at the Rochester Institute of Technology have shown that for non-defective observers, a just-noticable color difference can range from 0.5 to 5.0 CIELAB color difference units.

[Billmeyer 81] Billmeyer, F.W., Jr., and Saltzman, M., *Principles of Color Technology*, Second Edition, John Wiley and Sons, New York, 1981. This book, used as the Colorimetry text at RIT's Center for Imaging Science, is perhaps the best up-to-date introduction to the topics of colorimetry and color science. No graphic reproduction specific information is presented.

Gordon, J., Holub, R., Poe, R., "On the Rendition of Unprintable Colors." *TAGA Proceedings, 1987.* Exact reproduction of a colored original is most often not possible due to limited gamut range of the printer. This paper presents a mathematical formalism for describing the mapping of images from one gamut to another to yield pleasing results. A colorimetric approach is used by chosing coordinates in an approximation of uniform color space: L*u*v*.

[Hunt 87] Hunt,Dr. R. G. W., *The Reproduction of Colour.* Fourth Edition, Fountain Press, Tolworth. England, 1987. This classic pro-

vides a very broad coverage of color photography, color television, and color printing.

Judd, Dean B. and Wyszecki, Gunter, *Color in Business, Science, and Industry*. Third Edition, John Wiley and Sons, New York, 1975. This book has long been highly regarded in the field of color science. It does not address the graphic arts directly but it does provide the necessary foundations of color science which are becoming more important for graphic reproduction.

[Laihanen 88] Laihanen, P., "Colour Reproduction Theory Based on the Principles of Colour Science." *Advances in Printing Science and Technology: Proceedings of the 19th International Conference of Printing Research Institutes, Eisenstadt, Austria, June 1987*. Pentech Press Limited, London, 1988. This lengthy article begins with a discussion of the shortcomings of conventional image reproduction principles, citing especially the uncontrolled manner in which color balance is altered when cyan, magenta, and yellow tone curves are manipulated. Color reproduction based on color science is reviewed with special emphasis on its advantages for image manipulation. Optimum colorimetric gamut compression is discussed. Color transformation into printing ink densities is addressed first with classical Neugebauer equations, followed by n-modified, modern Neugebauer, and vector-corrected Neugebauer. Color errors are reduced to one fifth that of classical Neugebauer. The interpolation methods used share the same shortcomings found in Korman's methodology.

Pearson, Milton, "Image Reproduction Colorimetry." *Color: Research and Application*, Volume 11, Number 1, Spring, 1986. This is an easy to read though a bit sketchy overview of colorimetry as it applies to the graphic arts. Pearson makes an important distinction between colorimetry in the graphic arts, "image-reproduction colorimetry," and colorimetry in commercial colorant matching, "matching-and-formulation colorimetry." The widely disparate color error ranges encountered suggest the need for different instrument selection and calibration criterion. To further illustrate the relative importance of color error numbers, Pearson tabulates the changes in color

error which result in three important measurement factors: Using the 1931 versus 1964 standard observer; changing geometry from 0°/45° to sphere; and changing the color temperature of the illuminant. Metamerism, and its role in four-color image reproduction is summarized.

Schultz, U., "Density Measurement and Colour Measurement, Advantages and Disadvantages in the Printing Industry." *Advances in Printing Science and Technology: Proceedings of the 19th International Conference of Printing Research Institutes, Eisenstadt, Austria, June 1987.* Pentech Press Limited, London, 1988. This paper attempts to establish the status of measurement integrity of two color monitoring methods: Colorimetry and Densitometry. The serious shortcomings of densitometry as a color measurement tool are carefully illustrated. Possibilities for describing ink properties with colorimetry are examined. Colorimetry and denisitometry are shown to have quite different aims. Densitometry was originally developed to measure optical absorption in specific materials. Colorimetry attempts to quantify the visual color experience.

[Stamm 81] Stamm, S., "An investigation of color tolerances." *TAGA Proceedings, 1981.* This paper reports on an investigation of the acceptable tolerance for lithographic reproduction.

COLOR CORRECTION AND TRANSFORMATION FOR PRINTING

[Clapper 69] Clapper, F. R., "Computerized Colour Correction." *Printing Technology: Proceedings of the Institute of Printing,* Vol. 13, No. 1, April 1969. This is probably the first attempt at empirical color prediction through closed-loop measurement of synthesized test patches. Clapper printed a color chart with known combinations of dot areas. He measured the color of each patch and worked out a set of equations using least-squares methods. He then set up the scanner color correction and gradation to conform to these models.

[Korman 71] Korman, Nathaniel I., "Self-Adaptive System for the Reproduction of Color." *U.S Patent #3,612,753,* Issued October 12, 1971.

This patent, and the following Korman entries, describe one of the only published accounts of color transformation through look-up tables generated from interpolated measurements of synthesized color patches. This 1971 patent (which, interestingly, expires in 1988) is a surprisingly broad claim for look-up table color matching through interpolated color measurements of test patches.

[Korman 72-1] Korman, Nathaniel I., "Accuracy of Color Reproduction with the Digital Computer - Scanner System of Color Separation." *TAGA Proceedings, 1972.* This paper briefly outlines Korman's method of look-up table correction without giving any details of interpolation methods. Mention is made of "a great deal of effort" being spent on minimizing the apparently objectionable inaccuracies of the interpolation process. The problem is clearly not fully comprehended by the author who makes the following admission: "We can expect even further improvements as our understanding of the nature of the irregularities progresses; hopefully, improved understanding can also help reduce the irregularities and lead to improved printing." Korman mentions the additional system characterization benefits which can be reaped from printed cross sections of the look-up table.

[Korman 72-2] Korman, Nathanial I., "The digital computer-controlled scanner for colour separation." *The Penrose Graphic Arts International Annual,* Vol. 65 1972. This non-technical paper is included as the only published example of Korman's test pattern printed in color.

[Korman 73] Korman, Nathanial I., Yule, John A. C., "Digital Computation of Dot Areas in a Colour Scanner." *Advances in Printing Science and Technology: Proceedings of the 11th International Conference of Printing Research Institutes, Canandaigua, New York, May 1971.* Keppler-Verlag KG, Frankfurt, Germany, 1973. This paper expands on the overview of Korman's look-up table method found in the 1972 *TAGA Proceedings.* An in depth treatment of the interpolation method is presented. Though the authors use convex tetrahedral hulls, the

method used within the hull is not a true 3-space linear interpolation algorithm. The tetrahedrons are also arbitrarily chosen for each interpolation. The authors concede: "...improvements in the accuracy of the computations are needed." The authors mention a problem of "smoothness" in the reproduction. Discontinuities, that is jumps in color or tone scales, are an observed complication.

[Molla 88] Molla, Dr. R. K., *Electronic Color Separation.* Chapter 10: "Color Correction," R. K. Printing & Publishing Company, Montgomery, West Virginia, 1988. This new book, which purports to be *the* reference on color scanning, makes no reference to look-up table color transformation – no surprise. The authors obviously shallow understanding of color theory colorimetry detracts from an otherwise credible book.

Pobboravski, I. and Pearson, M., "Computation of dot areas required to match a colorimetrically specified color using the modified Neugebauer equations." *TAGA Proceedings, 1984.* This paper is rarely passed over in any recent discussions of Neugebauer equations and their mutations. A preferable treatment of this topic, however, is found in the Laihanen paper referenced above.

[Pugsley 75] Pugsley, Peter C., "Colour Correcting Image Reproducing Methods and Apparatus." *U.S. Patent #3,893,166,* Issued July 1, 1975. This is the only non-Korman reference found for look-up table color matching. No claim is made for auto-calibration (covered by Korman's patent). This patent details an interpolation method which which uses trilinear techniques. It's efficacy is dependent on the preliminary knot ordering techniques used. These techniques are not mentioned.

[Rhodes 88] Rhodes, Warren (Dusty) L., *Towards "WYWSIWYG" Color: A Simplified Method for Improving the Printed Appearance of Computer Generated Images.* EDL-88-2, Xerox Corporation, April, 1988. This paper, written by one of the recognized experts in the field, is a description of a method for matching output from electronic printers to an RGB monitor image. The goal is a transform which processes digital monitor data of a specific monitor/printer pair, for

pleasant rendition on the printer. "It was developed to serve the needs of a community of users who were dissatisfied with the quality of their prints and who placed more value on a quick and significant improvement than on obtaining optimum graphic arts quality." The technique introduces an L*a*b* equivalent to Equivalent Neutral Density (END). First, gray balance is corrected, then the black printer is added for optimum balanced gray range and density range. A saturation boost and hue adjustment consummate the correction process yielding a very respectable product. The paper includes reproductions of prints showing the progressive improvements at each stage of the process. A lengthy listing of references and a bibliography is included. Included are excellent printed examples of color images reproduced at Level 0, Level 2, and Level 3 color fidelity. (See discussion of levels in Chapter 2)

[Saunders 88] Saunders, Bert, Private communication.

[Yule 67] Yule, J.A.C., *Principles of Color Reproduction.* John Wiley and Sons, New York, 1967. This out-of-print book is highly regarded as the technical reference for color reproduction. Yule provides an in depth treatment of the color correction problem from photographic masking to modified Neugebauer equations.

ELECTRONIC IMAGING IN THE GRAPHIC ARTS

[Johnson 88] Johnson, A. J., "Requirements for Digital Color Proofing." *Advances in Printing Science and Technology: Proceedings of the 19th International Conference of Printing Research Institutes, Eisenstadt, Austria, June 1987,* Pentech Press Limited, London, 1988. This paper is a short summary of the image fidelity requirements for digital color proofing. Gray-level resolution, spacial resolution, and color transformation are all discussed. The author attempts to dislodge the conventional perception that a proofing system's colorants should match that of the inks to be used on the press.

[Kriss 87] Kriss, Michael A., "Electronic Imaging, The Challenge, The Promise." *J. Soc. Photogr. Sci. Technol. Japan,* Vol. 50, No 5, 1987. This is an excellent, though quite technical, paper on the imaging science

and technology. Comparisons are made between the available CCD imaging technologies and photographic films. A useful chart assigns equivalent pixel density to each of the more popular photographic films.

[Rzeszewski 83] Rzeszewski, Ted, *Color Television,* IEEE Press, John Wiley & Sons, New York, NY., 1983. This book is a collection of papers about color television. Of particular interest is the first section, called Background, which covers the theory of television colorimetry. A comprehensive history of the NTSC standard is included.

[Saarelma 84] Saarelma, H., Oittinen, P., Kekolahti, P., Tuovinen, P., "Performance Aspects of Digital Picture Reproduction." *Advances in Printing Science and Technology: Proceedings of the 17th International Conference of Printing Research Institutes, Saltsjöbadan, Sweden, June 1983,* Pentech Press Limited, London, 1984. Though specifically oriented toward newspaper production, this paper provides a good general overview of digital imaging in the graphic arts. All factors of image input, assembly and correction, and output, are addressed. An interesting explanation of the generation of screen angles by the "rational tangents" method is provided.

NUMERICAL METHODS FOR COLOR PREDICTION MODELING

[Dahlquist 74] Dahlquist, Germund, *Numerical Methods,* Prentice-Hall, Inc., Englewood Cliffs, N.J. This is a good and quite comprehensive text on numerical methods. Clear treatment of matrix calculations and error sources found in this book are well suited to color space interpolation concerns. This reference also deals with *barycentric interpolation,* though the treatment is very brief and limited to interpolation within triangular grids. No mention is made of the possibility of extending barycentric interpolation concepts to higher dimensions.

[Neugebauer 37] Neugebauer, H.E.J., "Die theoretischen Grundlagen des Mehrfarbenbuchdrucks," Zeitschrift für wissenschaftliche Photographie, Photophysik und Photochemie, 36, 1937. This is

the original document where the now famous *Neugebauer Equations* were first published.

[Thalmann 87] Thalmann, Daniel, and Magnenat-Thalman, Nadia, *Image Synthesis: Theory and Practice,* Springer-Verlag, Tokyo, 1987. Chapter 3 of this book contains a good description of interpolation and approximation methods as pertaining to their essential role in the construction of 3D objects for image synthesis. These techniques apply to *surface interpolation* within three dimensions with no mention being made to the possibility of extending discussed techniques to *solid interpolation* with four dimensions. Rigorous mathematical treatment is provided.

[Schneider 82] Schneider, Dennis M., Steeg, Manfred, and Young, Frank H., *Linear Algebra: a concrete introduction.*

APPENDIX B
PARTITIONING THE HEXAHEDRON

In order to facilitate interpolation using the method of barycentric coordinates derived in Chapter 6, a means of partitioning the printable color gamut into tetrahedra must be realized. The gamut can first be partitioned into hexahedra, then this aggregation of hexahedra can be systematically further partitioned to form a new packing of space-filling of tetrahedra. This decomposition must follow the constraints effected by the *three conditions* outlined in §6.5. The task at hand is to determine all possible modes of space-filling a hexahedron with tetrahedra where only the eight vertices of the hexahedron are used (no new ones allowed internal to the hexahedron).

B.1 THE FIVE PROTOTYPE TETRAHEDRA

All possible prototype tetrahedra can be formally discovered through procedures which explore all configuration alternatives. To start, a vertex of the hexahedron (which will henceforth be referred to and illustrated as a cube) will be chosen as the anchor for all prototypes. This can be done due to the vertex symmetry of the cube. The anchor will be the farthest most vertex of the upper face as shown in the illustration at the top of the next page. It is impossible for this cube to contain a tetrahedron oriented in such a way that each face of the cube touches not more than one tetrahedral vertex—that is, one cube face (and in fact two faces) must have an least two vertices—and therefore an edge—of the tetrahedron. The top cube face will be

THE FIVE PROTOTYPE TETRAHEDRA

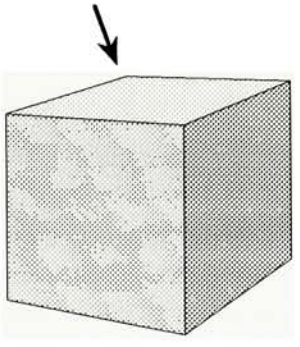

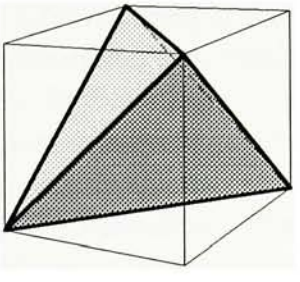

TYPE 0

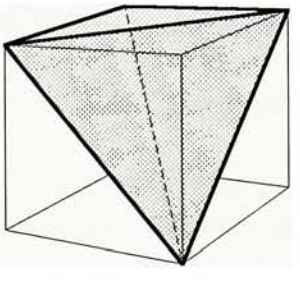

TYPE 1

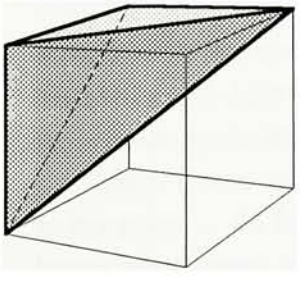

TYPE 2A

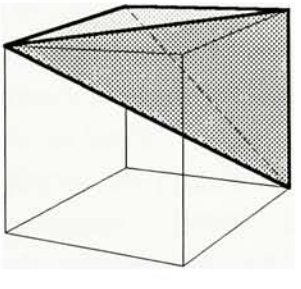

TYPE 2B

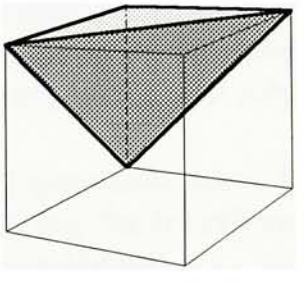

TYPE 3

chosen as the anchor face of the cube. The first iterations will include all possible tetrahedra with a single edge on the diagonal of the anchor face. This allows only *one* prototype configuration. This Type 0 prototype (see diagram on page B-2) has no tetrahedral faces coincident with any cube faces. The prototype is a *regular tetrahedron* composed of four equilateral triangles and equal dihedral angles: $2\sin\sqrt{3}/3 = 70°31'44"$. The Type 0 volume (for a unit cube) is 1/3. This type has reflection symmetry with itself.

For the next iteration, the anchor point will be the right-angle vertex of a tetrahedron's face lying coincident with the anchor face. This triangle locates three of the vertices leaving one for the iterations. That remaining vertex can take position at any of the lower four vertices of the cube. A Type 1 prototype is realized with the fourth vertex being at the nearest alternative. This irregular tetrahedron has only *one* coincident face. The dihedral angle for the longest edge is $2\pi/3 = 120°$. The volume is 1/6. This type also exhibits reflection symmetry with itself.

Moving the lower vertex clockwise to the next position yields a Type 2A tetrahedron. This prototype and its mirror image, the Type 2B (reflection symmetrical), enjoy two coincident faces with the cube. Those two faces share a common edge at a 90° dihedral angle. These prototypes contains a second 90°, two 45°, and a single 60° dihedral.

The Type 3 prototype shares three faces with the cube (by now it may be obvious how the prototype's name corresponds to its characteristics: the number of coincident sides). Contained are three 90° and three 45 degree dihedral angles. The volume is 1/6 and it exhibits reflection symmetry with itself.

With these variations, all possible configurations have been exhausted – all four possible corners for placing the fourth vertex have been used and all mirror symmetries considered.

B.2 THE FOUR HEXAHEDRON PARTITIONING MODES

The diagram on page B-4 illustrates the four possible modes for space-filling of the cube using these five prototypes. Mode A incor-

THE FOUR PARTITIONING MODES

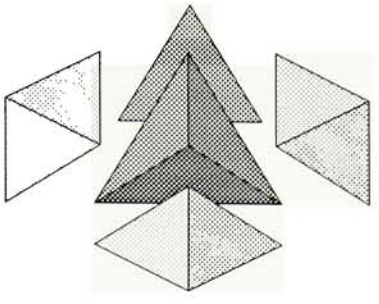

MODE A

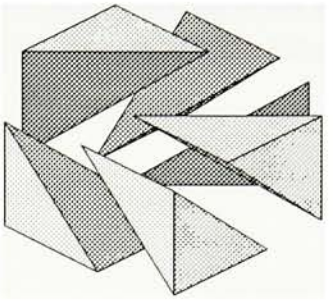

MODE B

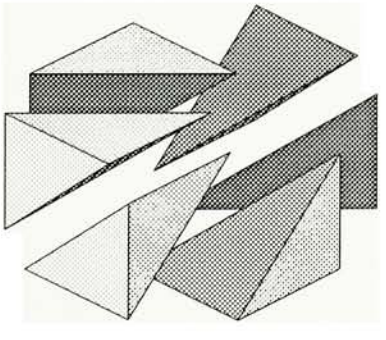

MODE C

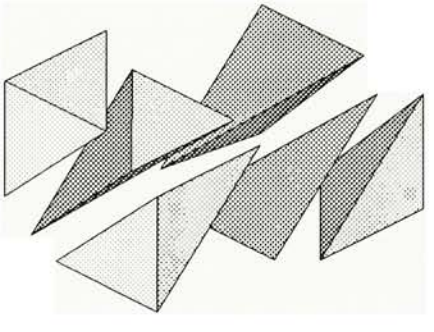

MODE D

porates a Type 0 tetrahedron and four Type 3's. Mode B consists of three Type 2A's and three Type 2B's as does Mode C. Mode D is truly unique. It contains two Type 1's (the projection of the Type 1's is a little clearer in this diagram than in the original prototype illustration), a Type 2A, a Type 2B, and two Type 3's. Mode D, like Mode C, exhibits external slide symmetry: these cubes can be stacked directly without first building a cluster as with Mode A (See Diagram and discussion on page 6-18).

APPENDIX C
INTERPOLATION STATE DIAGRAM

Interpolation within a hull defined by a convex polygon requires identification of the addressable points contained on or within that hull. In §6.6 a method was introduced for finding the points which fall within this hull. This appendix contains a state diagram explaining the sequence of events for just such a procedure. At the bottom of the diagram on the next page is shown the tetrahedron-in-a-box, first introduced in §6.6., which will be used to illustrate the state diagram.

The process begins at the *START* state (See state diagram on the next page) where x, y, and z are initialized to zero. The axes x, y, and z represent the color space coordinates; but the respective pairing with color axes is not fixed. The side of the box which is, on average, closest to all four vertices is chosen to be the $x=0$ plane. The side with the next closest average distance is $y=0$, and similarly for $z=0$. This is a very significant step in the effort to minimize the calculation overhead. All transitions between states in the diagram are marked with the state variable test (a logic expression) followed by a slash and the process performed.

The point $x=y=z=0$ is either in the tetrahedral hull or it is not. If in, the first state transition is to *IN* and generates an interpolation (*interp*) followed by an x increment (*inx*). If out, there is only and x increment and the new state is *OUT1*. While in *OUT1*, x and y are incremented until the point is *IN* the hull. Interpolation occurs at every point while in the hull and upon piercing through to the outside x

INTERPOLATION STATE DIAGRAM

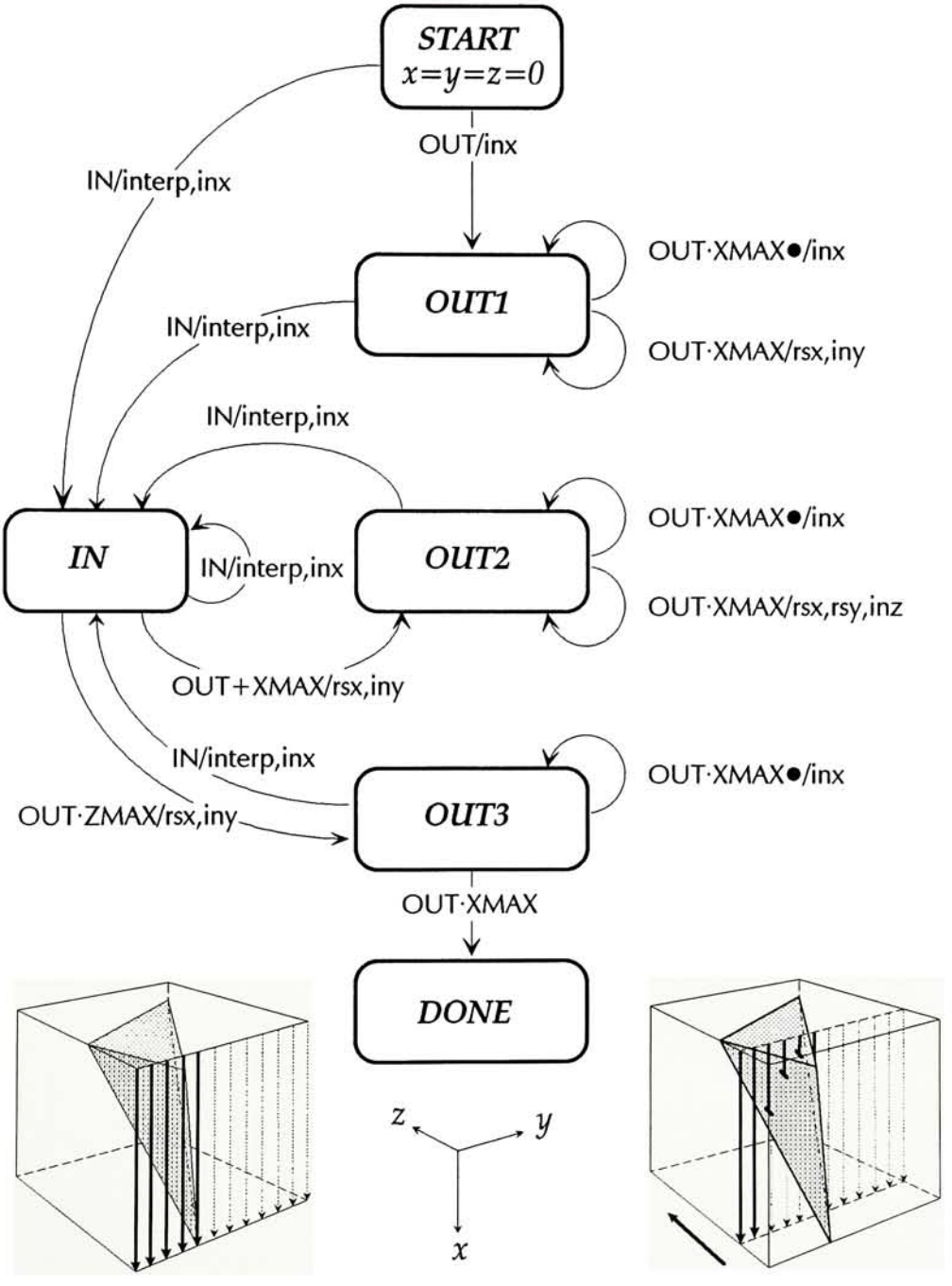

is immediatly reset (*rsx*) and *y* incremented (*iny*). The state transition is to *OUT2* (unless *z* is at its maximum). With *x* reset and *y* incremented, a new arrow is traversed and upon reaching the hull again, the transition is back to *IN*. If the hull is not seen before *x* reaches its maximum, then *x* and *y* are reset and *z* is incremented (*OUT·XMAX/ rsx,rsy,inz*) beginning a new plane of tests. The operation alternates back and forth between *IN* and *OUT2* for most of the duration. When *z* reaches *ZMAX*, each time the hull is exited the transition is to *OUT3* instead of *OUT2*. While in *OUT3*, any sight of the hull returns the state to *IN*. If an entire full length arrow of tests transpire without entering the hull (*OUT·XMAX*), *OUT2* is exited to the *DONE* state. This process is repeated for each tetrahedron within the aggregation.

APPENDIX D
COLOR ERROR TEST IMAGE

Color error tolerance for the different types of color error (§6.2) must be analyzed in order to maximize the efficiency of any color modeling or color space interpolation schemes. This appendix includes a synthetically generated test image designed to verify the relative impact of Type 1 (constant or gradually changing error), Type 2 (systematically arranged step error), and Type 3 (non-differentiable kink) color errors.

The test image is divided into 12 vertical bands. Each band contains a split gradation. Each half of the split gradations start with color *A* and end with color *B* but the paths from *A* to *B* are different. The right half of each split gradation includes a straight-line detour to a different color, *C*, then back to *B* as illustrated in the right half of the diagram below. Each of the 12 bands traverses to a new *C*

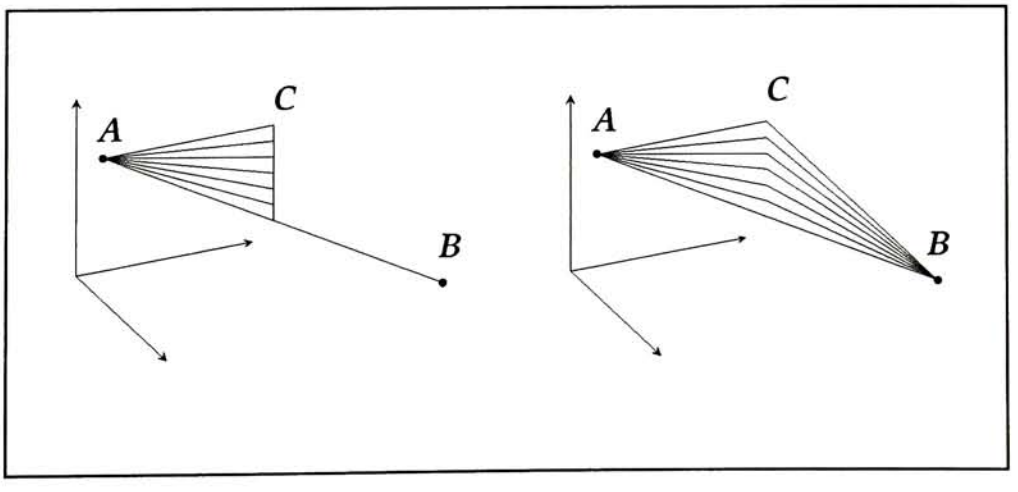

which is a different magnitude of color difference from the straight-line path. This illustrates Type 1 and Type 3 color error. The other half of each band reverts to the straight-line gradation upon reaching color *C* as illustrated by the left half of the diagram. This generates varying amounts of Type 2 (step) color error in equal magnitude as the adjacent Type 1 error.

From the printed test image, one can clearly see the definite ranking of perceptibility. The step error becomes immediately obvious with a just-noticable color difference. It is quite obvious all along the split from *C* to *B*. The Type 1 error becomes (which should be viewed with all but the gradation covered) noticable soon after the Type 2 step error. Of particular interest is the fact that the Type 3 error located at color *C* is undetectable even at large amounts of step change in color error rate-of-change. Specifically, the location of the kink is not perceptable – and the very presence of the sharp kink is not even obvious. Clearly, large amounts of Type 3 error would become a problem, if at all, only after clearly unacceptable amounts of the other two error types existed.

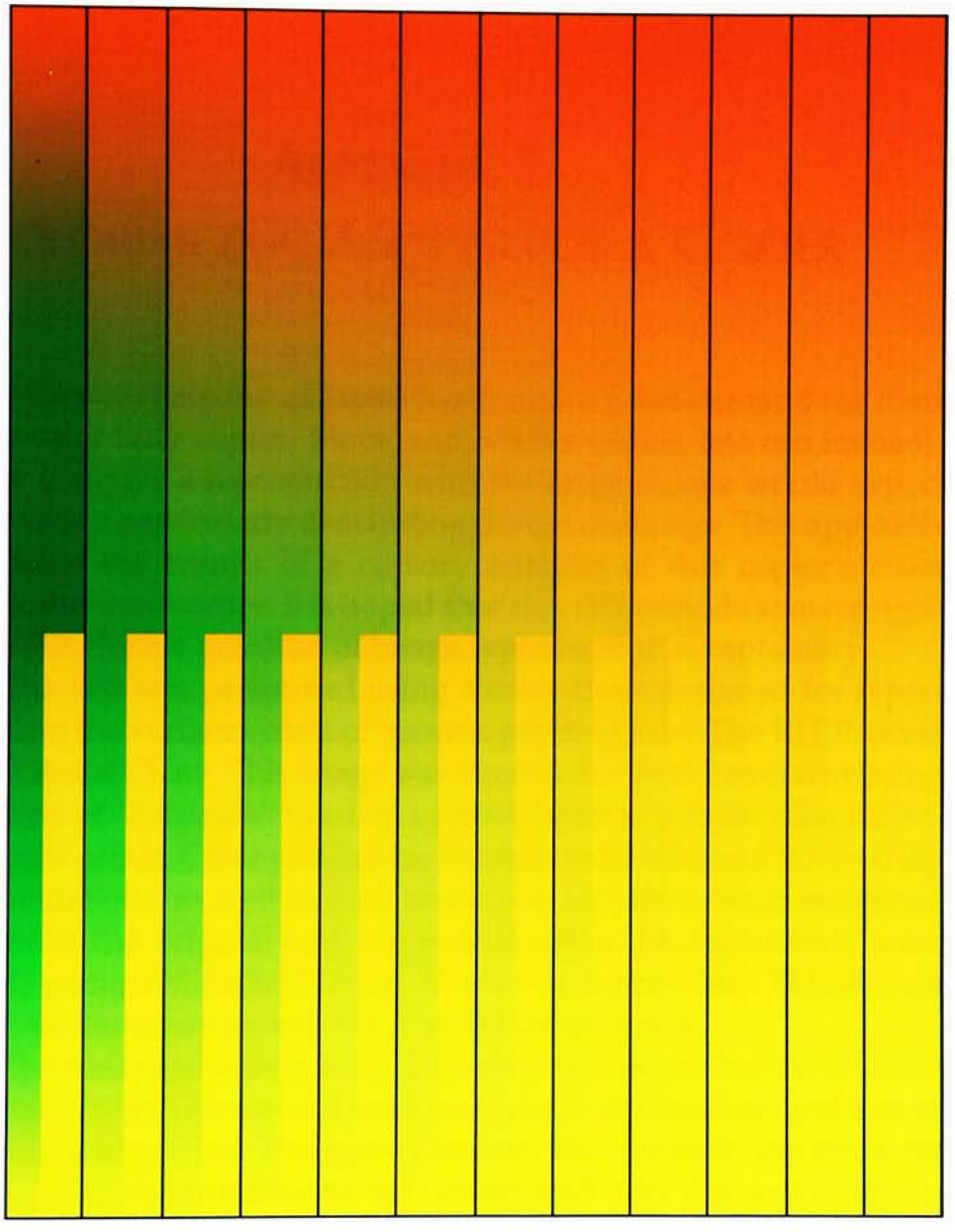

APPENDIX E
COLORIMETRIC ANALYSIS OF A COPIER

The Canon company of Japan has found a great demand for their new color laser copier. Since, with such a copier, one can immediately compare a reproduction with the original, one would expect this to be a particularly demanding design challenge. This appendix contains the results of a cursory analysis of this copier's color reproduction fidelity. It is hoped that this will provide some insight into the elusive question of image reproduction acceptability.

The test was performed using a color chart designed for representing the surface colors of process printing inks: The RIT Process Ink Gamut Chart. This image was chosen due to the overwhelming portion of "originals" used on a photocopier which are offset lithographic prints. Color patches for all eight solid inks and ink overlap combinations, as well as their respective 50% tints, were measured on both the original and the reproduction. Measurements were made using a Minolta Chroma Meter which provides CIELAB data for D65 illumination and the 2° standard observer.

The next page shows, in CIELAB coordinates, the hue error of the reproduction. The colored markers indicate the location and hue of the original patches. The arrows indicate the hue shift: the arrow tip being at the coordinates of the reproduced hue. The solid patches generally became desaturated while the tints were reproduced with slightly exaggerated saturation. The following page contains the data in tabulated form. Note the general compression of the lightness range.

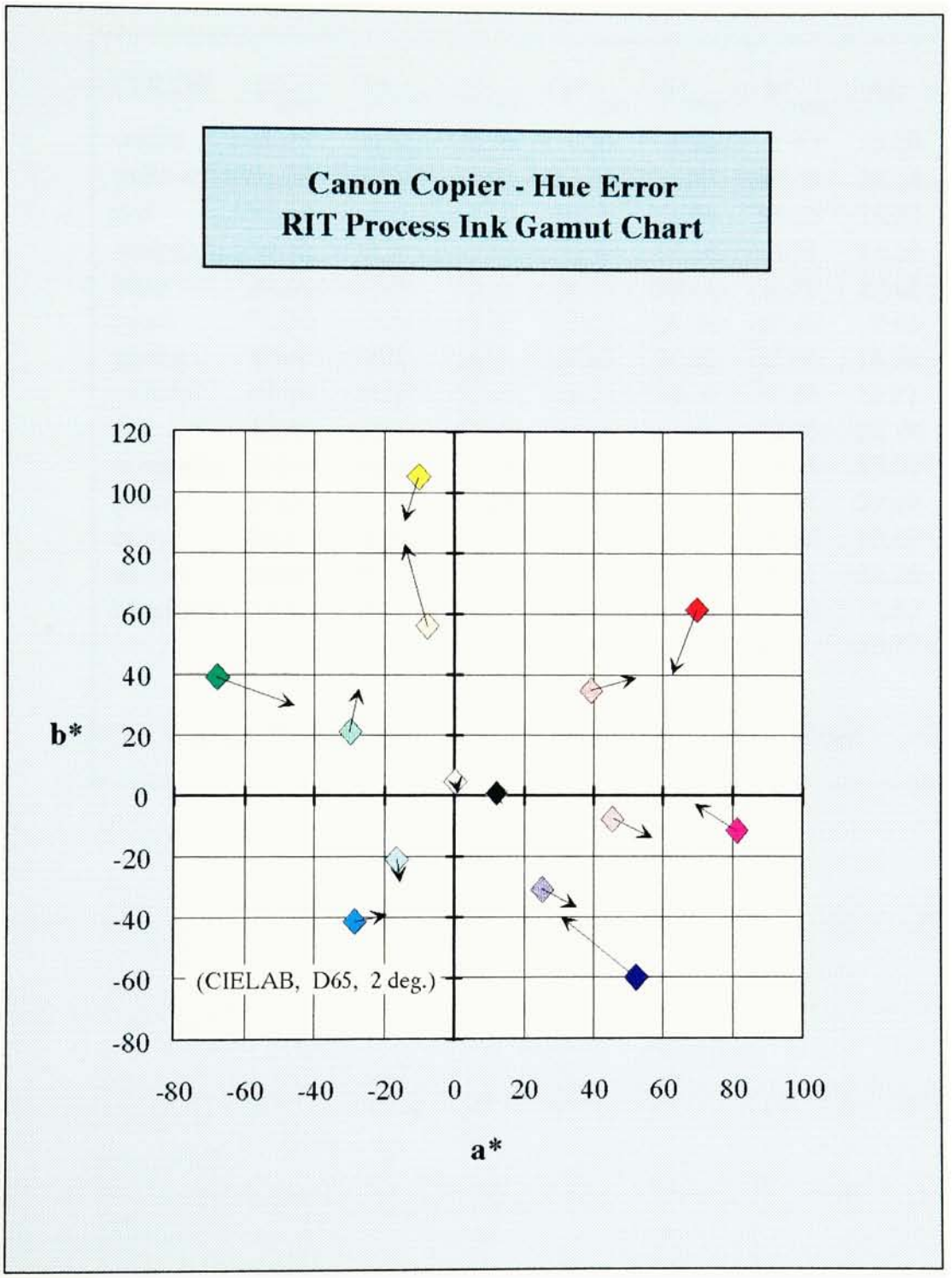
Canon Copier - Hue Error
RIT Process Ink Gamut Chart
b*
a*
120
100
80
60
40
20
0
-20
-40
-60
-80
-80 -60 -40 -20 0 20 40 60 80 100
(CIELAB, D65, 2 deg.)

COLOR	L^*_{ORIG}	L^*_{COPY}	a^*_{ORIG}	a^*_{COPY}	b^*_{ORIG}	b^*_{COPY}	ΔE
white	98.48	94.50	0.22	0.91	4.54	1.13	5.29
yellow	91.67	90.13	-7.90	-14.35	55.77	83.10	28.12
red	66.32	54.11	39.06	52.08	34.93	39.12	18.33
magenta	66.18	59.64	45.59	56.59	-7.68	-13.91	14.23
blue	50.14	43.26	25.20	34.99	-30.64	-36.70	13.41
cyan	72.79	70.26	-16.41	-15.77	-20.94	-28.33	7.84
green	69.07	62.29	-30.06	-27.55	21.22	35.02	15.58
yellow	89.69	89.55	-10.44	-14.37	104.98	90.81	14.71
red	48.56	46.53	69.68	62.85	61.30	40.28	22.19
magenta	49.54	48.47	81.29	69.12	-11.63	-2.86	15.04
blue	15.55	17.75	52.28	30.59	-60.13	-40.11	29.60
cyan	53.17	58.91	-28.31	-19.60	-41.53	-39.18	10.69
green	48.50	43.34	-67.76	-45.98	39.16	29.81	24.26
black(3c)	17.17	16.69	11.96	10.63	0.82	1.33	1.50
						Average:	15.77

CANON COLOR COPIER — COLOR ERROR, RIT GAMUT CHART

APPENDIX F
MEASURED GAMUT DATA

Characterization of the size, shape, and internal structure of a printing process's printable color gamut is an important facet of optimized color transformation modeling, whether for interpolation, mathematical modeling or some combination of both.

This appendix contains relevant data for two different printing processes: ink-jet and offset lithograph. The ink-jet data, comprising §F.1, was measured from a test image similar to the one included on page F-3. This image was printed on an Iris Graphics Series 3000 printer at 240 spots per inch and 32 spot sizes dithered to 256 gray levels. The paper used was Crystal White from Aussedat Rey in France. The inks are standard issue from Iris and were printed with 50% GCR.

The process ink measurements are from the *Process Color Guide* by S. D. Scott. The paper used was Hammermill Offset Opaque basis 80. The inks are manufactured by Superior Printing Ink Company in New York City. The sequence was K,C,M,Y. A Miehle-Roland 28×40 4-color press was used.

All measurements were performed with a colorimeter from Minolta using D65 illumination and CIELAB color coordinates for the 2° Standard Observer. All 12 edges of the printer's color gamut were measured. Additional measurements were made in the interior of the cube faces and within the cube. For additional details and extracted information see Chapter 7.

F.1 INK-JET GAMUT DATA

Page F-3 contains an example of the test image measured for these plots. Pages F-4 through F-6 are the 2D projections of the gamut mapped into CIELAB color space. The color of the diamond line markers along each edge indicate the final color (maximum ink) of the edge. For example the yellow diamonds delineate the white-to-yellow edge and the red diamonds indicate the yellow-to-red and magenta-to-red edges.

Pages F-7 through F-9 show incremental color change per drop along the 12 edges of the cube. The final value (for 31 drops) then is the total length of the edge in CIELAB ΔE units. These first six plots are printed with a pink background.

The remaining pages of section F.1 (F-10 through F-21) are plots of the color coordinates of the 12 edges, one per page, showing the CIELAB values and the color change per drop (the plots on F-7 through F-9 are integrations of this color change data), as well as the color difference from the originating vertex directly to each point. The final value of this last curve gives the vertex-to-vertex distance of the edge. These 12 pages are printed with a blue background. The a* and b* values are printed with red and yellow line markers, respectively, in keeping with the measured redness and blueness as represented in CIELAB space.

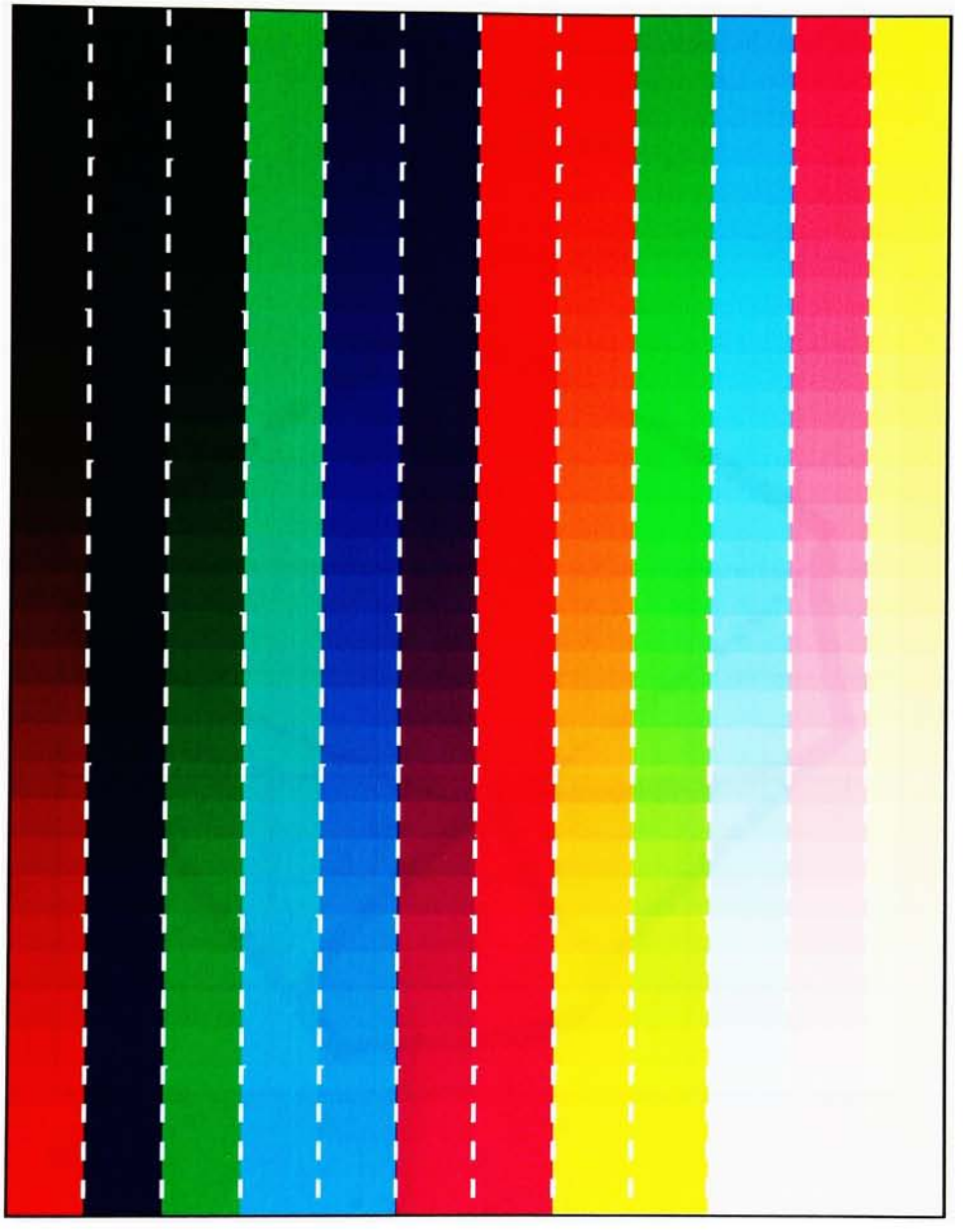

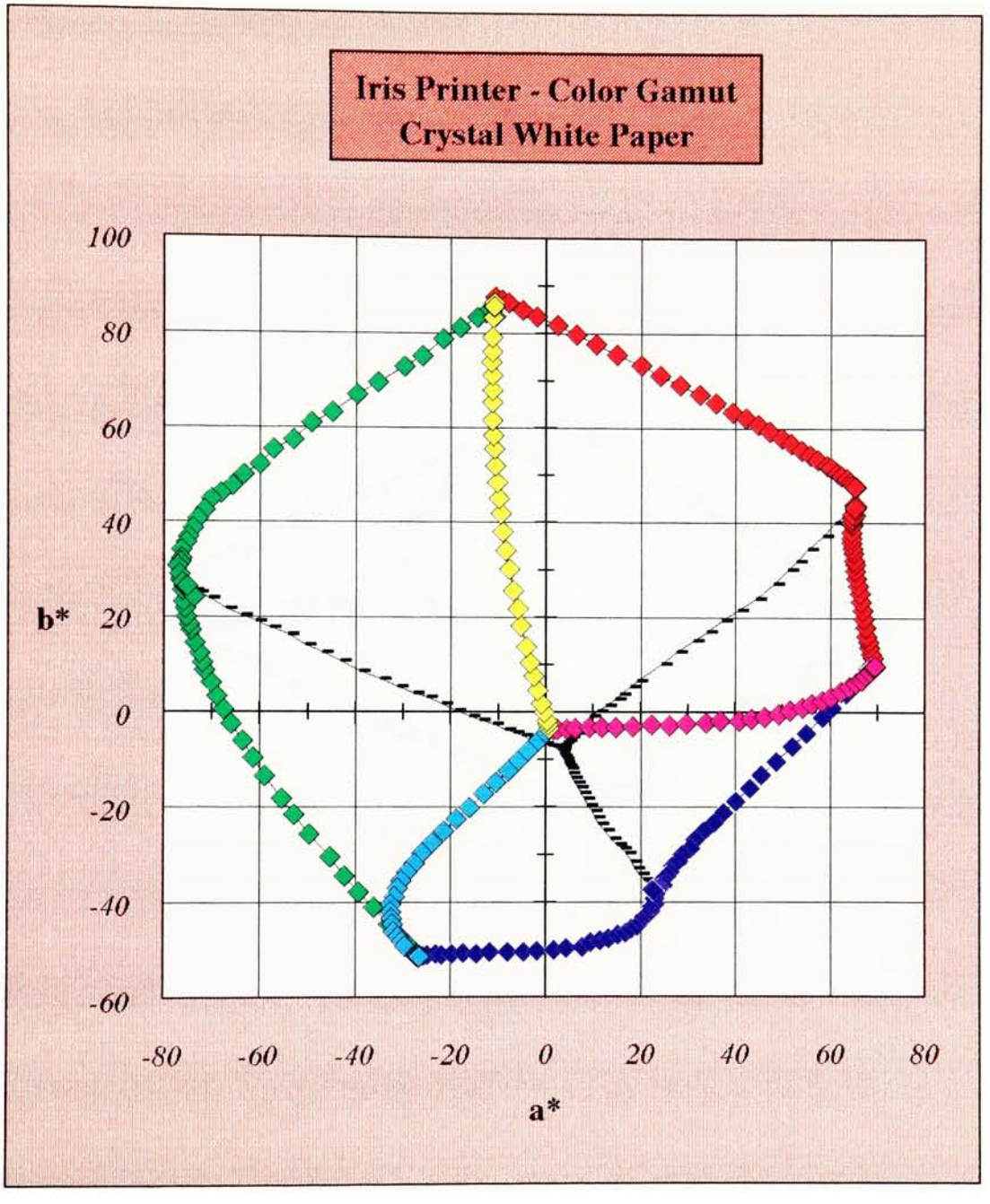
Iris Printer - Color Gamut
Crystal White Paper
100
80
60
40
b* 20
0
-20
-40
-60
-80
-60
-40
-20
0
20
40
60
80
a*

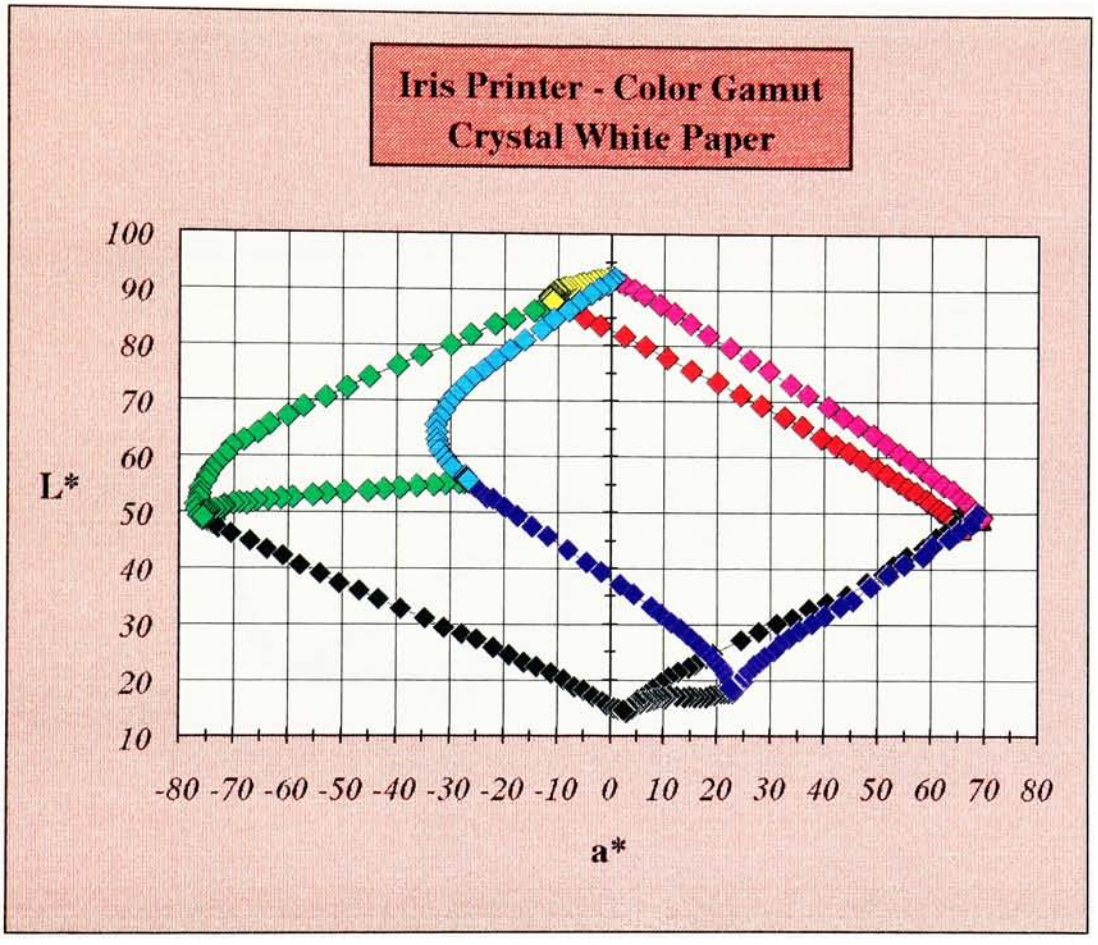
Iris Printer - Color Gamut
Crystal White Paper
L*
100
90
80
70
60
50
40
30
20
10
-80 -70 -60 -50 -40 -30 -20 -10 0 10 20 30 40 50 60 70 80
a*

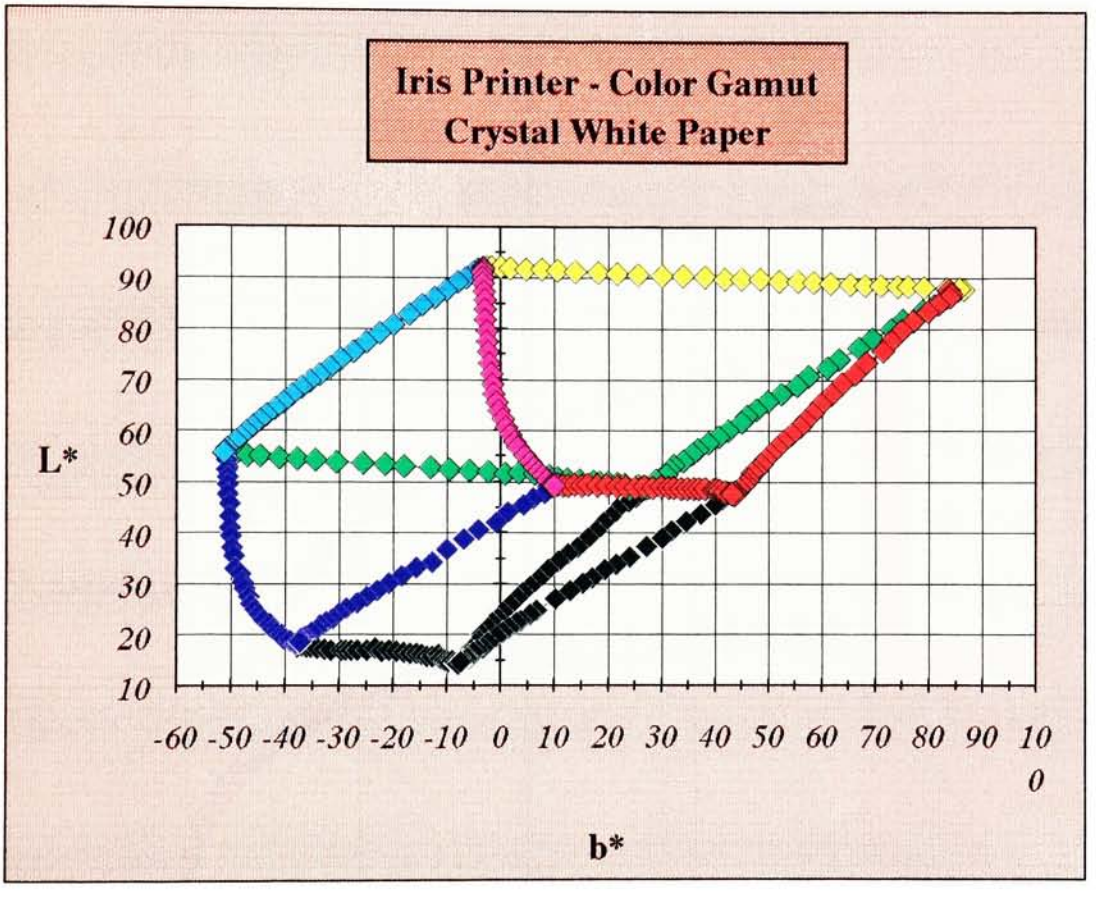
Iris Printer - Color Gamut
Crystal White Paper
L*
100
90
80
70
60
50
40
30
20
10
-60 -50 -40 -30 -20 -10 0 10 20 30 40 50 60 70 80 90 100
b*

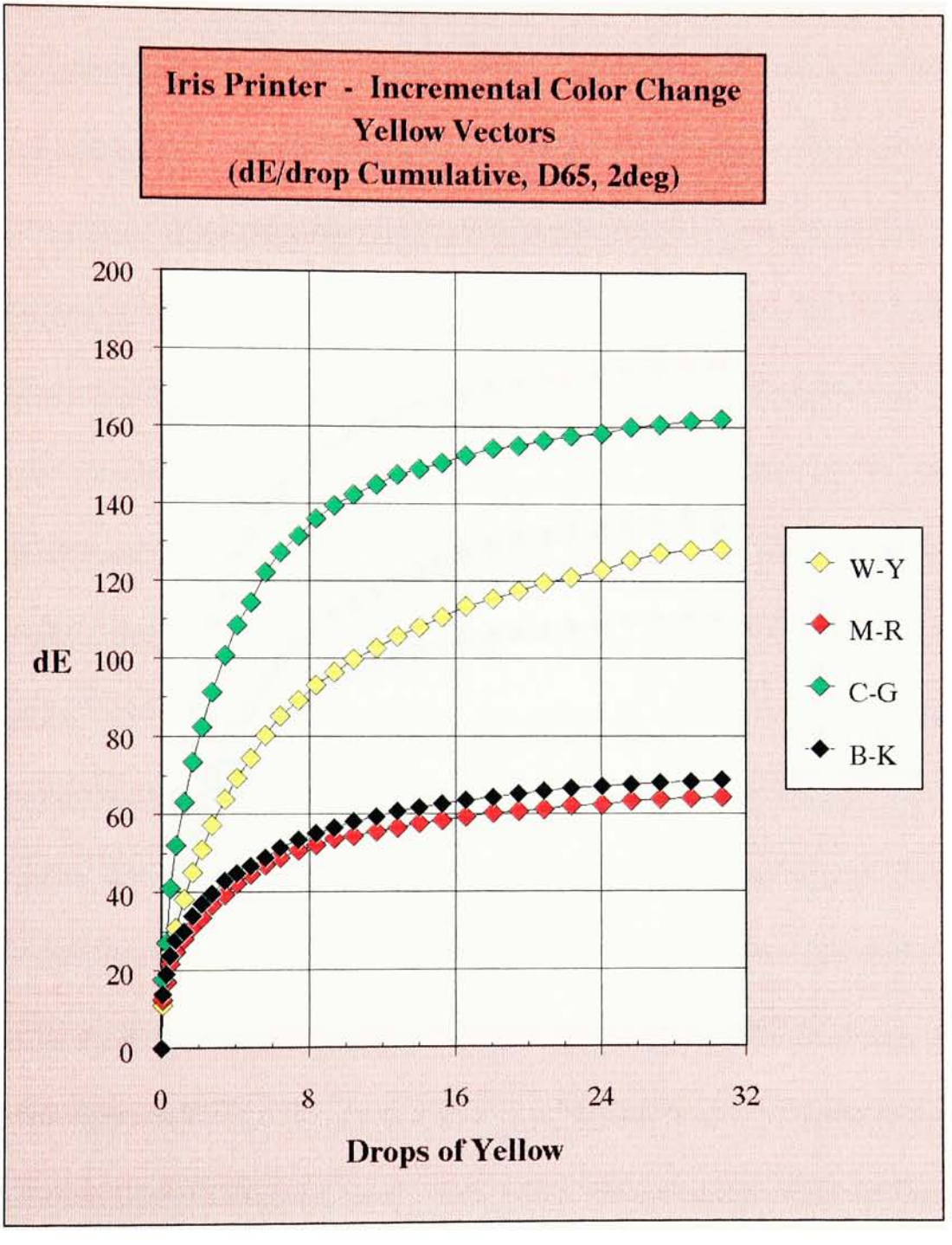
Iris Printer - Incremental Color Change
Yellow Vectors
(dE/drop Cumulative, D65, 2deg)
dE
200
180
160
140
120
100
80
60
40
20
0
0
8
16
24
32
Drops of Yellow
W-Y
M-R
C-G
B-K

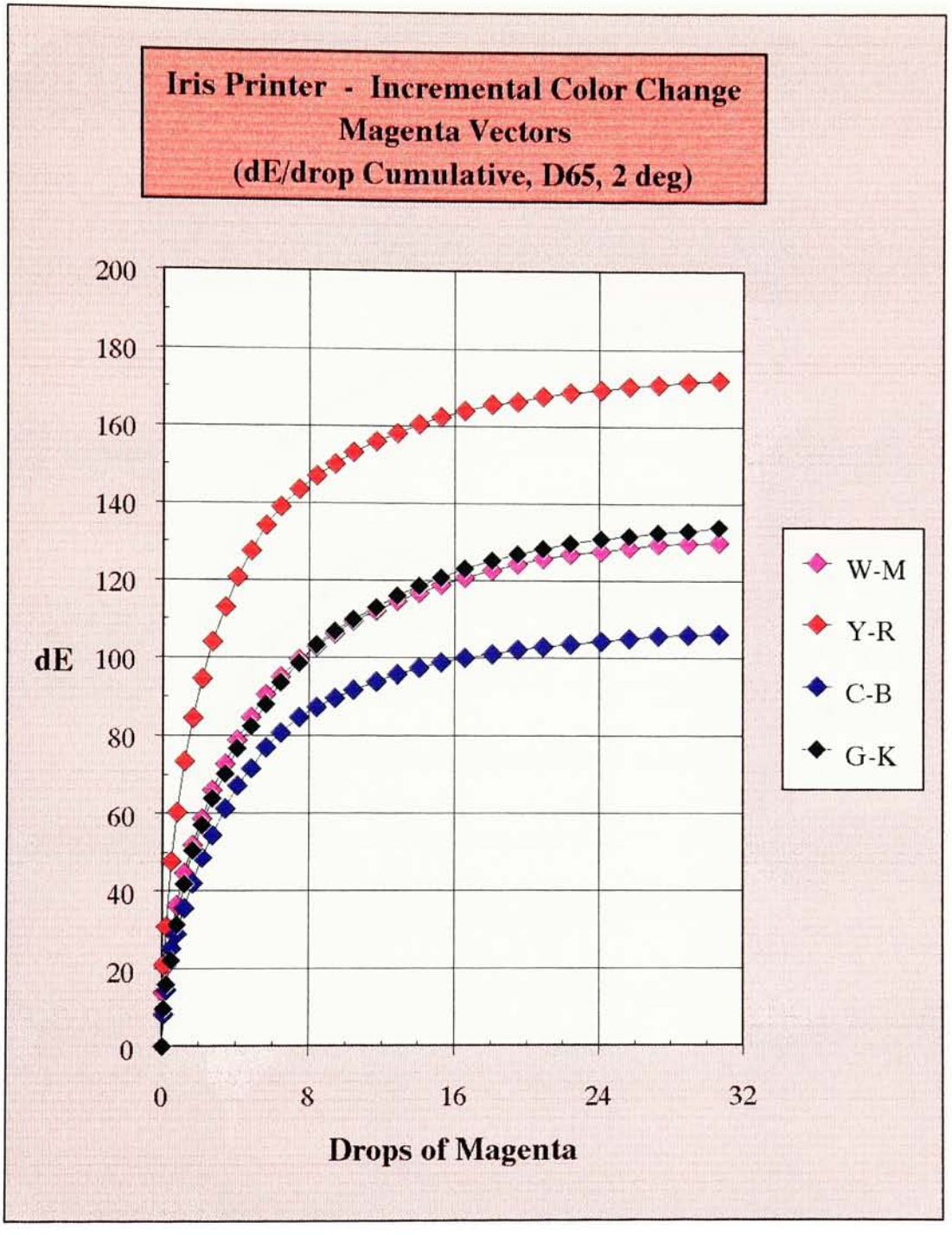
Iris Printer - Incremental Color Change
Magenta Vectors
(dE/drop Cumulative, D65, 2 deg)
dE
200
180
160
140
120
100
80
60
40
20
0
0
8
16
24
32
Drops of Magenta
W-M
Y-R
C-B
G-K

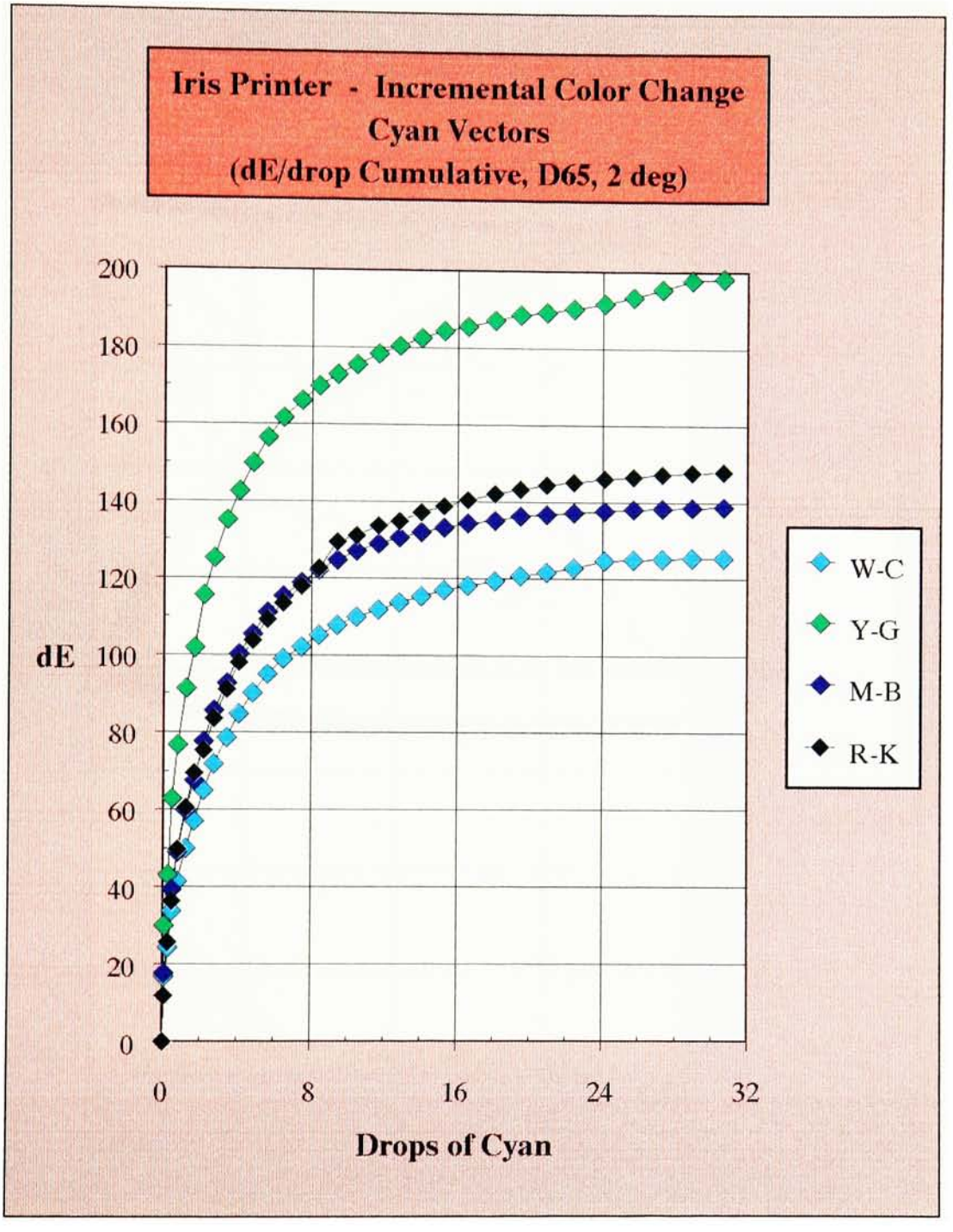
Iris Printer - Incremental Color Change
Cyan Vectors
(dE/drop Cumulative, D65, 2 deg)
dE
200
180
160
140
120
100
80
60
40
20
0
0
8
16
24
32
Drops of Cyan
W-C
Y-G
M-B
R-K

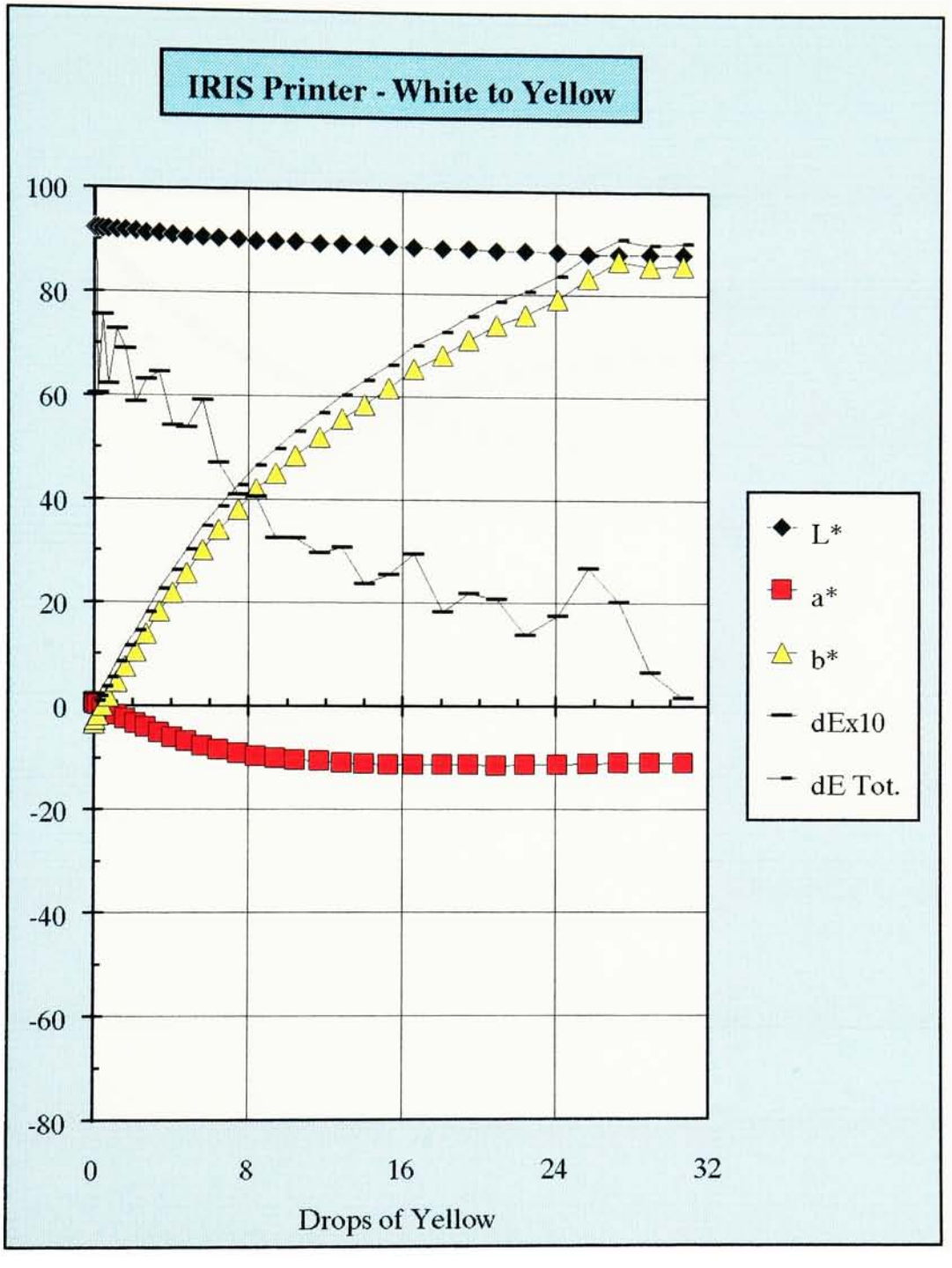
IRIS Printer - White to Yellow
100
80
60
40
20
0
-20
-40
-60
-80
0
8
16
24
32
Drops of Yellow
L*
a*
b*
dEx10
dE Tot.

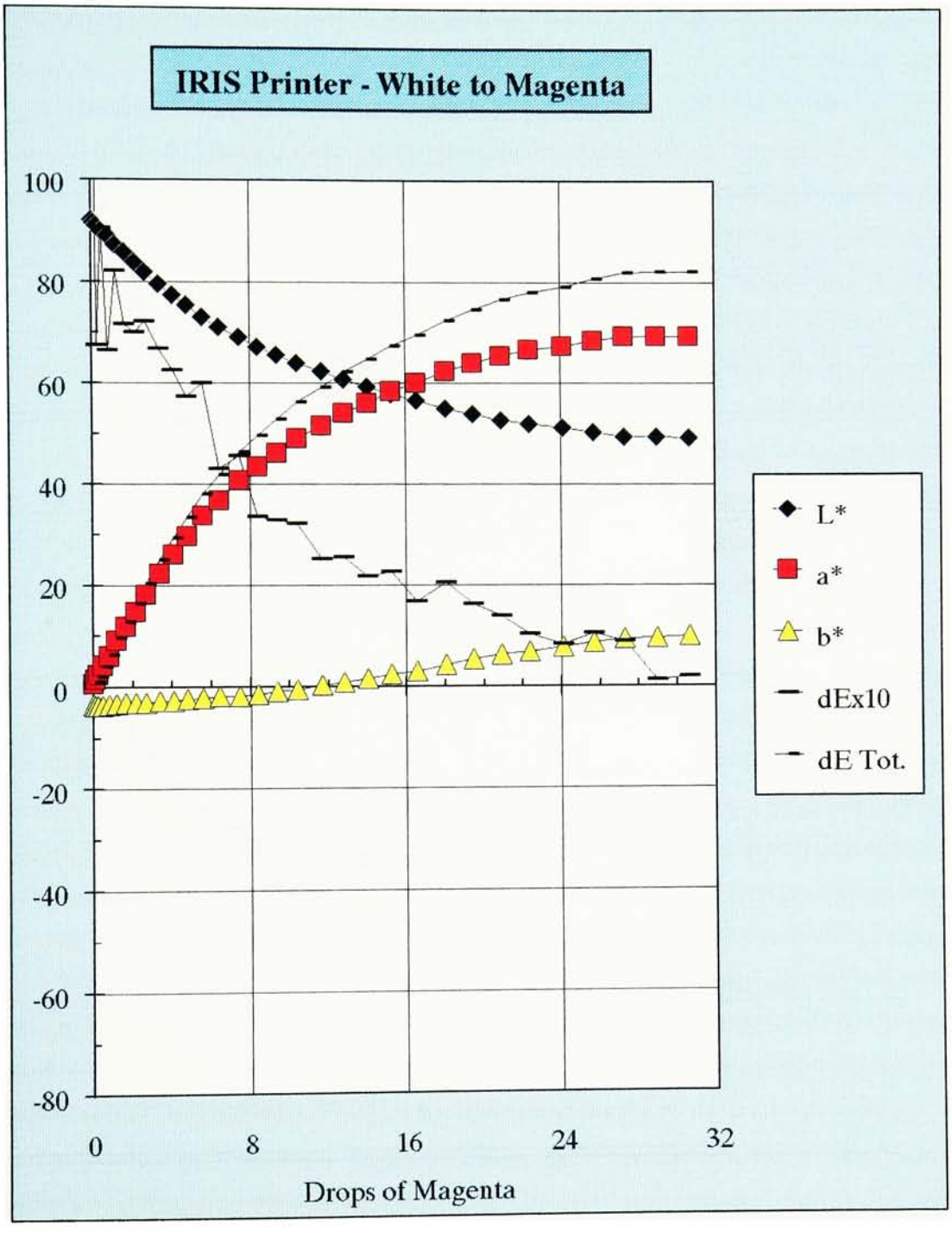
IRIS Printer - White to Magenta
100
80
60
40
20
0
-20
-40
-60
-80
0
8
16
24
32
Drops of Magenta
L*
a*
b*
dEx10
dE Tot.

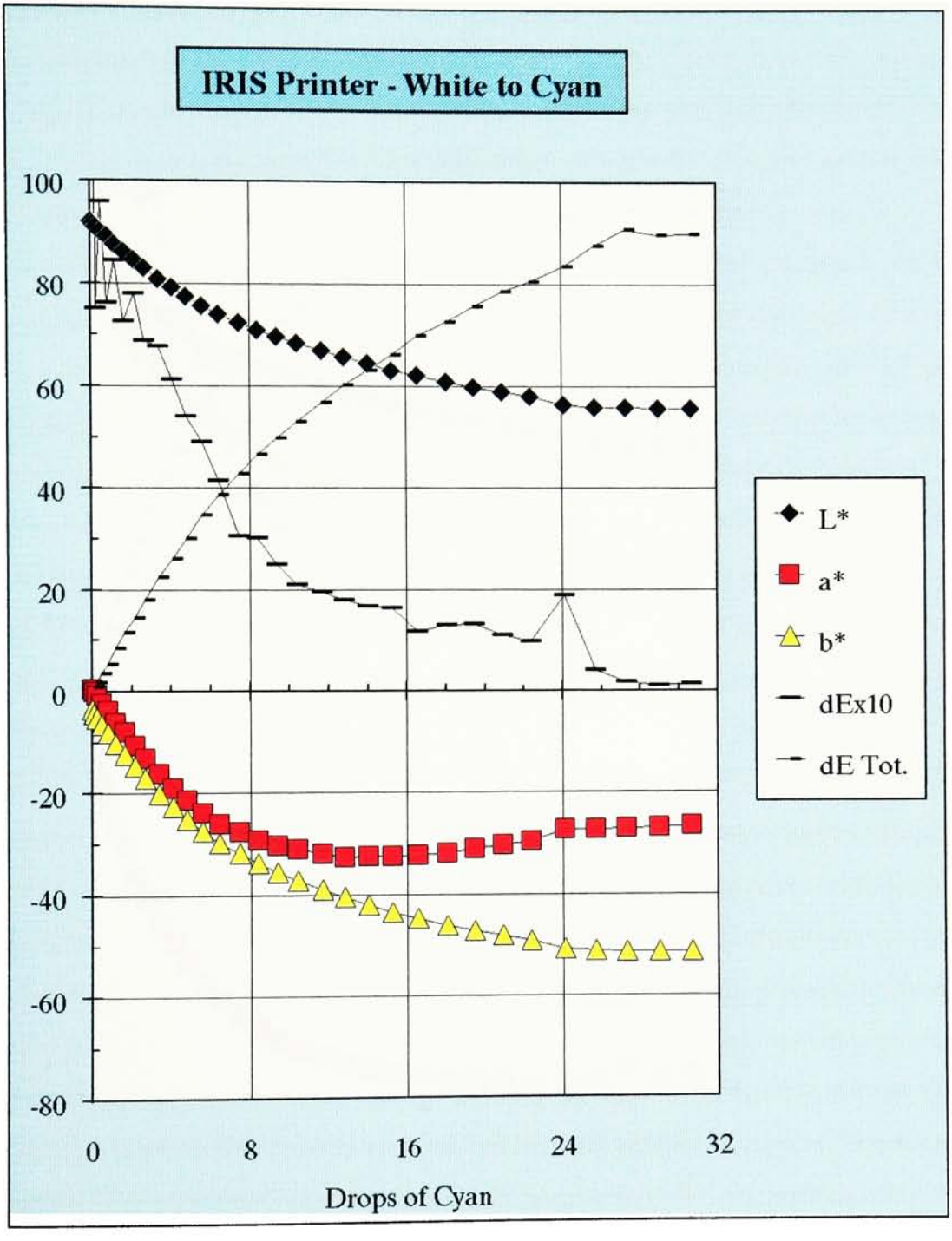
IRIS Printer - White to Cyan
100
80
60
40
20
0
-20
-40
-60
-80
0
8
16
24
32
Drops of Cyan
L*
a*
b*
dEx10
dE Tot.

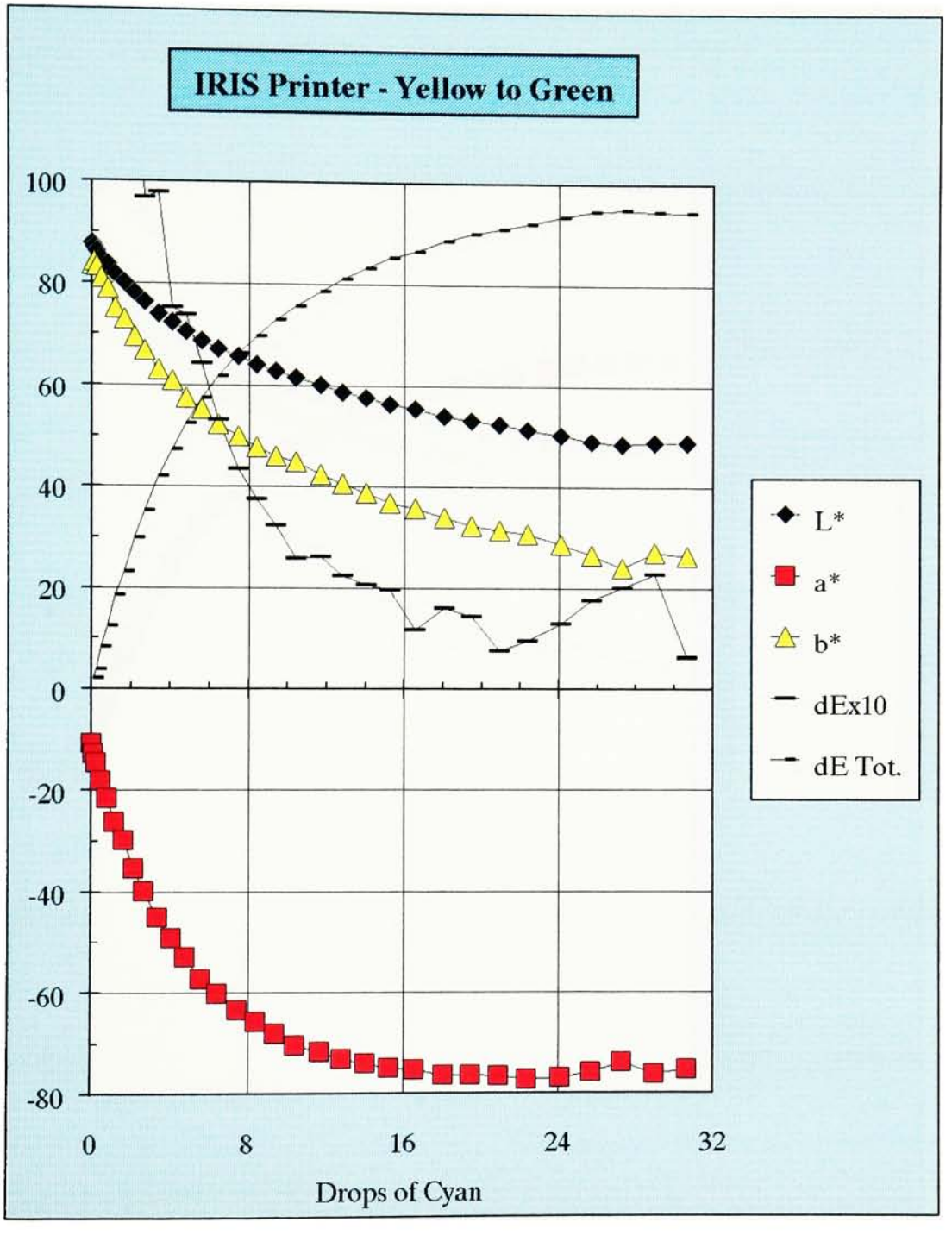
IRIS Printer - Yellow to Green
100
80
60
40
20
0
-20
-40
-60
-80
0
8
16
24
32
Drops of Cyan
L*
a*
b*
dEx10
dE Tot.

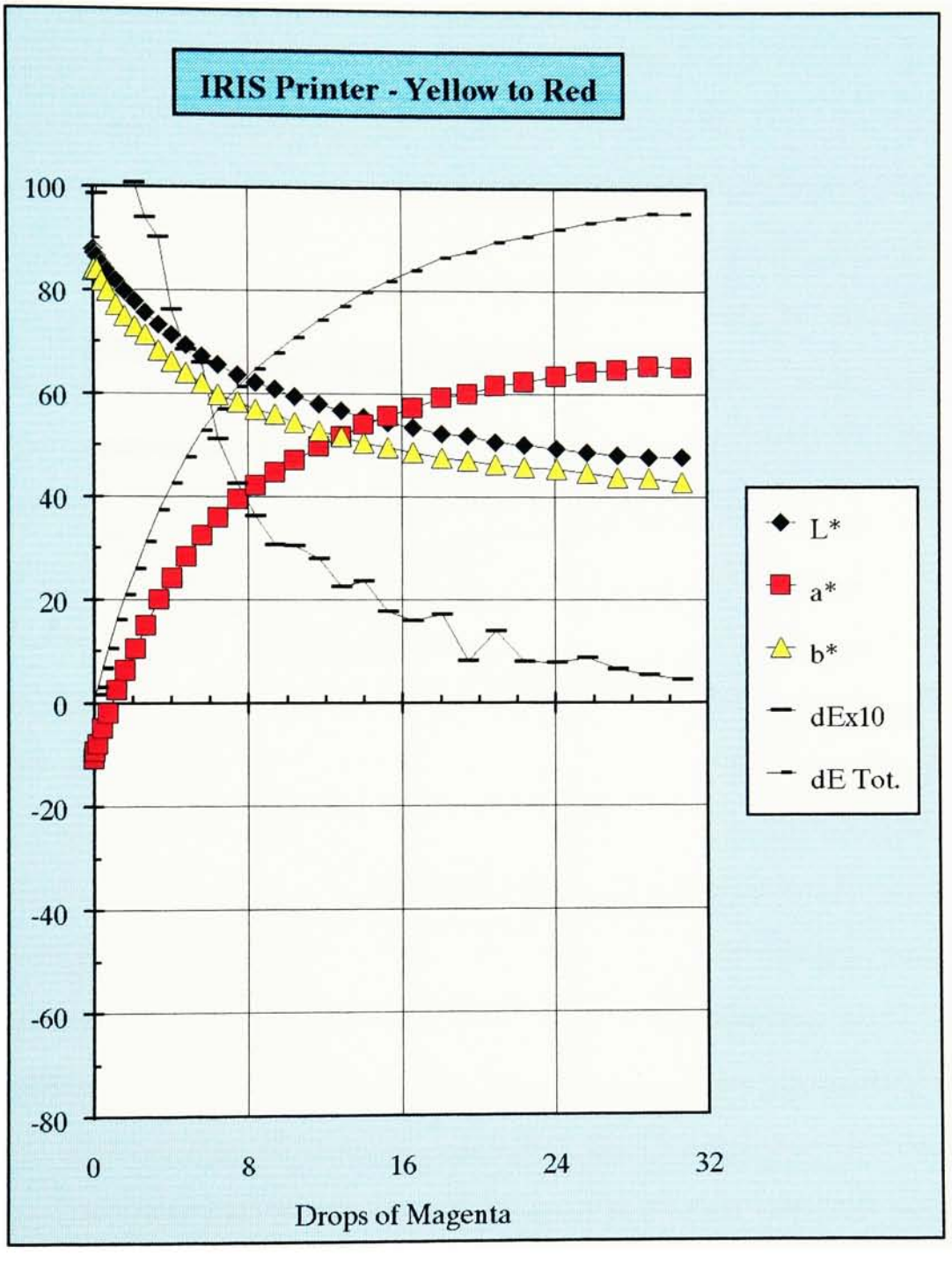
IRIS Printer - Yellow to Red
100
80
60
40
20
0
-20
-40
-60
-80
0
8
16
24
32
Drops of Magenta
L*
a*
b*
dEx10
dE Tot.

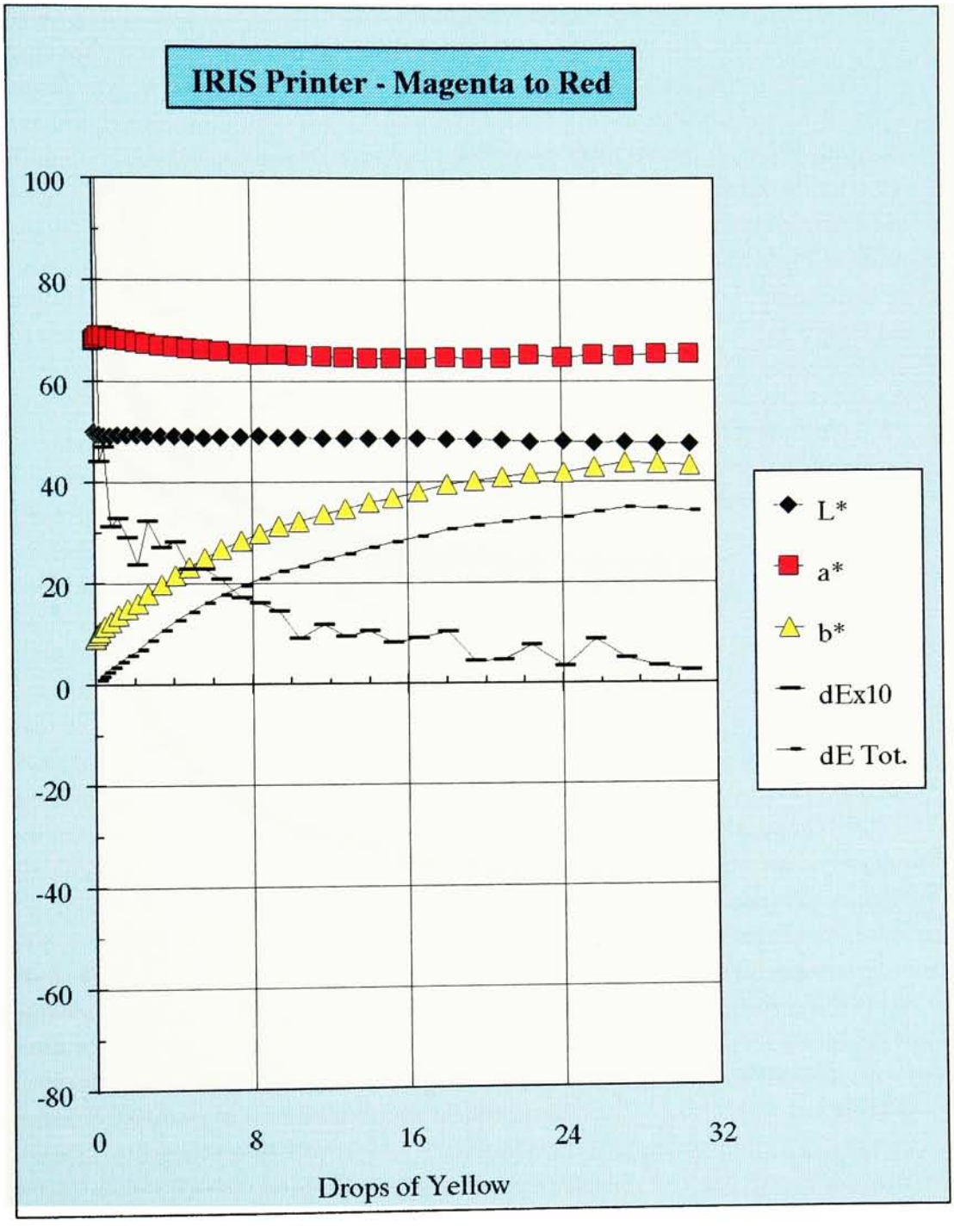
IRIS Printer - Magenta to Red
100
80
60
40
20
0
-20
-40
-60
-80
0
8
16
24
32
Drops of Yellow
L*
a*
b*
dEx10
dE Tot.

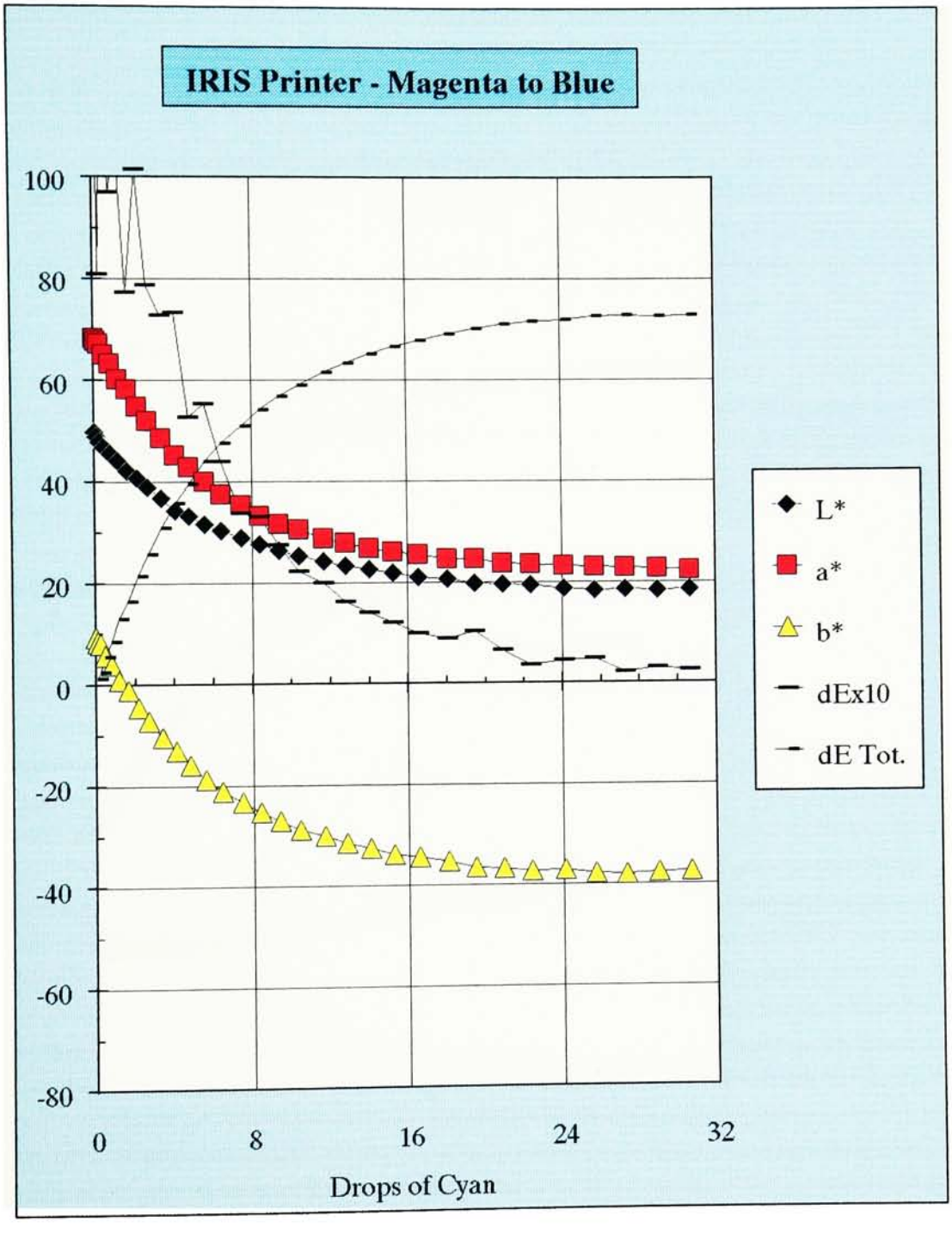
IRIS Printer - Magenta to Blue
100
80
60
40
20
0
-20
-40
-60
-80
0
8
16
24
32
Drops of Cyan
L*
a*
b*
dEx10
dE Tot.

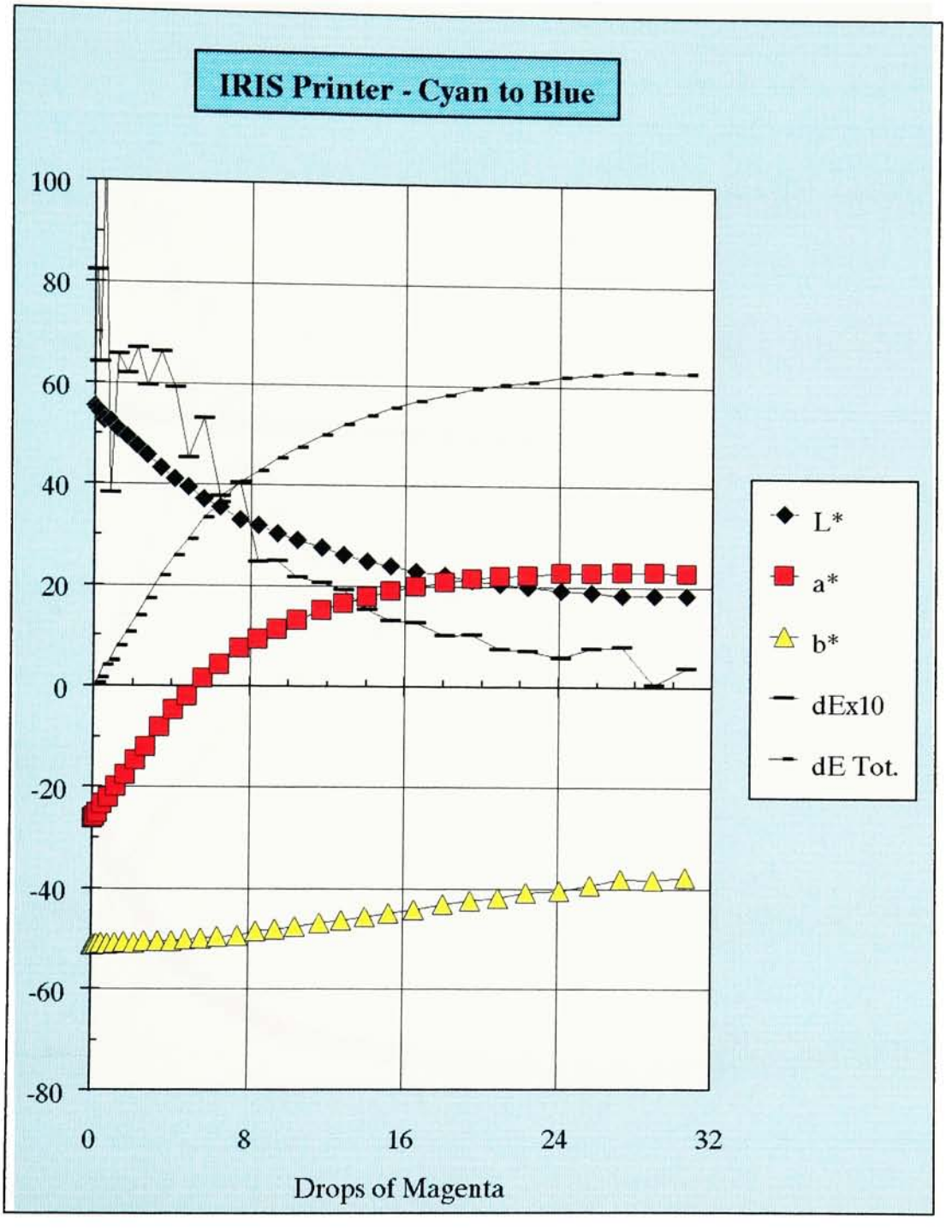
IRIS Printer - Cyan to Blue
100
80
60
40
20
0
-20
-40
-60
-80
0
8
16
24
32
Drops of Magenta
L*
a*
b*
dEx10
dE Tot.

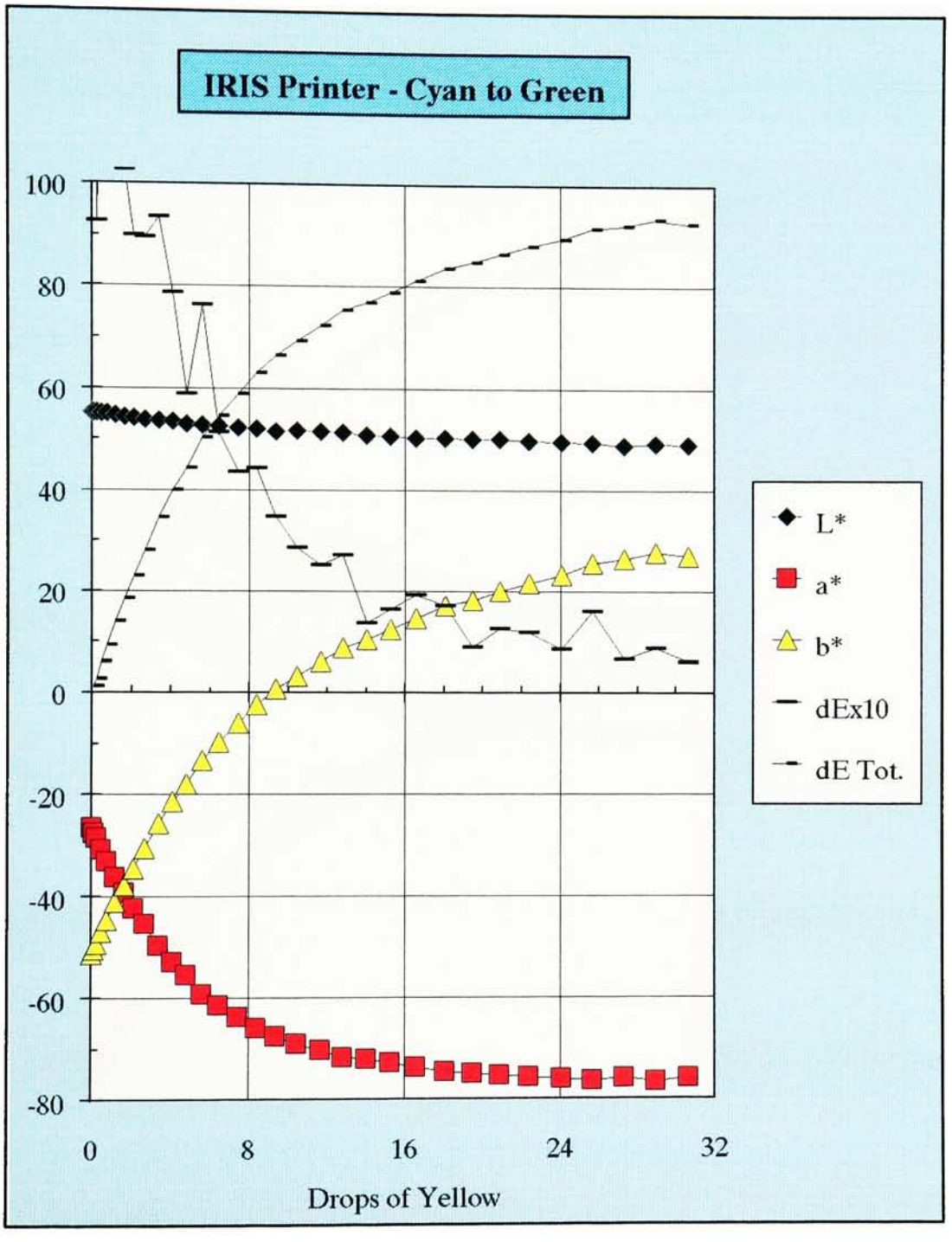
IRIS Printer - Cyan to Green
100
80
60
40
20
0
-20
-40
-60
-80
0
8
16
24
32
Drops of Yellow
L*
a*
b*
dEx10
dE Tot.

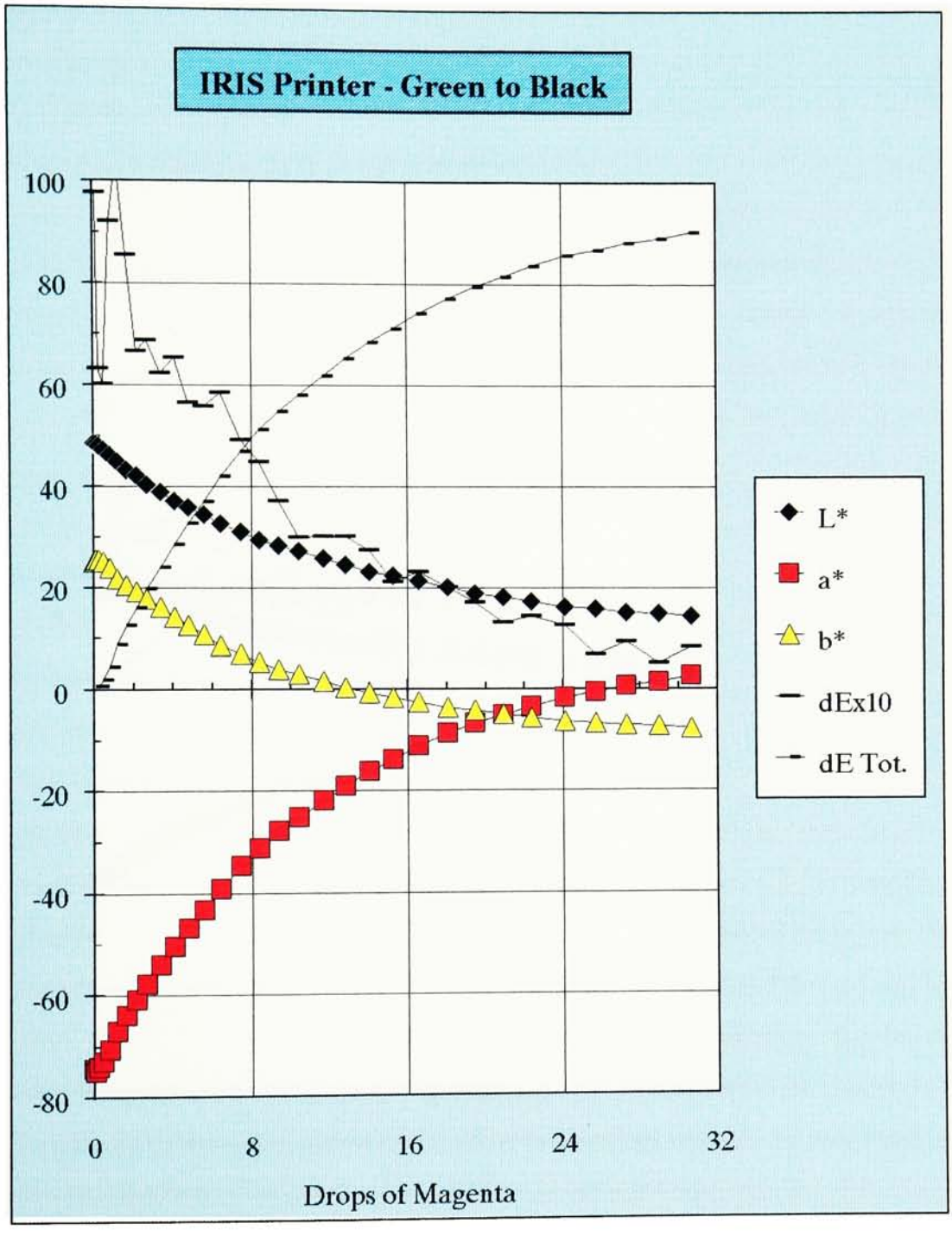
IRIS Printer - Green to Black
100
80
60
40
20
0
-20
-40
-60
-80
0
8
16
24
32
Drops of Magenta
L*
a*
b*
dEx10
dE Tot.

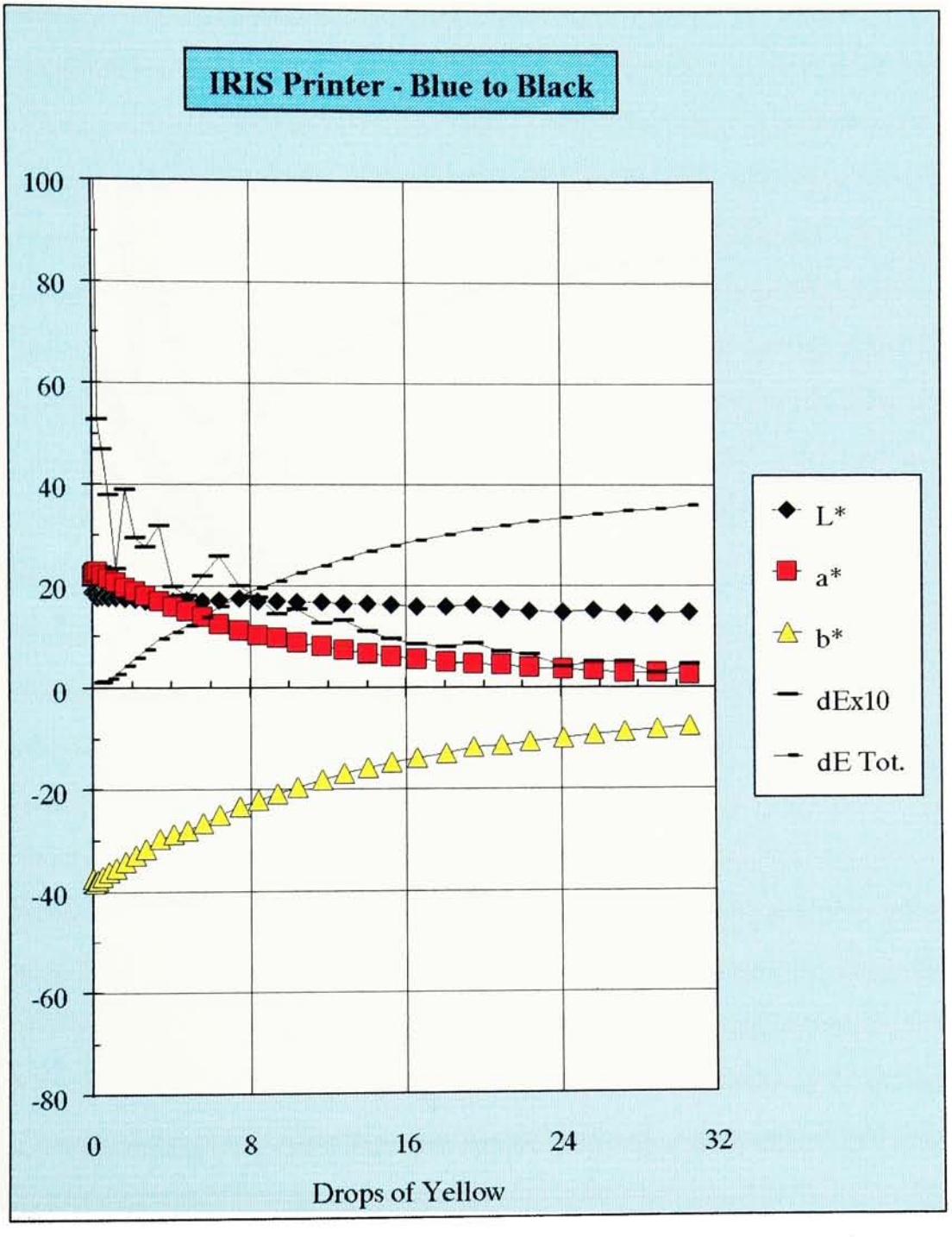
IRIS Printer - Blue to Black
100
80
60
40
20
0
-20
-40
-60
-80
0
8
16
24
32
Drops of Yellow
L*
a*
b*
dEx10
dE Tot.

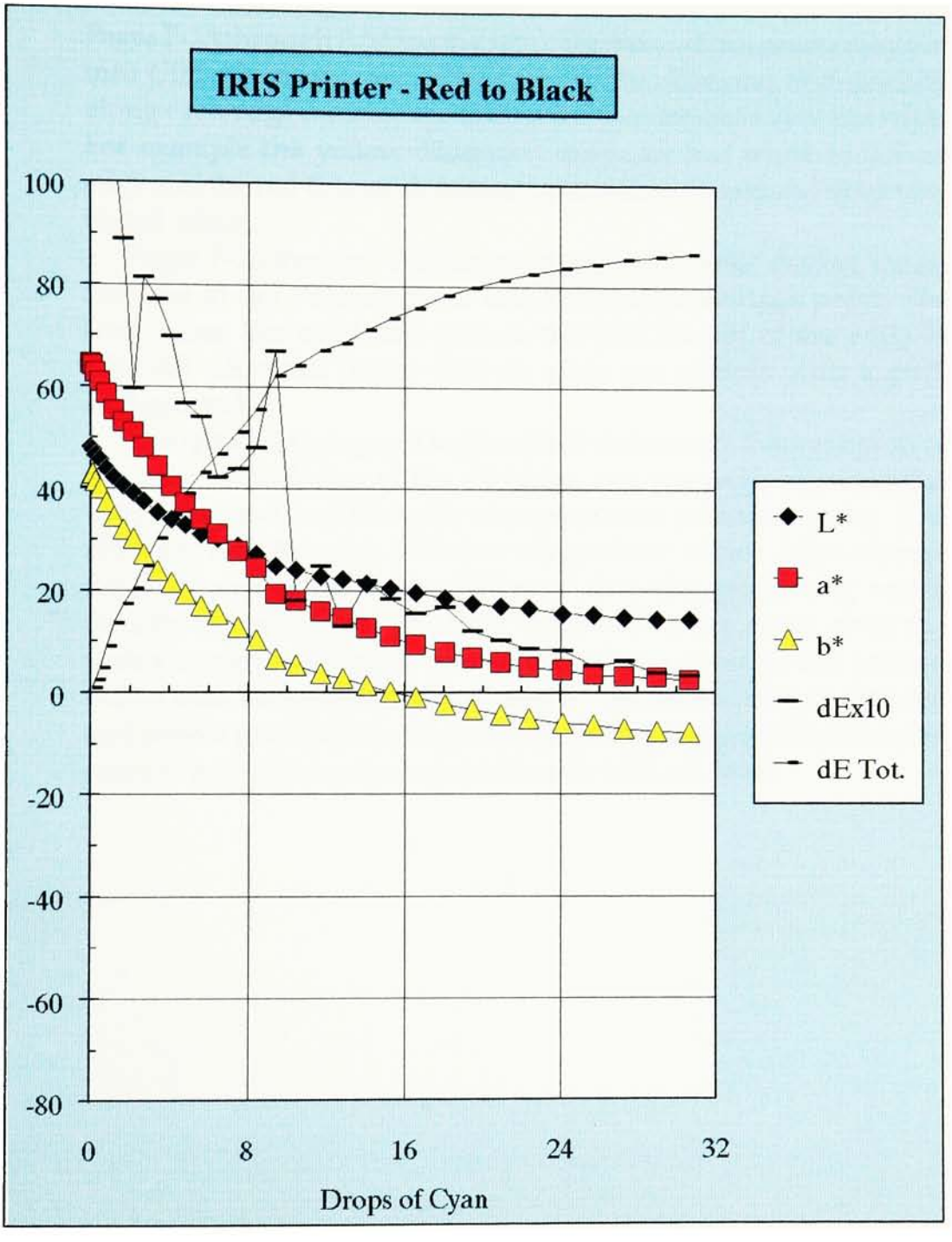
IRIS Printer - Red to Black
100
80
60
40
20
0
-20
-40
-60
-80
0
8
16
24
32
Drops of Cyan
L*
a*
b*
dEx10
dE Tot.

F.2 OFFSET LITHOGRAPHY GAMUT DATA

Pages F-23 through F-25 are the 2D projections of the gamut mapped into CIELAB color space. The color of the diamond line markers along each edge indicate the final color (maximum ink) of the edge. For example the yellow diamonds delineate the white-to-yellow edge and the red diamonds indicate the yellow-to-red and magenta-to-red edges.

Pages F-26 through F-28 show incremental color change for an increase in dot percentage of one nominal percentage point. The final value (for solid ink) then is the total length of the edge in CIELAB ΔE units. These first six plots are printed with a pink background.

The remaining pages of section F.2 (F-29 through F-40) are plots of the color coordinates of the 12 edges, one per page, showing the CIELAB values and the color change per dot percenate point (the plots on F-26 through F-28 are integrations of this color change data), as well as the color difference from the originating vertex directly to each point. The final value of this last curve gives the vertex-to-vertex distance of the edge. These 12 pages are printed with a blue background. The a* and b* values are printed with red and yellow line markers, respectively, in keeping with the measured redness and blueness as represented in CIELAB space.

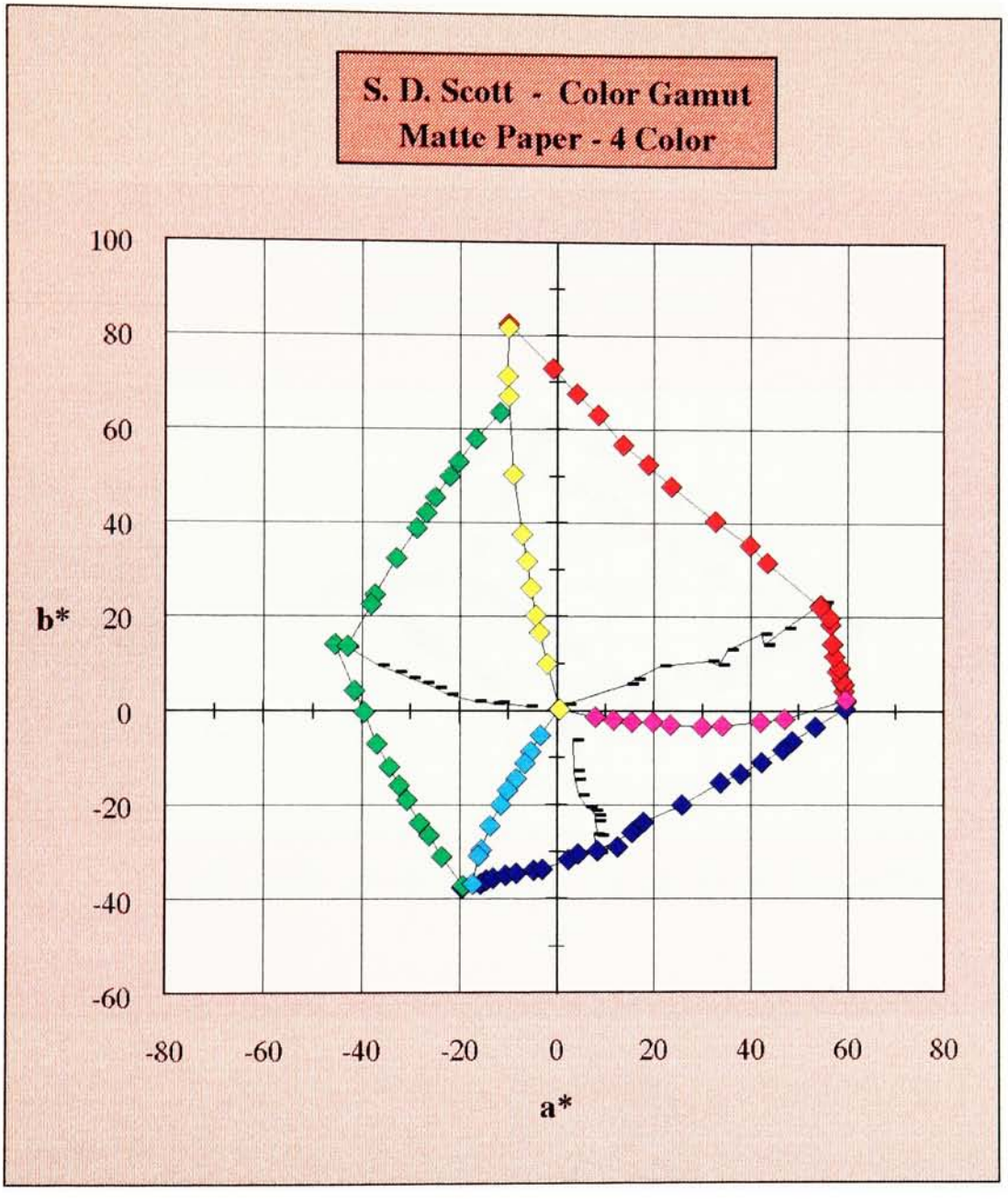
S. D. Scott - Color Gamut
Matte Paper - 4 Color
b*
a*
100
80
60
40
20
0
-20
-40
-60
-80
-60
-40
-20
0
20
40
60
80

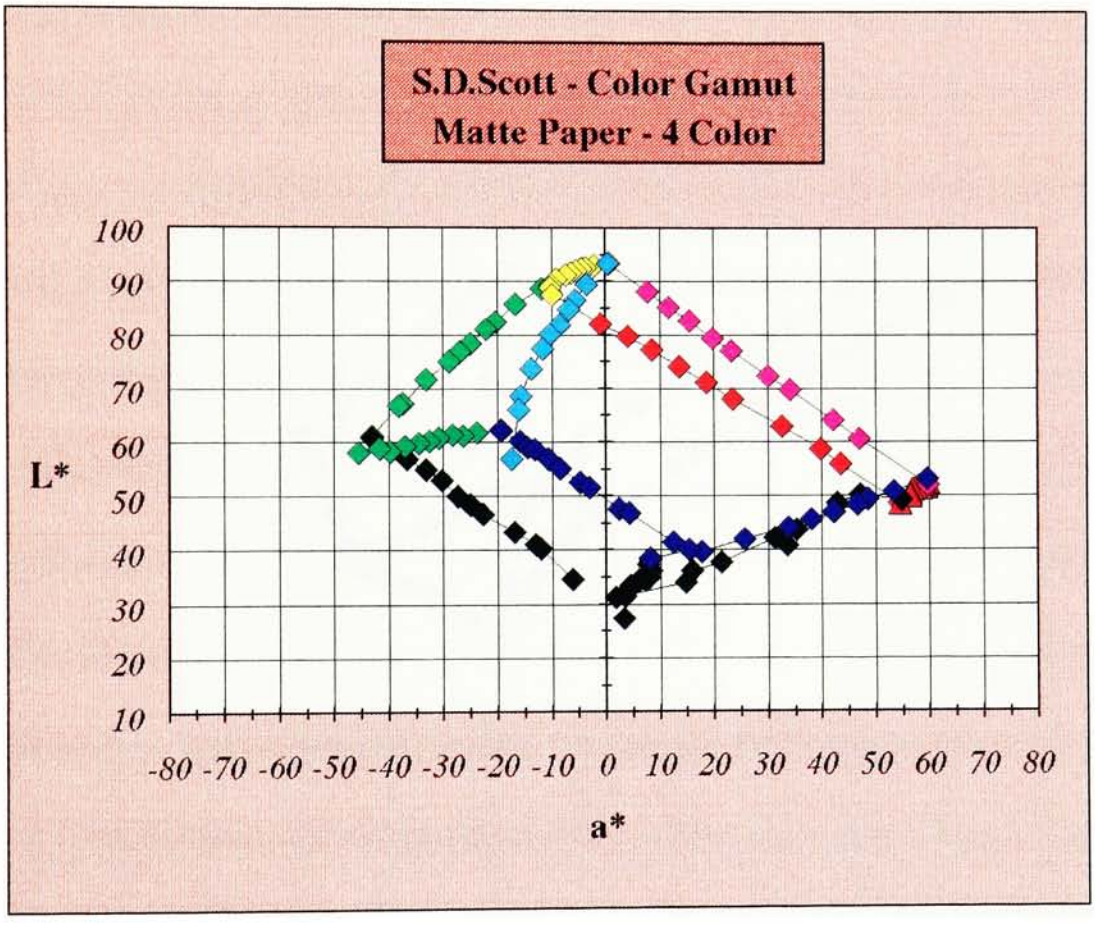
S.D.Scott - Color Gamut
Matte Paper - 4 Color
L*
100
90
80
70
60
50
40
30
20
10
-80 -70 -60 -50 -40 -30 -20 -10 0 10 20 30 40 50 60 70 80
a*

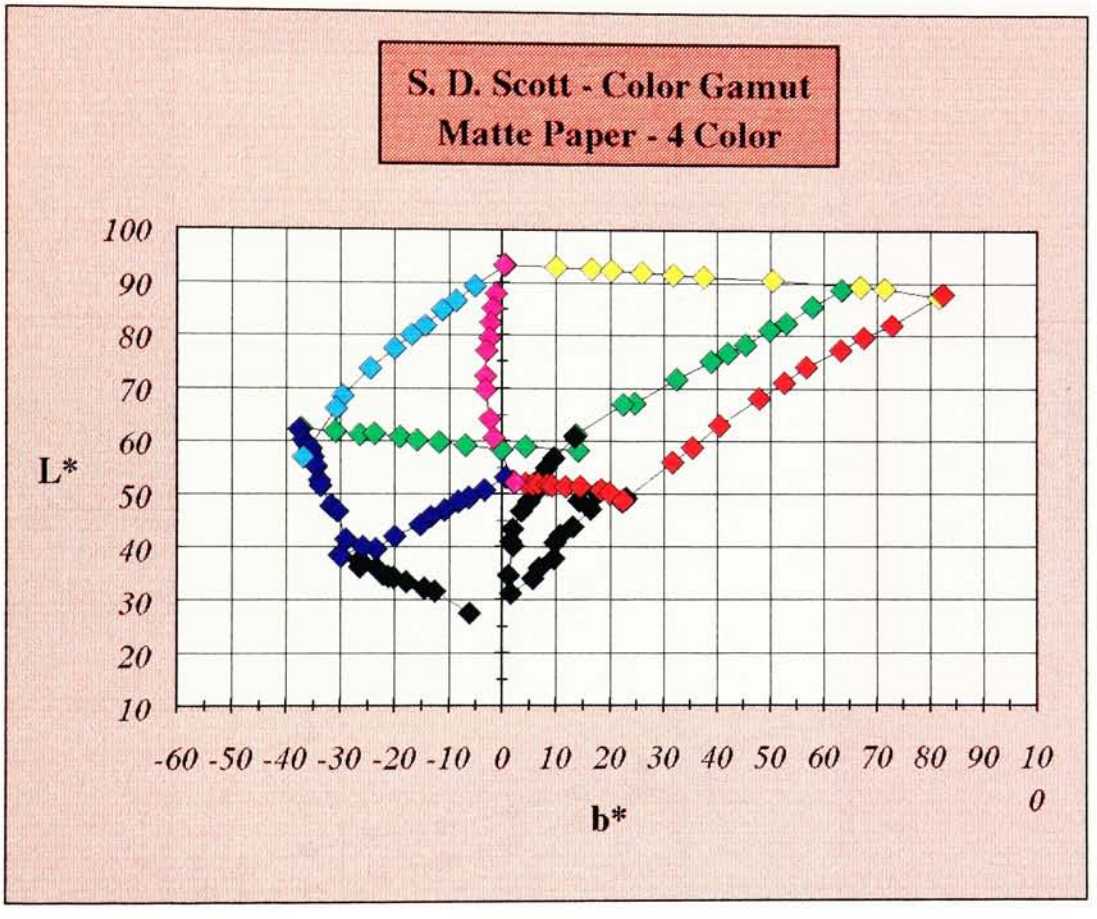
S. D. Scott - Color Gamut
Matte Paper - 4 Color
L*
100
90
80
70
60
50
40
30
20
10
-60 -50 -40 -30 -20 -10 0 10 20 30 40 50 60 70 80 90 10 0
b*

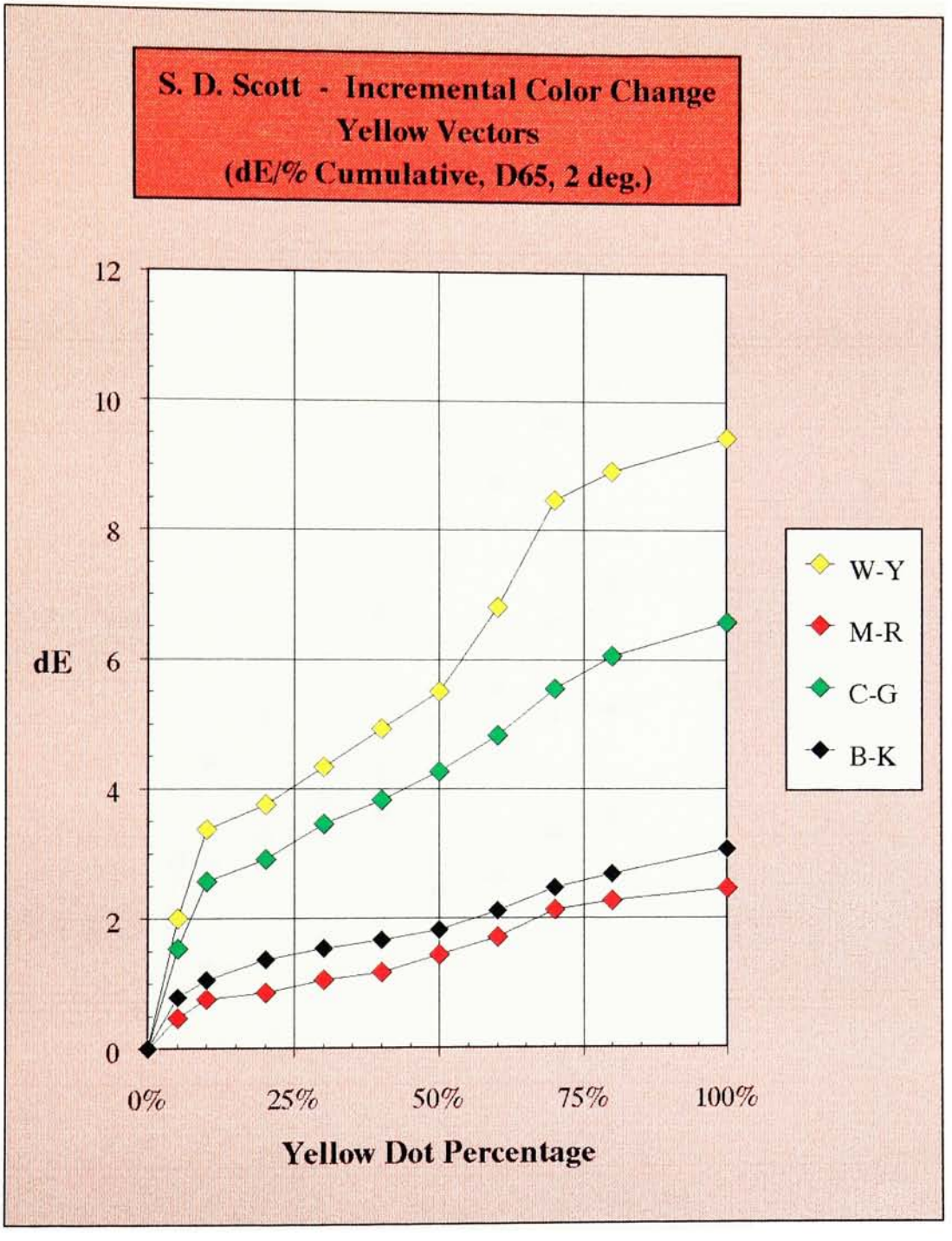
S. D. Scott - Incremental Color Change
Yellow Vectors
(dE/% Cumulative, D65, 2 deg.)
dE
12
10
8
6
4
2
0
0%
25%
50%
75%
100%
Yellow Dot Percentage
W-Y
M-R
C-G
B-K

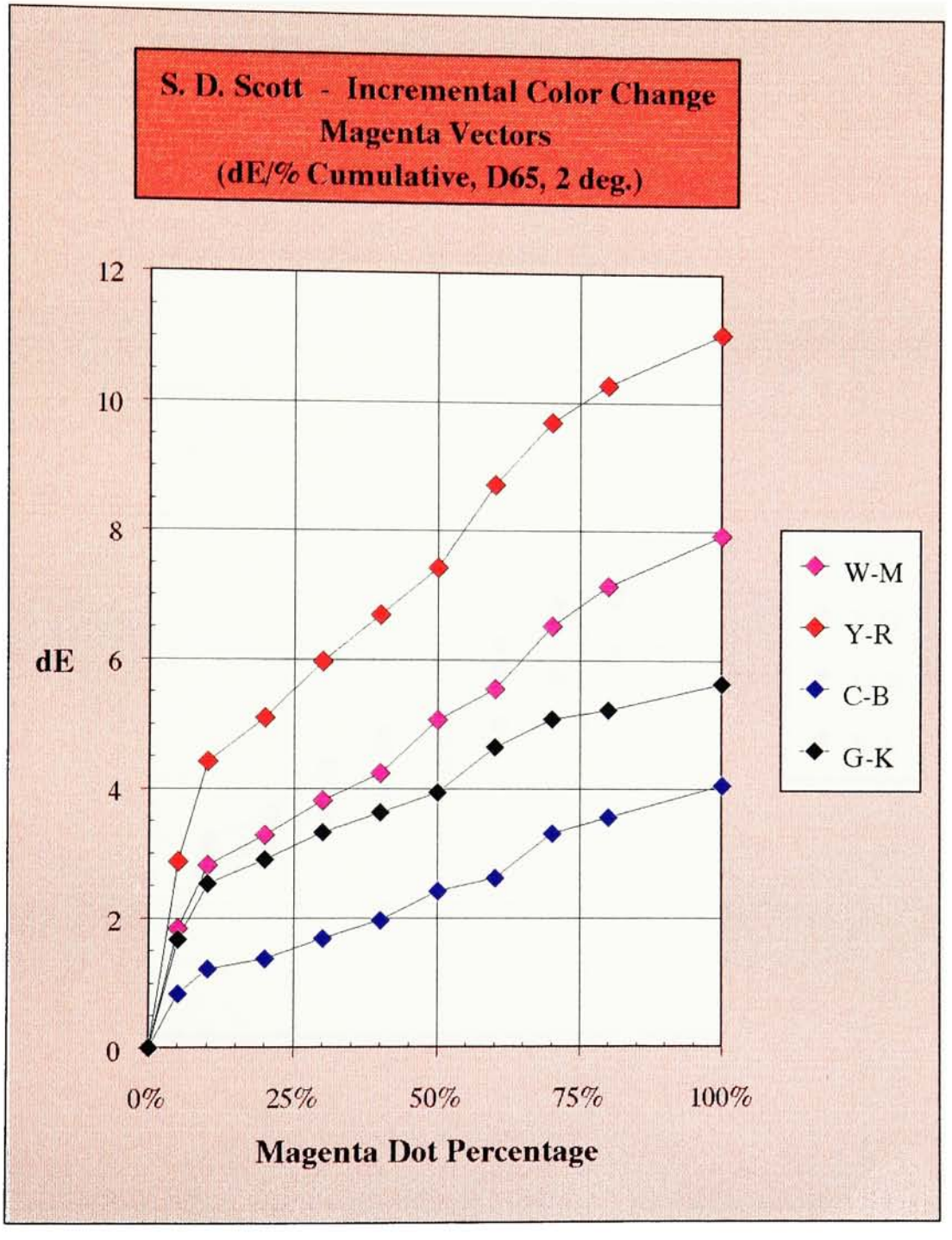
S. D. Scott - Incremental Color Change
Magenta Vectors
(dE/% Cumulative, D65, 2 deg.)
12
10
8
6
4
2
0
dE
0%
25%
50%
75%
100%
Magenta Dot Percentage
W-M
Y-R
C-B
G-K

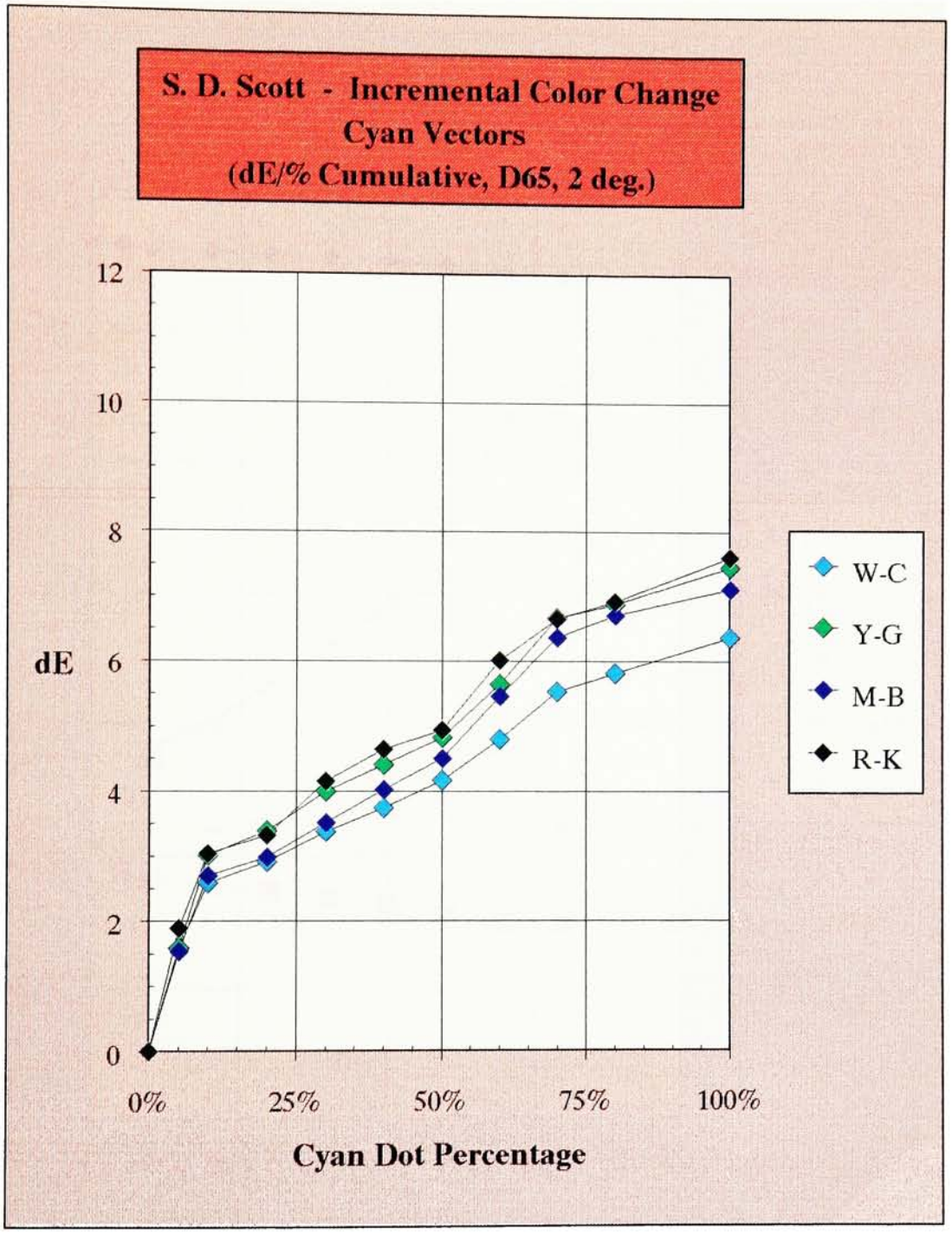
S. D. Scott - Incremental Color Change
Cyan Vectors
(dE/% Cumulative, D65, 2 deg.)
12
10
8
6
4
2
0
dE
0%
25%
50%
75%
100%
Cyan Dot Percentage
W-C
Y-G
M-B
R-K

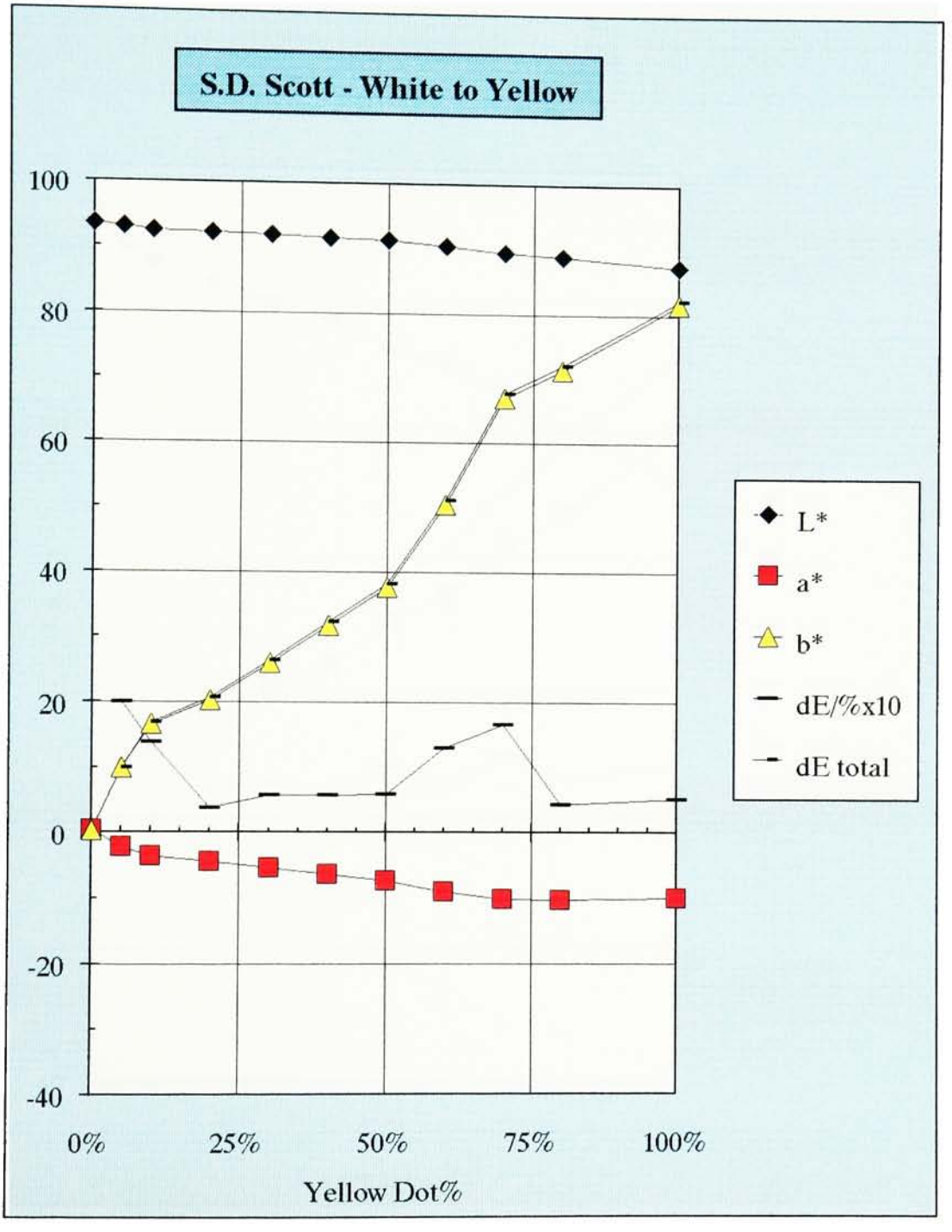
S.D. Scott - White to Yellow
100
80
60
40
20
0
-20
-40
0%
25%
50%
75%
100%
Yellow Dot%
L*
a*
b*
dE/%x10
dE total

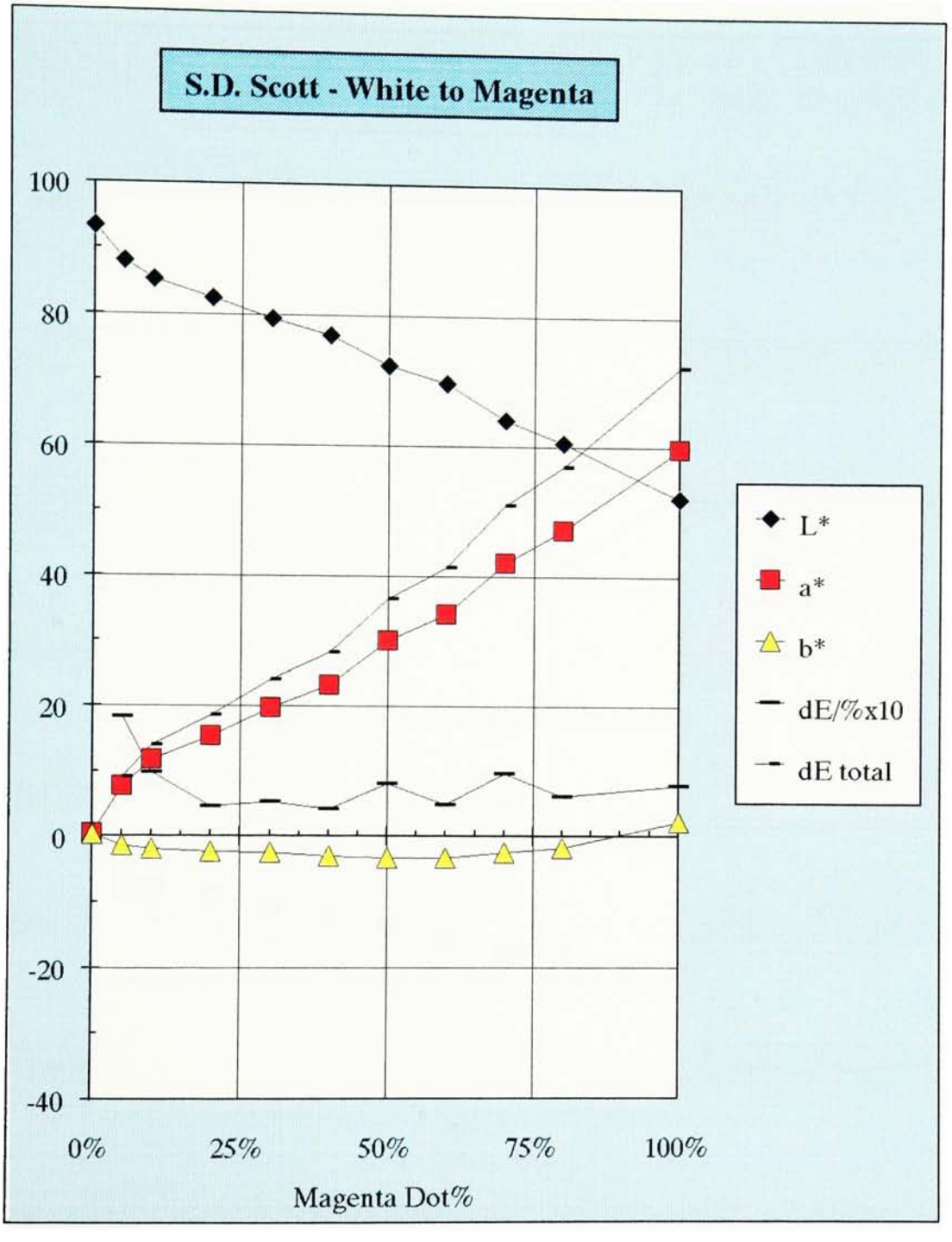
S.D. Scott - White to Magenta
100
80
60
40
20
0
-20
-40
0%
25%
50%
75%
100%
Magenta Dot%
L*
a*
b*
dE/%x10
dE total

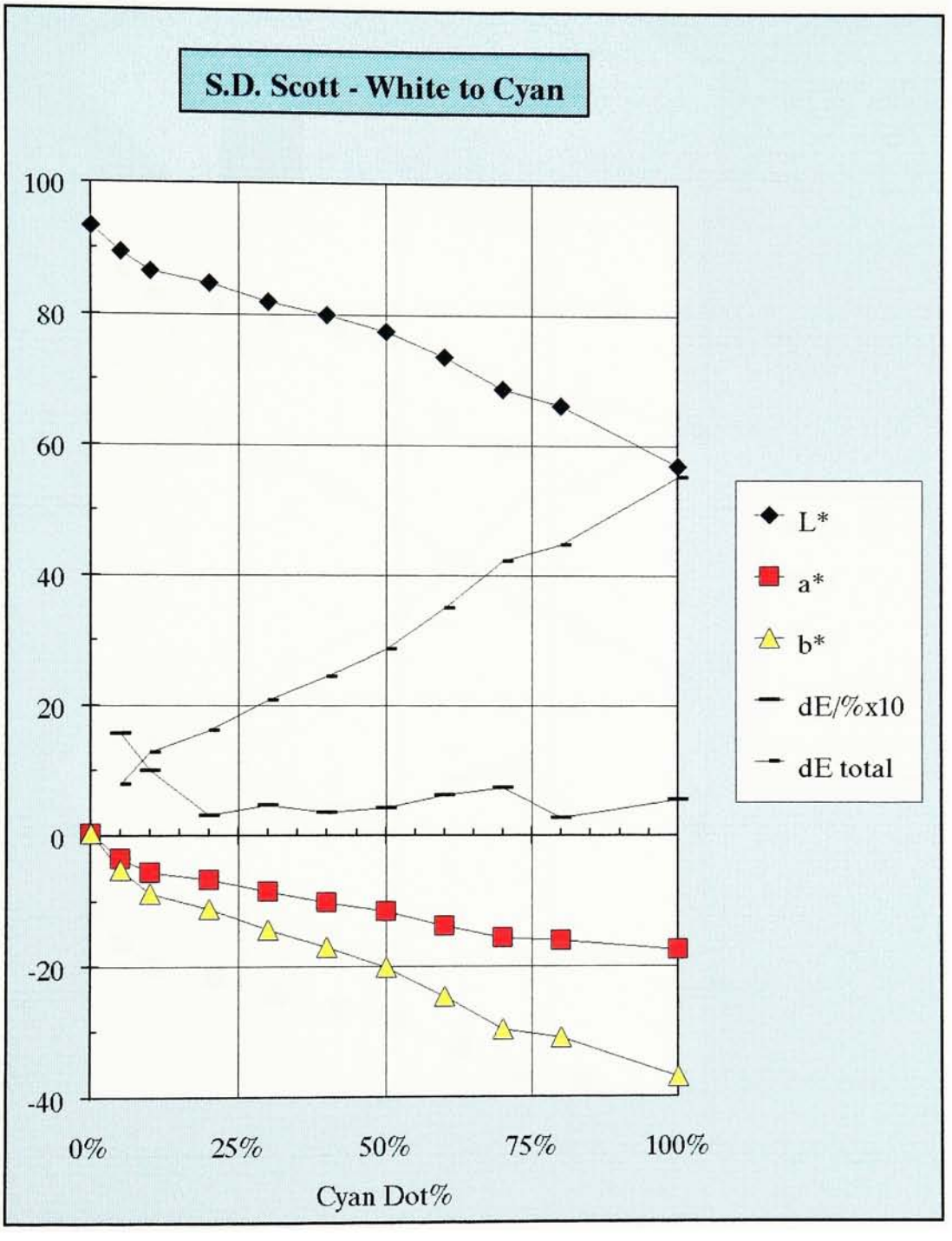
S.D. Scott - White to Cyan
100
80
60
40
20
0
-20
-40
0%
25%
50%
75%
100%
Cyan Dot%
L*
a*
b*
dE/%x10
dE total

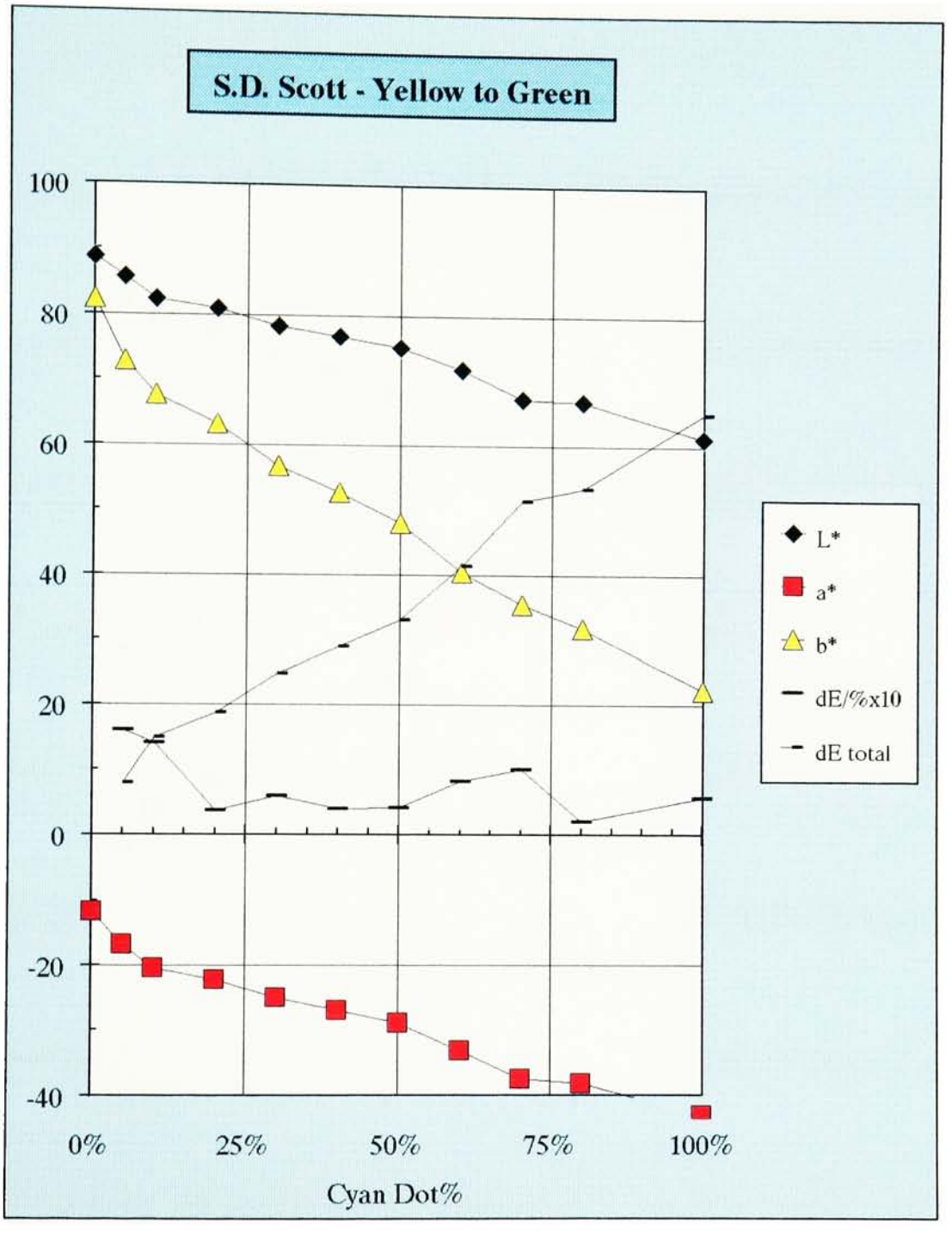
S.D. Scott - Yellow to Green
100
80
60
40
20
0
-20
-40
0%
25%
50%
75%
100%
Cyan Dot%
L*
a*
b*
dE/%x10
dE total

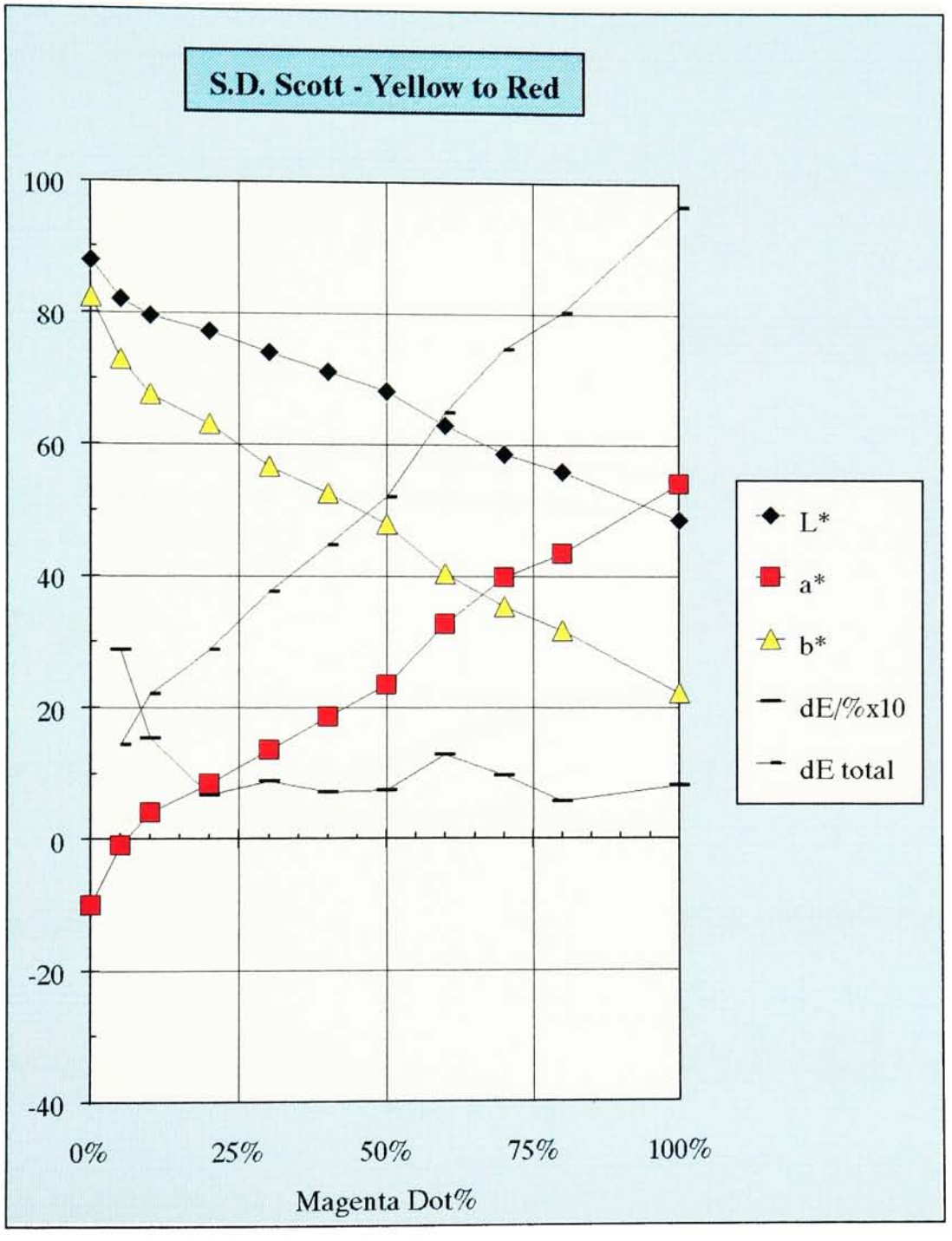
S.D. Scott - Yellow to Red
100
80
60
40
20
0
-20
-40
0%
25%
50%
75%
100%
Magenta Dot%
L*
a*
b*
dE/%x10
dE total

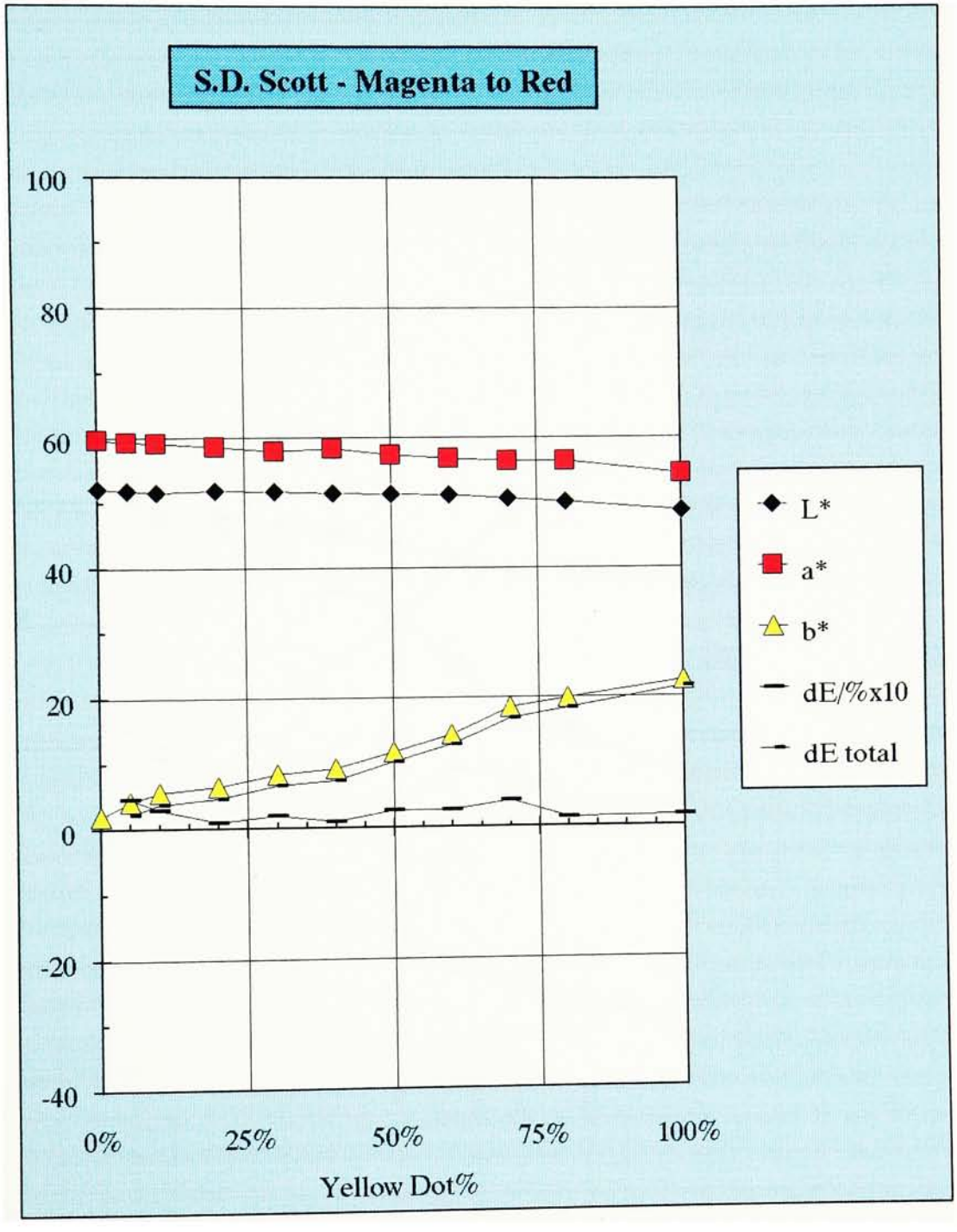
S.D. Scott - Magenta to Red
100
80
60
40
20
0
-20
-40
0%
25%
50%
75%
100%
Yellow Dot%
L*
a*
b*
dE/%x10
dE total

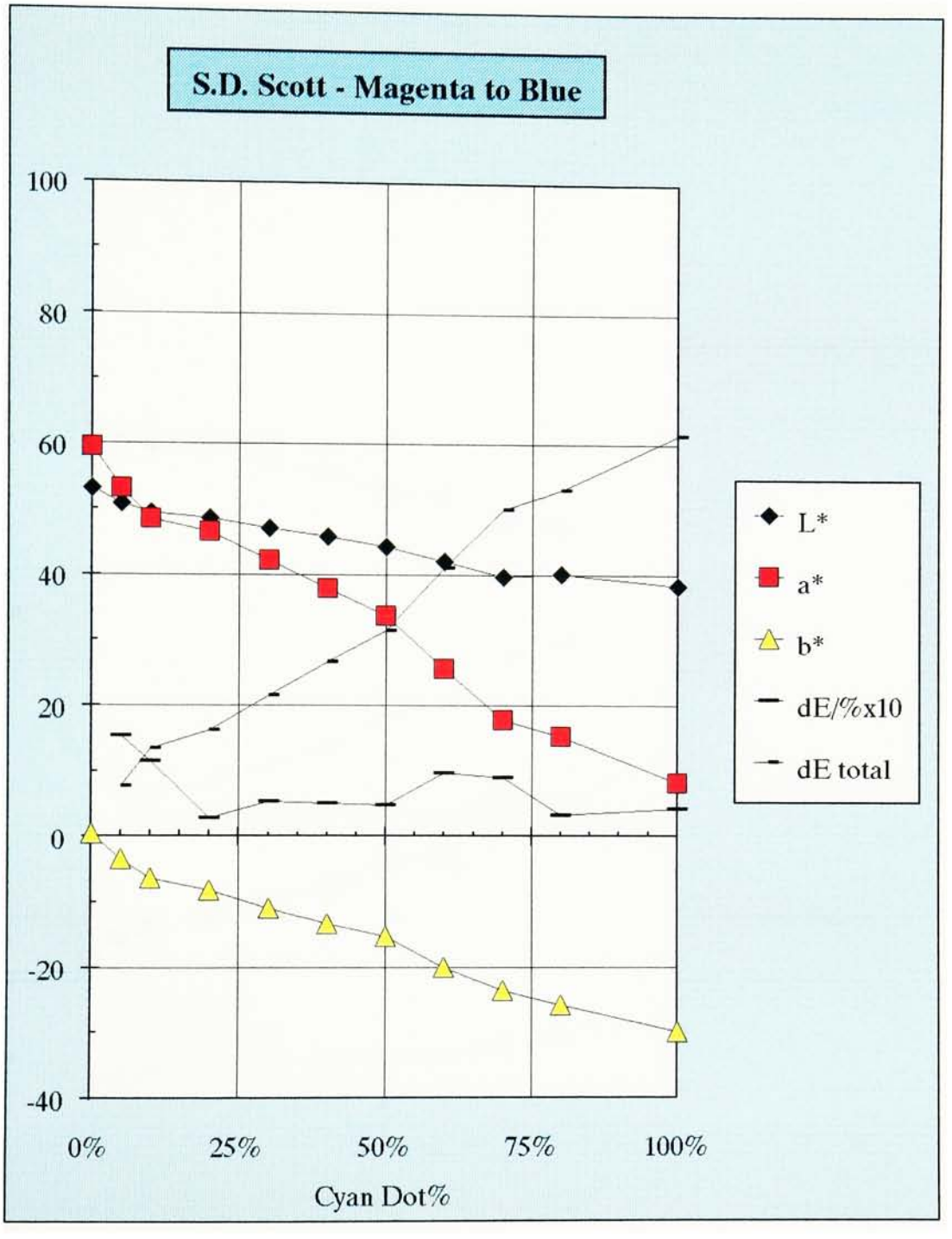
S.D. Scott - Magenta to Blue
100
80
60
40
20
0
-20
-40
0%
25%
50%
75%
100%
Cyan Dot%
L*
a*
b*
dE/%x10
dE total

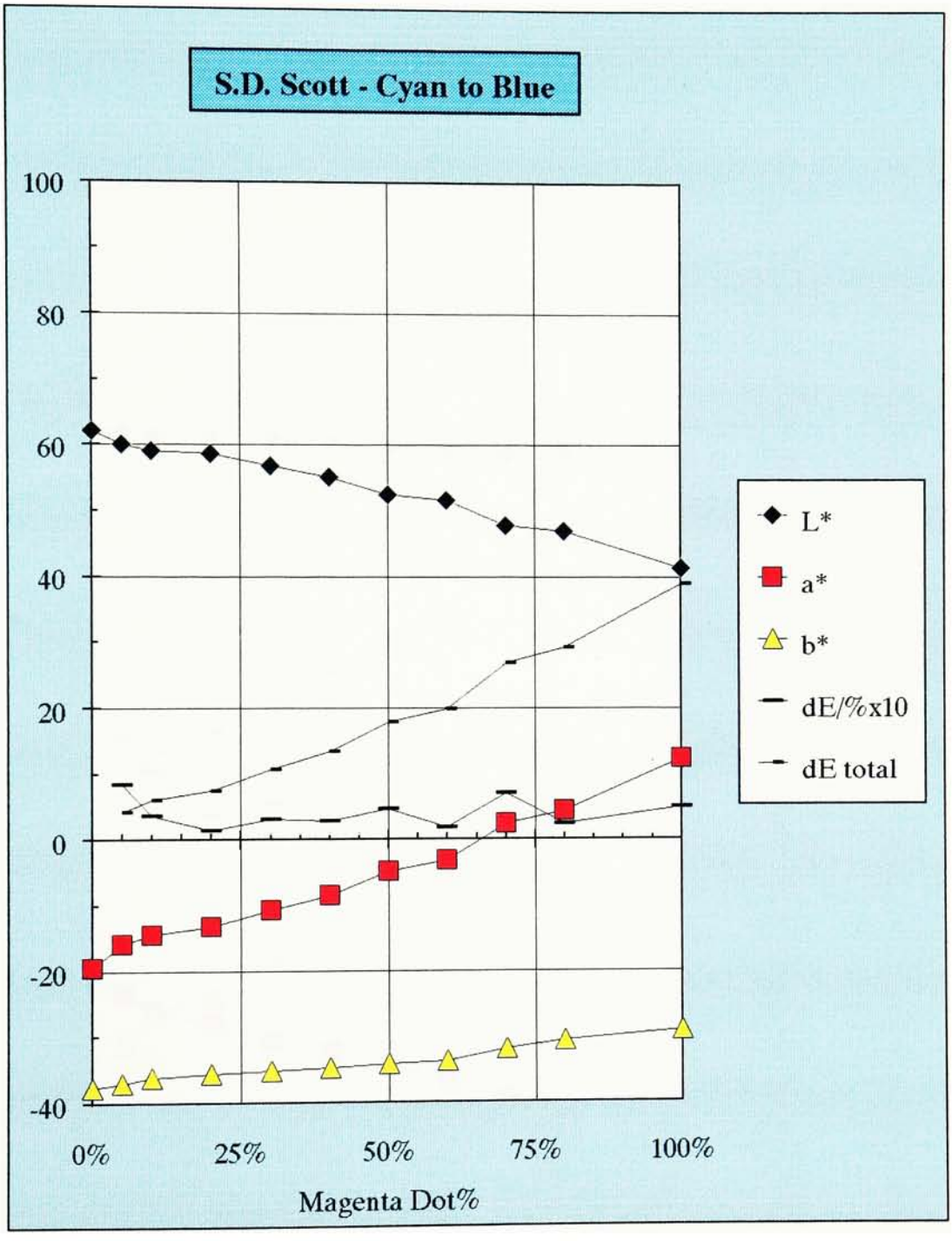
S.D. Scott - Cyan to Blue
100
80
60
40
20
0
-20
-40
0%
25%
50%
75%
100%
Magenta Dot%
L*
a*
b*
dE/%x10
dE total

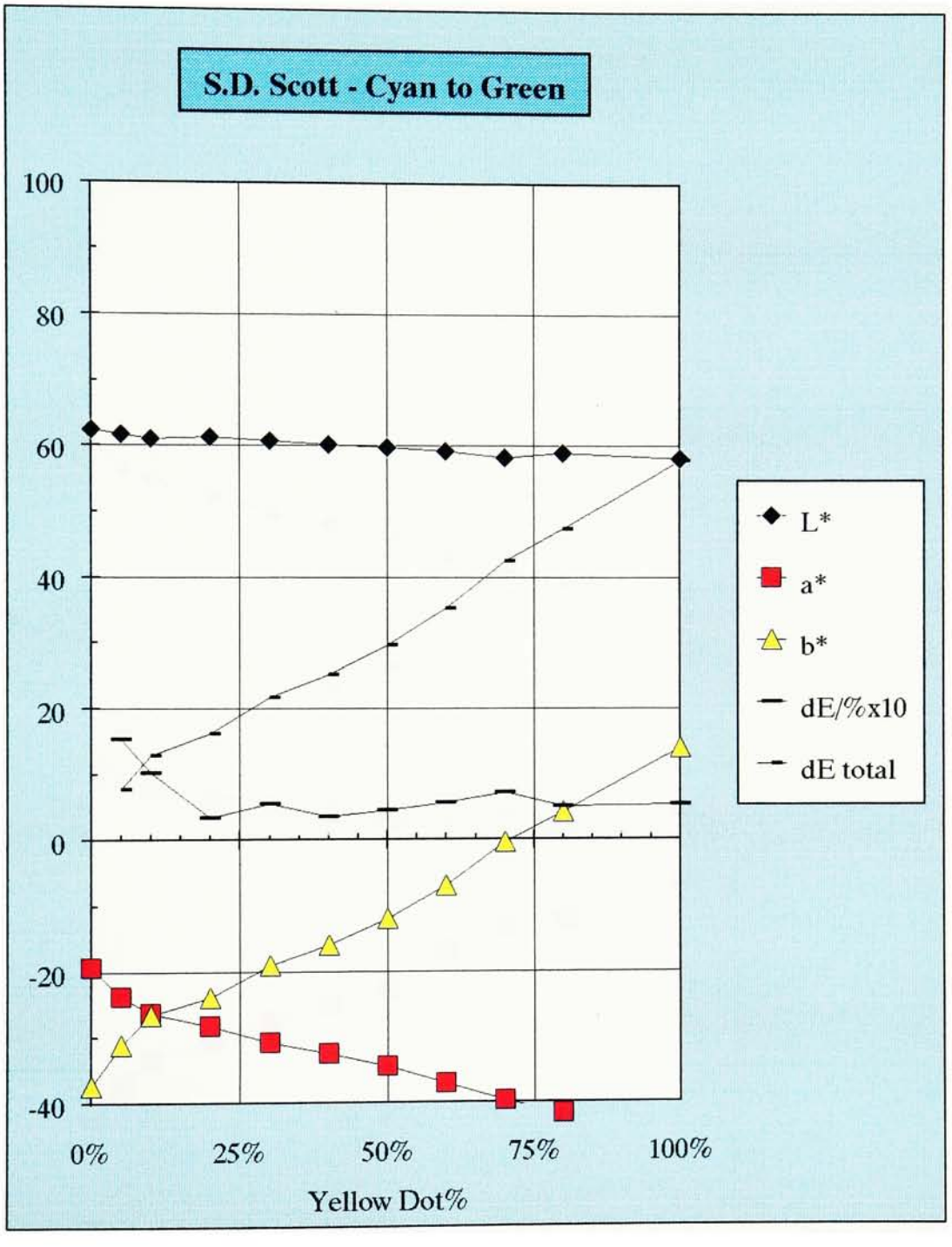
S.D. Scott - Cyan to Green
100
80
60
40
20
0
-20
-40
0%
25%
50%
75%
100%
Yellow Dot%
L*
a*
b*
dE/%x10
dE total

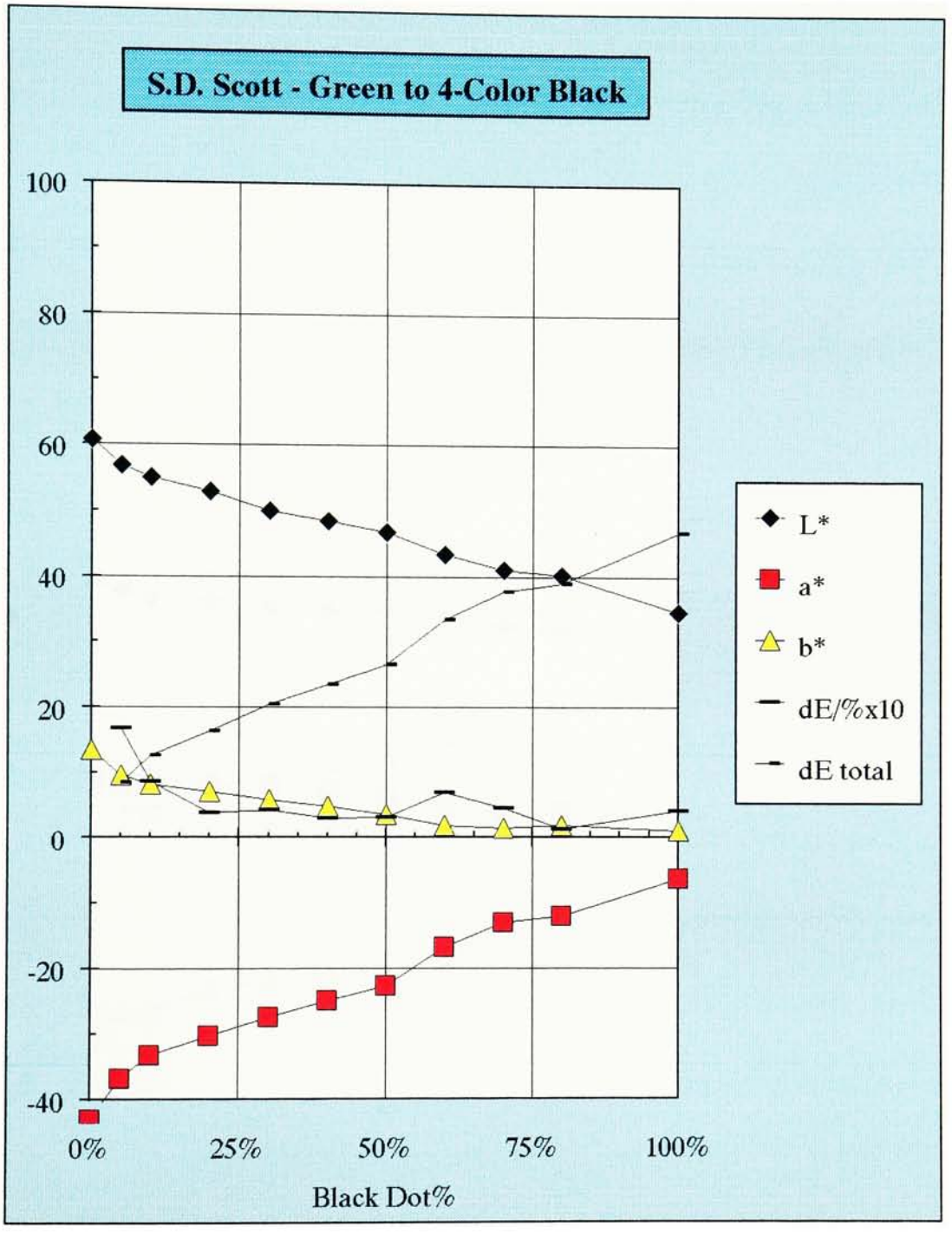
S.D. Scott - Green to 4-Color Black
100
80
60
40
20
0
-20
-40
0%
25%
50%
75%
100%
Black Dot%
L*
a*
b*
dE/%x10
dE total

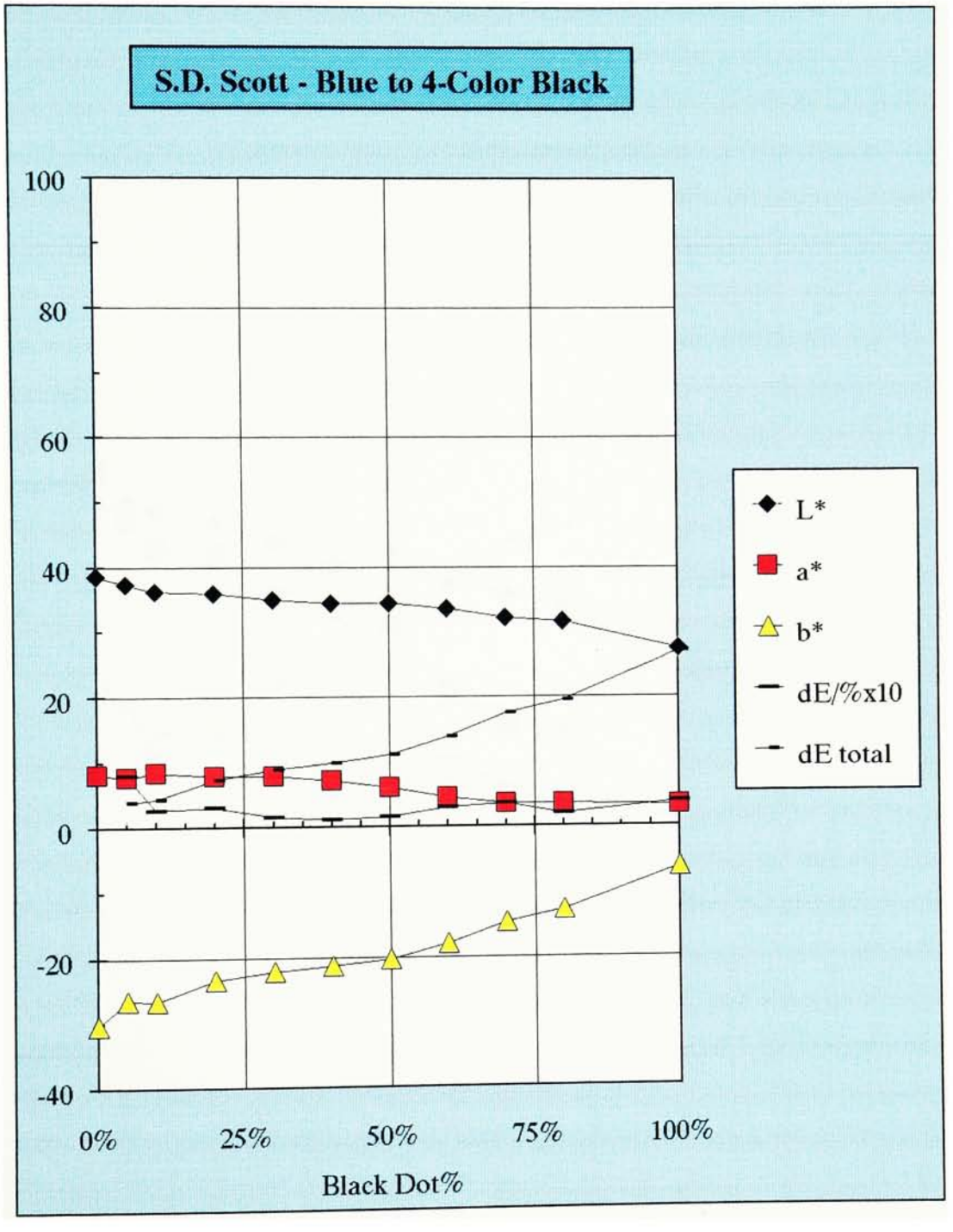
S.D. Scott - Blue to 4-Color Black
100
80
60
40
20
0
-20
-40
0%
25%
50%
75%
100%
Black Dot%
L*
a*
b*
dE/%x10
dE total

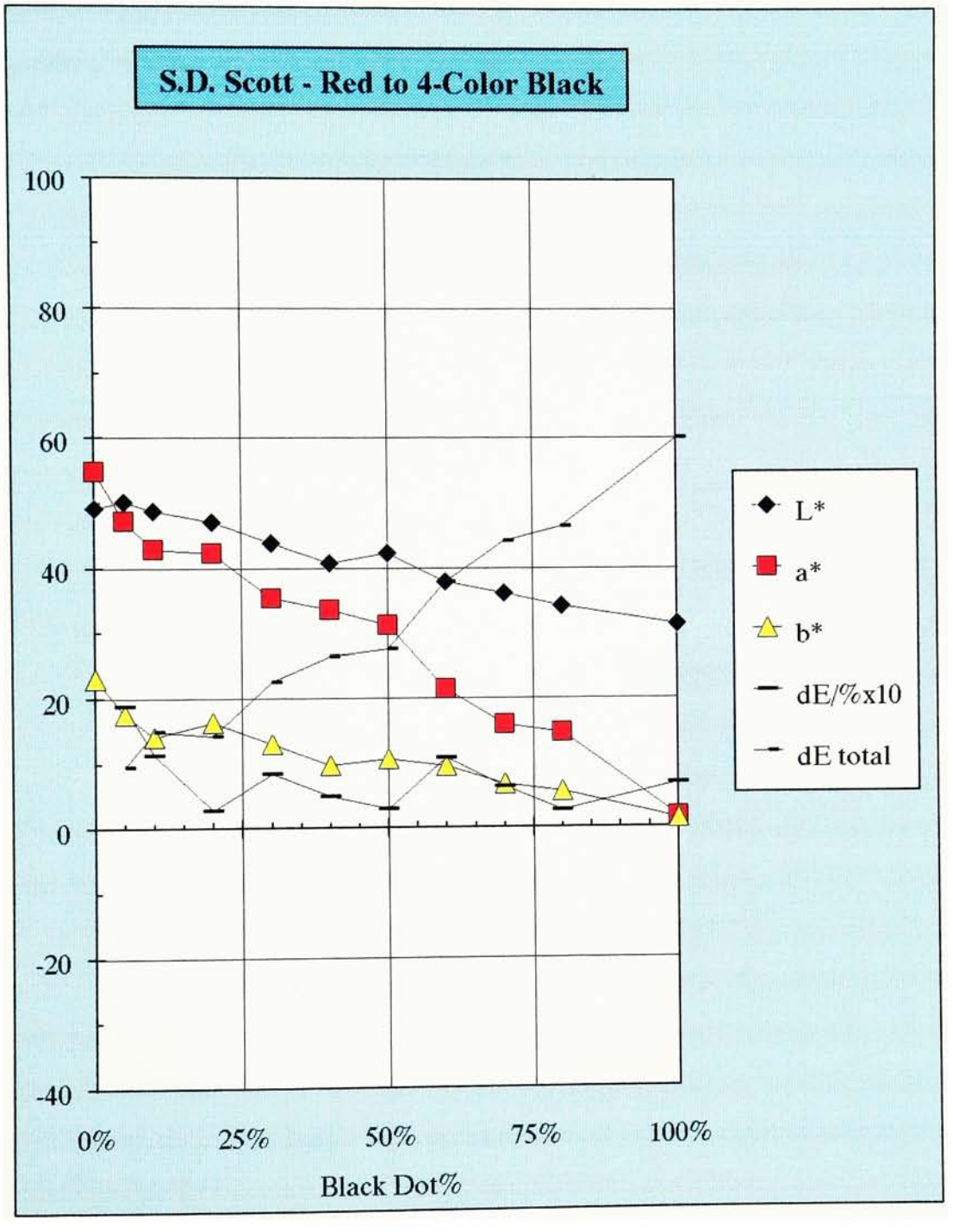
S.D. Scott - Red to 4-Color Black
100
80
60
40
20
0
-20
-40
0%
25%
50%
75%
100%
Black Dot%
L*
a*
b*
dE/%x10
dE total